

REVIEW

Reassessing the *Dlx* code: the genetic regulation of branchial arch skeletal pattern and development

Michael J. Depew,¹ Carol A. Simpson,¹ Maria Morasso² and John L. R. Rubenstein³

¹Department of Craniofacial Development, King's College London, Guy's Hospital, London, UK

²Developmental Skin Biology Unit, NIAMS, Bethesda, MD, USA

³Nina Ireland Laboratories of Developmental Neurobiology, University of California, San Francisco, USA

Abstract

The branchial arches are meristic vertebrate structures, being metameric both between each other within the rostro-caudal series along the ventrocephalic surface of the embryonic head and within each individual arch: thus, just as each branchial arch must acquire a unique identity along the rostrocaudal axis, each structure within the proximodistal axis of an arch must also acquire a unique identity. It is believed that regional specification of metameric structures is controlled by the nested expression of related genes resulting in a regional code, a principal that is though to be demonstrated by the regulation of rostrocaudal axis development in animals exerted by the nested *HOM-C/**Hox* homeobox genes. The nested expression pattern of the *Dlx* genes within the murine branchial arch ectomesenchyme has more recently led to the proposal of a *Dlx* code for the regional specification along the proximodistal axis of the branchial arches (i.e. it establishes intra-arch identity). This review re-examines this hypothesis, and presents new work on an allelic series of *Dlx* loss-of-function mouse mutants that includes various combinations of *Dlx1*, *Dlx2*, *Dlx3*, *Dlx5* and *Dlx6*. Although we confirm fundamental aspects of the hypothesis, we further report a number of novel findings. First, contrary to initial reports, *Dlx1*, *Dlx2* and *Dlx1/2* heterozygotes exhibit alterations of branchial arch structures and *Dlx2*^{-/-} and *Dlx1/2*^{-/-} mutants have slight alterations of structures derived from the distal portions of their branchial arches. Second, we present evidence for a role for murine *Dlx3* in the development of the branchial arches. Third, analysis of compound *Dlx* mutants reveals four grades of mandibular arch transformations and that the genetic interactions of *cis* first-order (e.g. *Dlx5* and *Dlx6*), *trans* second-order (e.g. *Dlx5* and *Dlx2*) and *trans* third-order paralogues (e.g. *Dlx5* and *Dlx1*) result in significant and distinct morphological differences in mandibular arch development. We conclude by integrating functions of the *Dlx* genes within the context of a hypothesized general mechanism for the establishment of pattern and polarity in the first branchial arch of gnathostomes that includes regionally secreted growth factors such as *Fgf8* and *Bmp* and other transcription factors such as *Msx1*, and is consistent both with the structure of the conserved gnathostome jaw bauplan and the elaboration of this bauplan to meet organismal end-point designs.

Key words branchial arch; development; *Dlx*; genetic; gnathostome; hinge and caps; jaws; pattern; skeleton.

Introduction

The branchial (pharyngeal) arches (BA) are metameric, meristic vertebrate structures filled with cranial neural

crest and mesoderm and sandwiched between points of endodermal–ectodermal contact along the ventrolateral cephalic surface (Fig. 1; Wolf, 1769; von Sömmerring, 1799; Meckel, 1809–1811; Rathke, 1825a,b, 1828, 1839, 1843, 1857; Huschke, 1827; von Baer, 1827; Huxley, 1869; His, 1881; Gegenbaur, 1888; Liessner, 1888; Wiedersheim & Parker, 1897; Gaupp, 1898, 1899; Gregory, 1904, 1933; Sewertzoff, 1911, 1928; Reynolds, 1913; Wilder, 1923; Kingsley, 1925; Kingsbury, 1926; de Beer, 1937; Nelsen, 1953; Goodrich, 1958; Romanoff, 1960; Jollie, 1962, 1977; Young, 1962; Adelman, 1966; Romer, 1966, 1972; Barghusen & Hopson, 1979; Moore,

Correspondence

Dr M. J. Depew, Department of Craniofacial Development, King's College London, Floors 27–28, Guy's Hospital, London Bridge, London SE1 9RT, UK. T: +44 207188 7388; E: michael.depew@kcl.ac.uk; and Dr J. L. R. Rubenstein, Nina Ireland Laboratories of Developmental Neurobiology, 1550 4th Street, University of California, San Francisco, San Francisco, CA 94143-2611 USA. T: +1 415476 7862; E: jlrr@itsa.ucsf.edu

Accepted for publication 13 September 2005

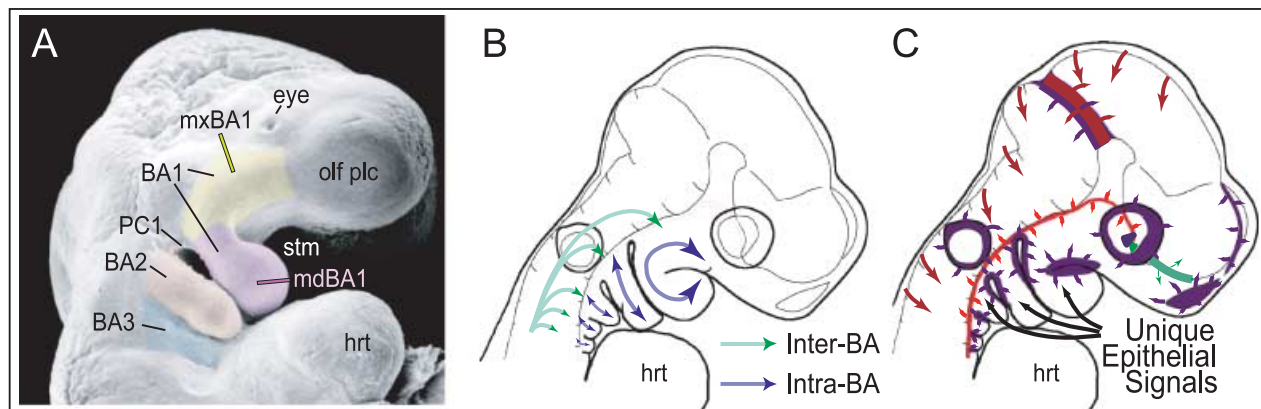


Fig. 1 Branchial arch (BA) organization and development. (A) Scanning electron micrograph of an E9.5 mouse embryo highlighting the meristic nature of the branchial arches. Yellow indicates the maxillary branch of the first arch (mxBA1), lavender the mandibular branch of the first arch (mdBA1), salmon the second, or hyoid, arch (BA2), and light blue the third arch (BA3). (B) Schema of patterning tasks in BA skeletal development. Green arrows highlight the task of establishing Inter-Arch identity, while blue arrows indicate the establishment of Intra-Arch identity (modified from Depew et al. 2002b). (C) Schema of an E9.5 mouse embryo depicting various sources (coloured patches and arrows) of patterning information influencing the development of the murine skull (modified from Depew et al. 2002b). Abbreviations: hrt, heart; olf plc, olfactory placode; PC1, first pharyngeal cleft; stm, stomodeum. See list after acknowledgements for full list of abbreviations.

1981; Carroll, 1988; Langille & Hall, 1989; Northcutt, 1990; Hunt et al. 1991a,b; Noden, 1991; Krumlauf, 1993; Kuratani et al. 1997; Hall, 1999; Shigetani et al. 2000, 2002, 2005; Graham, 2001; Kimmel et al. 2001; Depew et al. 2002a,b; Kuratani, 2003a, 2004, 2005; Kuratani et al. 2004). Traditionally, it has been recognized that the branchial arches are metameric along the rostrocaudal axis of a vertebrate; they are, after all, clearly defined outgrowths along the ventrolateral surface of the embryonic head and there are more than one. Also clear, yet often under-appreciated as such in the literature, is the fact that the branchial arches may be metameric, or homeomeric, within (Depew et al. 2002a,b). Thus, just as each branchial arch must acquire a unique identity along the rostrocaudal axis, each structure within the proximodistal axis of an arch must acquire a unique identity.

Clues to the genetic basis of how metameric structures develop have been gained by genetic, molecular and morphological analyses of development in many model organisms and from the first principals of organization. Studies principally of fruit flies and mice have shown that a nested pattern of related genes can result in a metameric set of structures; key among these were studies suggesting a combinatorial *Hox* code for inter-rhombomeric and inter-BA identity (e.g. Lewis, 1978; Nüsslein-Volhard & Wieschaus, 1980; Hunt et al. 1991a,b; Lawrence, 1992; McGinnis & Krumlauf, 1992; Krumlauf, 1993; Slack et al. 1993; Duboule, 1994). Like-

wise, the unique nested expression pattern within the murine branchial arch ectomesenchyme of the *Dlx* homeobox transcription factor genes made them attractive as candidates for genetic regulators of intra-arch development and identity: they were transcription factors, they were expressed in the right places and times, and the fly homologue was known to regulate the growth of appendages (reviewed in Pangani-ban & Rubenstein, 2002). Moreover, as the BA were known to give rise to an ordered series of skeletal elements, it was hypothesized that this nested pattern resulted in a combinatorial *Dlx* code wherein the combination of *Dlx* genes expressed in any particular portion of a BA primordia would be responsible for the development, pattern and subsequent morphology of the skeletal elements that formed from that primordia (Qiu et al. 1995, 1997; Depew et al. 1999, 2002a,b). A corollary, then, of this hypothesis was that a change in the combination either by loss- or gain-of-expression domains would change the identity of the skeletal elements.

Herein we re-examine this hypothesis. We begin by reviewing what has been done to address it genetically in mice, and then present new work on an allelic series of *Dlx* loss-of-function mutants that provides a fuller understanding of the roles that these genes have in BA development and gives insight into potential mechanisms through which the *Dlx* code defines proximodistal BA identity. This review contains a synthesis of both published and previously unpublished anatomical

studies that may be unfamiliar to some readers. Therefore, to aid readers unfamiliar with this field, we have constructed each subsequent section to be semi-independent and have included brief introductions to branchial arch development, genetics and derived anatomy. We have also included below an organizational road map of the contents of this review.

Dlx combinatorial code: correlation of BA skeleton and skeletal pattern

- 1 Structural components derived from the branchial arches
- 2 Molecular components of pattern in the branchial arches
- 3 *Dlx* BA gene expression and chromosomal organization
- 4 The combinatorial *Dlx* code hypothesis: predictions and examination of morphological change

Initial genetic tests of the code

- 1 *Dlx2*^{-/-} murine mutants
- 2 Evidence for a genetic interaction of the first-order paralogues, *Dlx1* and *Dlx2*, without evidence of distal BA alterations
- 3 Demonstration of *Dlx* regulation of distal BA structure: *Dlx5*^{-/-}
- 4 Testing the notion of a homeotic transformation as a prediction of the nested *Dlx* code hypothesis

Reassessing the regulation of *Dlx1* and *Dlx2* in distal BA-derived structures

- 1 Augmenting the phenotypic descriptions of mice carrying *Dlx1* mutant alleles
- 2 Augmenting the phenotypic descriptions of mice carrying *Dlx2* mutant alleles
- 3 Augmenting the phenotypic descriptions of mice carrying compound *Dlx1/2* mutant alleles
- 4 The *Dlx1*, *Dlx2* and *Dlx1/2* mutant phenotypes in relation to the hypothesized combinatorial *Dlx* code and the nature of heterozygous phenotypes

Reassessing the code: regulation of distal BA morphology and rationale for further examining the loss-of-function of distal *Dlx* genes

- 1 Testing genetic interactions: utilizing the loss of a nested *Dlx* gene to further address the code

- 2 Evidence of a genetic interaction between second-order paralogues: *Dlx2*^{-/-}; *Dlx5*^{-/-} mutants have extensively altered BA derivatives, including cleft mandibles
- 3 *Dlx2*^{-/-}; *Dlx5*^{+/-} mutants: phenotypic similarity to, but not identity with, the distal BA transformations seen in *Dlx5*^{-/-} mutants
- 4 *Dlx2*^{+/-}; *Dlx5*^{-/-}: exacerbation of the *Dlx5*^{-/-} phenotype with transformation of the body of Meckel's cartilage to a morphology reminiscent of an ala temporalis
- 5 Genetic interaction of the third-order paralogues, *Dlx1* and *Dlx5*: evidence that *Dlx1*^{-/-}; *Dlx5*^{-/-} mutants are phenotypically more similar to *Dlx2*^{+/-}; *Dlx5*^{-/-} mutants than to *Dlx2*^{-/-}; *Dlx5*^{-/-} mutants.
- 6 Evidence for a role for *Dlx3* in BA development: genetic interaction of *Dlx3* and *Dlx5*
- 7 *Dlx1/2*^{-/-}; *Dlx5*^{-/-} mutants: BA development in light of the loss of both a linked-pair partner and a paralogous partner
- 8 *Dlx1/2*^{-/-}; *Dlx5*^{+/-} and *Dlx1/2*^{+/-}; *Dlx5*^{-/-} mutants
- 9 Minimal transformation of the BA in the *Dlx3*^{+/-}; *Dlx1/2*^{-/-} mutants

Transformations resulting from the compound loss of single *Dlx* gene alleles

- 1 Neonatal lethality with phenotypic similarity to *Dlx5*^{-/-} mutants in compound *Dlx1/2*^{+/-}; *Dlx5/6*^{+/-} heterozygotes
- 2 Similar neonatal lethality in *Dlx2*^{+/-}; *Dlx5/6*^{+/-} heterozygotes
- 3 Extensive heterozygosity: [*Dlx1*^{+/-}; *Dlx2*^{+/-}; *Dlx3*^{+/-}; *Dlx5*^{+/-}; *Dlx6*^{+/-}] mutants

Testing equivalents: comparing first-, second- and third-order paralogues and comparing unique combinations and numbers of *Dlx* alleles

- 1 *Dlx6*^{-/-}; *Dlx5*^{+/-} mutants: phenotypic similarity to, but not identity with, *Dlx2*^{+/-}; *Dlx5*^{-/-} and *Dlx1*^{-/-}; *Dlx5*^{-/-} mutants
- 2 Comparisons of [*Dlx2*^{+/-}; *Dlx5*^{-/-}; *Dlx6*^{+/-}], [*Dlx3*^{+/-}; *Dlx5*^{-/-}; *Dlx6*^{+/-}], [*Dlx1*^{+/-}; *Dlx2*^{+/-}; *Dlx5*^{-/-}; *Dlx6*^{+/-}] and [*Dlx5*^{-/-}; *Dlx6*^{-/-}] mutants

Denouement – getting your head on straight in a *Dlx* world

- 1 Insights into the nature of the *Dlx* functions in patterning of the branchial arch-derived skeleton

- 2 *Dlx* dosage in the BA1 development: regional specification and regional growth
- 3 *Dlx* in the development and evolution of the jaw
- 4 Soft tissue phenotypes in the jaws of *Dlx5/6*^{-/-} and *Dlx2*^{-/-}; *Dlx5*^{-/-} mutants
- 5 Implications of the *Dlx* mutants for human developmental disorders
- 6 Summary

Dlx combinatorial code: correlation of BA skeleton and skeletal pattern

Structural components derived from the branchial arches

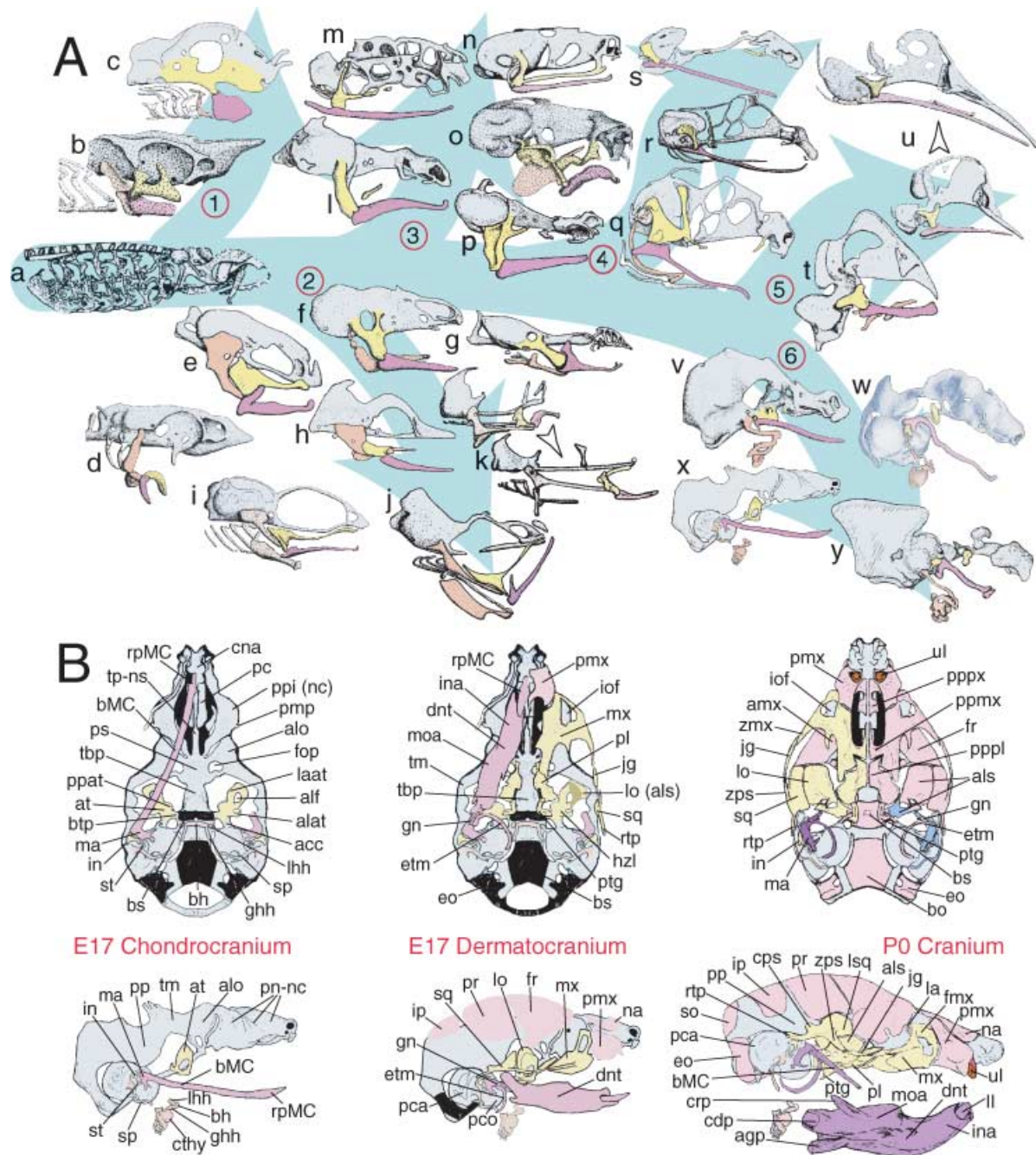
It has typically been thought that the BA are meristic (branchiomeristic) structures (Fig. 1; Rathke, 1825a,b, 1857; Huschke, 1827; von Baer, 1827; Huxley, 1869; His, 1881; Gegenbaur, 1888; Liessner, 1888; Wiedersheim & Parker, 1897; Gaupp, 1898; Gregory, 1904, 1933; Reynolds, 1913; Wilder, 1923; Kingsley, 1925; Kingsbury, 1926; de Beer, 1937; Nelsen, 1953; Goodrich, 1958; Romanoff, 1960; Jollie, 1962, 1977; Young, 1962; Romer, 1966, 1972; Barghusen & Hopson, 1979; Moore, 1981; Carroll, 1988; Langille & Hall, 1989; Northcutt, 1990; Hunt et al. 1991a,b; Noden, 1991; Krumlauf, 1993; Kuratani et al. 1997, 2003, 2005; Hall, 1999; Kimmel et al. 2001; Depew et al. 2002a,b; Kuratani, 2003a, 2004, 2005). Evidence, principally derived from palaeontological series and comparative embryology, has suggested that the prototypical gnathostome (jawed vertebrate) BA contained a proximodistal (PD) series of chondrocranial elements and (in those vertebrates with an ossified skeleton) an associated, ordered series of dermatocranial bones. Although healthy debate has been re-kindled as to whether the first BA (BA1, from which the gnathostome jaws are largely, but not entirely, derived) or the second BA (BA2, with which the jaw suspension has typically been associated) were ever 'typical', the first two BA of all gnathostomes are characterized by their possession of ordered splanchnocranial elements (Reichert, 1837; Parker, 1866, 1869, 1871, 1873; Huxley, 1869, 1876; Parker, 1876, 1877, 1878, 1879, 1881, 1882, 1883, 1885a,b; Gegenbaur,

1888; Wiedersheim & Parker, 1897; Gregory, 1904, 1913, 1933; Sewertzoff, 1911, 1928; Reynolds, 1913; de Beer, 1937; Paterson, 1939; Romer, 1956, 1966; Jollie, 1957, 1962; Goodrich, 1958; Romanoff, 1960; Young, 1962; Schmalhausen, 1968; Allin, 1975; Presley & Steel, 1976; Crompton & Parker, 1978; Barghusen & Hopson, 1979; Jarvik, 1980; Bellairs & Kamal, 1981; Moore, 1981; Kuhn & Zeller, 1987; Radinsky, 1987; Carroll, 1988; Langille & Hall, 1989; Vorster, 1989; Allin & Hopson, 1992; Couly et al. 1993; Novacek, 1993; Schultze, 1993; Trueb, 1993; Zusi, 1993; Kimmel et al. 1995; Cubbage & Mabee, 1996; Janvier, 1996; Kuratani et al. 1997; Depew et al. 2002b; Kuratani, 2003a,b, 2004, 2005). Regardless of origin or order in its evolution, the splanchnocranial chondrocranium of BA1 of all observed gnathostomes is composed of two major PD components: the maxillary first arch (mxBA1, proximal) and mandibular first arch (mdBA1, distal) derivatives of the palatoquadrate cartilage (PQ) and Meckel's cartilage (MC), respectively (Fig. 2A). BA2 likewise gives rise to an ordered series of elements, often collectively known as Reichert's cartilage. Typical of mammals, mice possess two highly derived PQ-associated elements: the ala temporalis and the incus (quadrate homologue of non-mammalian gnathostomes); they further possess a Meckel's cartilage and its constituent malleal (articular homologue of non-mammalian gnathostomes), body and rostral process components (Figs 2B and 21A–C). These chondrocranial elements are further associated with an ordered series of dermatocranial bones, including the mxBA1-derived maxilla, palatine, pterygoid and squamosal, and the mdBA1-derived dentary, ectotympanic and gonial.

Molecular components of pattern in the branchial arches

Patterning of the BA includes at least two basic tasks: (1) the establishment of inter-BA identity such that each BA within the rostrocaudal series is unique, and (2) the establishment of intra-BA identity such that each element within the proximodistal axis of a given BA has a unique identity (Fig. 1B). Historical questions regarding the origin and basis of the segmental

Fig. 2 Structural organization of BA derivatives. (A) Schemae of gnathostome chondrocrania demonstrating the conservation of an ordered series of splanchnocranial elements in the gnathostome bauplan. Maxillary arch derivatives are depicted in yellow, mandibular arch in lavender and caudal arches in salmon and/or white. The neurocranial chondrocranium is in light blue. Skull groupings are organized as follows: 1, Chondrichthyes; 2, Osteichthyes; 3, Amphibia; 4, Reptilia; 5, Aves; and 6, Mammalia. Genera depicted: a, *Ptetromyzon* sp. (modified from Parker, 1883); b, *Squalus* sp. (modified from Nelsen, 1953); c, *Callorhynchus* sp.



(modified from de Beer, 1937); d, *Acipenser* sp. (modified from de Beer, 1937); e, *Amia* sp. (modified from de Beer & Moy-Thomas, 1935); f, *Ceratodus* sp. (modified from de Beer, 1937); g, *Lepidosiren* sp. (modified from de Beer, 1937); h, *Anguilla* sp. (modified from Norman, 1926); i, *Salmo* sp. (modified from de Beer, 1937); j, *Gadus* sp. (modified from de Beer, 1937); k, *Syngnathus* sp. (arrowhead indicates ontogenetic progression of the chondrocranium; modified from Kindred, 1921); l, *Salamandra* sp. (modified from de Beer, 1937); m, *Ichthyophis* sp. (modified from de Beer, 1937); n, *Eleutherodactylus* sp. (modified from Hanken et al. 1992); o, *Rana* sp. (modified from Nelsen, 1953; after de Beer, 1937); p, *Amblystoma* sp. (modified from de Beer, 1937; after Gaupp); q, *Sphenodon* sp. (modified from Bellairs & Kamal, 1981); r, *Lacerata* sp. (modified from de Beer, 1937); s, *Eryx* sp. (modified from Bellairs & Kamal, 1981); t, *Spheniscus* sp. (modified from Romanoff, 1960; after Crompton); u, *Anas* sp. (arrowhead indicates ontogenetic progression of the chondrocranium; modified from de Beer & Barrington, 1934); v, *Ornithorhynchus* sp. (modified from de Beer, 1937); w, *Xerus* sp. (modified from Fawcett, 1922); x, *Mus* sp. (modified from Depew et al. 2002b); y, *Homo sapiens* (modified from de Beer, 1937). (B) Schemata of murine skulls depicting the E17 chondrocranium, E17 dermatocranium and neonatal cranium seen in both norma basalis externa and norma lateralis. Elements in yellow are maxillary arch derivatives while those in lavender are mandibular arch derivatives. Caudal arch derivatives are depicted in salmon. For anatomical nomenclature, see the list of abbreviations.

organization of the BAs have been re-investigated with the discovery of candidate regulatory genes whose expression and activity within the BAs, and/or their antecedent tissues, suggest roles in the control of BA development and pattern (Fig. 1C). These include, among numerous others, genes for secreted molecules of the *Bmp*, *Fgf*, *Shh*, *Wnt*, *Retinoic Acid* and *Endothelin* gene families, genes encoding their inhibitors such as *Noggin*, *Chordin*, *Dkk1* and *sFRP*, and members of the *Dlx*, *Alx*, *Msx*, *Otx*, *Pax*, *Prx*, *Fox*, *Tbx*, *Gsc* and *Hox* homeodomain transcription factor (TF) gene families. Reviews of many of these have recently been presented elsewhere (e.g. Depew et al. 2002b; Francis-West et al. 2003; Santagati & Rijli, 2003; Trainor et al. 2003; Tucker & Sharpe, 2004) and thus need not be covered here.

Although the search for ever more proximate sources of patterning information of the developing BA and their precursor tissues – whether centred within the ectoderm, ectomesenchyme, mesoderm and/or endoderm – proceeds and intensifies, a large body of work has already established a framework from which patterning of the BA skeleton can be assessed. Conceptually, for instance, investigation of the *Hox* gene family has been of particular importance in understanding of the establishment of inter-BA identity (Hunt et al. 1991a,b; Gendron-Maguire et al. 1993; Krumlauf, 1993; Rijli et al. 1993; Takio et al. 2004), as have been the *Pbx* and *Otx* gene families (Matsuo et al. 1995; Selleri et al. 2001). Experimental embryological studies in mice have further suggested that the period between embryonic day (E)10 and E10.5 is of particular importance in the ontogeny of the specification, determination and potency of the mouse BA primordia (Lumsden, 1988; Ferguson et al. 2000; reviewed in Depew et al. 2002b); this, then, is a period when gene expression patterns within the BA reflect the seminal course of craniofacial patterning and from which craniofacial structural outcome will subsequently be defined. It is also a period during which the pattern of *Dlx* gene expression within the BA ectomesenchyme is nested.

***Dlx* BA gene expression and chromosomal organization**

In invertebrate species such as the fruit fly *Drosophila melanogaster*, the *Dlx* orthologue, *distal-less*, controls the proximodistal development of appendages (Cohen & Jurgens, 1989). *Distal-less* orthologues have been found in every bilateral organism in which they have

been sought, and their expression patterns have suggested that they regulate the development of appendages from the body axes (Stock et al. 1996; Panganiban et al. 1997; Panganiban & Rubenstein, 2002; Stock, 2005). Functional studies on the vast majority of this wide range of organisms have not yet, however, been made (Panganiban & Rubenstein, 2002).

As with invertebrates, vertebrate *Dlx* genes are expressed in appendages, or outgrowths, from the main body axis, including in the BA. In mice, six *Dlx* genes have been detected and described: *Dlx1*, *Dlx2*, *Dlx3*, *Dlx4* (previously *Dlx7*), *Dlx5* and *Dlx6* (Fig. 3; Dolle et al. 1992; Bulfone et al. 1993; Robinson & Mahon, 1994; Simeone et al. 1994; Qiu et al. 1995, 1997; Stock et al. 1996; Panganiban & Rubenstein, 2002). In the embryonic mouse, these six *Dlx* genes are differentially expressed in a regional, nested pattern in the ectomesenchyme along the proximodistal axis of the BA (though none is extensively expressed in the distal-most BA midline ectomesenchyme) (Fig. 3B; Qiu et al. 1995, 1997). It is noteworthy, moreover, that *Dlx* genes are also variably expressed in the cephalic surface ectoderm. For instance, whereas *Dlx5* and *Dlx6* are expressed early (e.g. E8.25) in the entire cephalic surface ectoderm, by E10.5 their ectodermal expression is essentially restricted to the olfactory pit and otic vesicle (Yang et al. 1998; Depew et al. 1999). Likewise, at E10.5 *Dlx2* and *Dlx3* are expressed in both the distal-most mandibular BA oral ectoderm and the ectoderm of the lambdoidal junction where the maxillary BA meets the frontonasal processes (green arrows, Fig. 3).

Mammalian *Dlx* genes are arranged as tightly linked, convergently transcribed (tail-to-tail) bigene pairs, or first-order (*cis*) paralogues, located near *Hox* gene clusters (Stock et al. 1996; Panganiban & Rubenstein, 2002). Potentially of great importance, similarity outside of the homeodomain plus chromosomal location indicates that the *Dlx* genes can be placed into two clades of second-order (*trans*) paralogous groups: *Dlx1/4/6* and *Dlx2/3/5* (Fig. 3A). Their linkage further enables the simultaneous, targeted mutation of both genes of a bigene pair (Qiu et al. 1997; Merlo et al. 2002; Robledo et al. 2002). Tightly linked *Dlx* genes appear to share regulatory regions and are expressed in similar patterns within the developing BA mesenchyme (Dolle et al. 1992; Bulfone et al. 1993; Robinson & Mahon, 1994; Simeone et al. 1994; Ellies et al. 1997; Depew et al. 2002a; Panganiban & Rubenstein, 2002; Ghanem et al. 2003; Sumiyama & Ruddle, 2003). Hence, first-

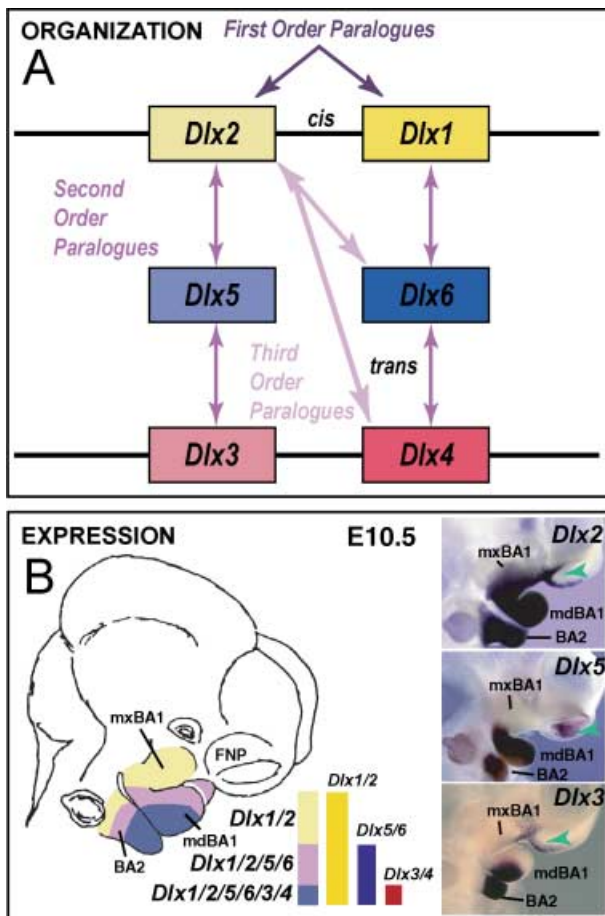


Fig. 3 *Dlx* gene organization and branchial arch expression. (A) Schema of *Dlx* chromosomal organization. In mice, the six known *Dlx* genes are arranged as tightly linked, convergently transcribed bigene pairs, delineated here as first-order (*cis*) paralogs. Similarity outside of the homeodomain plus chromosomal location indicates that the *Dlx* genes can be placed into two clades of second-order (*trans*) paralogous groups: *Dlx1*, 6 and 4 and *Dlx2*, 5 and 3. Third-order paralogs are those genes that are neither linked nor fall within the same clade, e.g. *Dlx2* and *Dlx4*. (B) Schema and *in situ* hybridization data of *Dlx* expression in the BA at E10.5. In the embryonic mouse, the six *Dlx* genes are differentially expressed in a regional, nested pattern in the ectomesenchyme along the proximodistal axis of the BA (though none is extensively expressed in the distal-most BA midline ectomesenchyme). *Dlx* genes are also variably expressed in the surface cephalic ectoderm (green arrowheads). Linked *Dlx* genes appear to share regulatory regions and are expressed in similar patterns within the developing BA mesenchyme: hence, first-order paralogous *Dlx* genes share nested expression patterns within the mesenchyme of the BAs: *Dlx1* and 2 are expressed throughout most of the proximodistal axis of the BA, while *Dlx5* and 6 and *Dlx3* and 4 share progressively restricted domains distally.

order paralogous *Dlx* genes share nested expression patterns within the mesenchyme of the BAs: *Dlx1* and 2 are expressed throughout most of the proximodistal axis of the BA, whereas *Dlx5* and 6 and *Dlx3* and 4 share progressively restricted domains distally (Fig. 3B).

The combinatorial *Dlx* code hypothesis: predictions and examination of morphological change

The correlation of this proximodistally nested pattern of ectomesenchymal expression within the BA with the proximodistal skeletal series derived from the BA of gnathostomes suggested that a combinatorial *Dlx* code may contribute to the establishment (pattern and development) of the distinct skeletal elements within a particular BA unit. Such a code might operate in a quantitative mode, a qualitative mode, or both: a quantitative mode would depend on the concentration of all *Dlx* proteins in a given nucleus, whereas a qualitative mode would depend on the concentration of specific *Dlx* proteins in a given nucleus. Thus, if the quantitative mode were the principal mechanism through which the *Dlx* proteins operate, any change of *Dlx* concentration (below or above a critical threshold) would alter the fate of that cell. By contrast, if the qualitative mechanism predominates, then distinct phenotypes would appear depending upon which *Dlx* proteins are expressed and where. One would predict, then, that either the loss of *Dlx* expression levels or the gain in either exogenous or endogenous domains within the BA primordia would result in the morphological alteration of those elements derived from tissues where the genes were contributing to the code. Thus, the code and the subsequent morphology might be defined by the number and type of functional *Dlx* alleles that are expressed in any particular portion of a BA. To test these hypothetical mechanisms, we have utilized an allelic subtraction strategy to study systematically the phenotype of mice that have reductions in specific combinations of *Dlx* genes.

Prior to presenting our morphological analyses of the single and compound *Dlx* mutants, it is important to address a number of methodological issues. For instance: What constitutes a change of morphology? How is it recognized? What are the components of morphology that are capable of alteration? Is a change in every element, or every portion thereof, necessitated by the precepts of a combinatorial code? Is it necessary that each member of the *Dlx* gene family

contribute equally to the code in every region in which it is expressed or with equal potency throughout its expression domain? Can there be a temporal component to the code or the change? How are ectopic structures, with or without necessarily changing endogenous structures, to be interpreted?

For most of these questions there are no established *a priori* answers, and in the studies described herein they have been operationally defined and limited. Here, we consider a transformation of an element to have occurred if an apparent alteration (generally, loss or gain) of any of the following is observed: (1) absolute size; (2) relative size; (3) presence and topology of structural components; (4) substructural cellular composition, including change of cellular differentiation, ectopias, and/or teratisms (anomalies of organic form and structure); or (5) relative topography, in particular in relation to an element's articulations (relationships) with other elements. Such alterations are recognized relative to wild-type control elements (the essential morphology of which we have previously ascertained and delineated, e.g. Qiu et al. 1995; Depew et al. 1999, 2002a,b). Moreover, a change in morphology of the structures of a BA will further be considered to have occurred if structurally independent ectopias and/or teratisms develop. We have detected alterations using one of two assays: (1) histological sectioning where the skeletal structures of late embryonic and neonatal crania are differentially stained, and (2) whole mount skeletal preparations of late embryonic and neonatal crania differentially stained for bone (and enamel) and cartilage by Alizarin red S and Alcian blue, respectively (McLeod, 1980). In summary, the principal components of endogenous morphology susceptible to change are size, shape, structural and cellular composition, and relation to other elements, and each structural component of an element need not be altered for the element to be considered morphologically transformed.

Initial genetic tests of the code

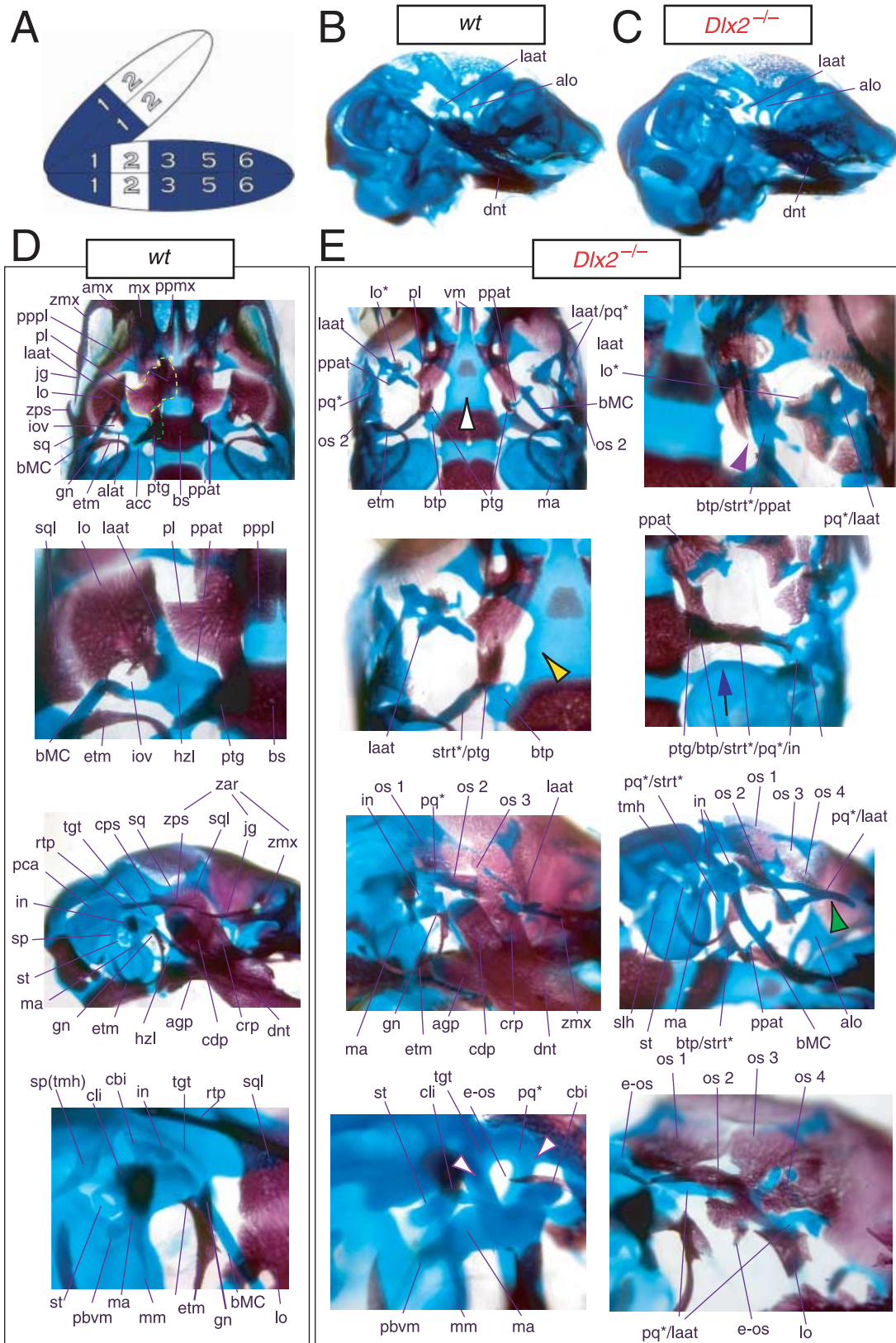
To best describe the allelic series of *Dlx* mutations that is the framework of this manuscript, it is expedient briefly to recount here some work already well embedded in the literature. Furthermore, owing to the nature of this review, the descriptions of the phenotypes cannot be exhaustive; we have attempted therefore to describe the most relevant and pertinent features of the mutants.

Dlx2^{-/-} murine mutants

The hypothesis of a combinatorial *Dlx* code and its predictions was initially examined genetically by use of a gene targeting strategy to generate a null allele of the murine *Dlx2* gene, which is expressed throughout most of the PD axis of the BAs (Qiu et al. 1995, 1997). *Dlx2*^{-/-} and *Dlx2*^{+/-} mice thus provided a seminal loss-of-function (decreased level) test of the code hypothesis.

Mice homozygous for the *Dlx2* mutant allele die as neonates with each of the mxBA1-derived elements being affected by the loss of both functional alleles of *Dlx2* (Qiu et al. 1995). The lateral aspects of the basisphenoid (though not the rostrocaudal) were transformed, principally by the deletion of most of the alisphenoid (Fig. 4). Although it was stated that the cartilaginous component of the ala temporalis was lost in postnatal day (P)0 animals, this was refined by stating that the ventromedial alisphenoid (in principal, the ala temporalis) was absent while its lateral wing (the lamina ascendens plus lamina obturans) is malformed; in place of the alisphenoid is a more lateral cartilage, given the appellation 'AT*' (for 'ala temporalis*') by Qiu et al. and an associated dermal bone. The lateral basisphenoids were further modified because the alicochlear commissure was lacking in approximately 50% of the mutants (blue and black arrow, Fig. 4E). The

Fig. 4 Skeletal analysis of *Dlx2*^{-/-} mutants through differential staining of bone (alizarin red) and cartilage (alcian blue). (A) Reference schema indicating the loss of two *Dlx2* alleles in BA1. (B) Wild-type E16.5 skull seen in oblique lateral view. (C) E16.5 skull of a *Dlx2*^{-/-} mutant littermate showing a normal dentary (dnt) and the isolated tip of the lamina ascendens of the ala temporalis (laat). (D) Wild-type P0 skull highlighting, top to bottom, the palatal region (norma basalis; yellow line outlining the palatine and green line outlining the pterygoid), the ala temporalis and lamina obturans components of the alisphenoid, the ear region with the primary and secondary jaw articulations, and the middle ear. (E) P0 *Dlx2*^{-/-} mutant skulls demonstrating alterations of mxBA1-derived structures. Purple arrowhead indicates an example exhibiting the loss of pterygoid bones. The green and black arrowhead points to the ectopic cartilage (pq*) running anterior from the region of the tegmen tympani and incorporating the lamina ascendens of the ala temporalis (laat). The purple and white arrowheads indicate the disassociation of the crus longus and crus brevis of the incus (cli and cbi), and the association of the crus longus with the tegman tympani (tgt), ectopic 'strut', and ectopic palatoquadrate ('pq*') cartilage. The blue and black arrow indicates the loss of the alicochlear commissure, while the yellow and black arrowhead indicates the ectopic lateral projection from the trabecular basal plate rostral to the basisphenoid body. See text for detailed descriptions and list for abbreviations.



incus, moreover, was malformed, missing the crus brevis and never articulated with the stapes – itself malformed. Approximately 50% of the incudi were continuous with an ectopic palatoquadrate cartilage (pq* in Figs 4E and 9B; see below). Within the second arch, the stapes lacked a central foramen and the styloid process lacked its connection to the crista parotica of the otic capsule (Fig. 4E).

Clefting of the secondary palate was found by Qiu et al. in 80% of the mutants, with the caudal aspects of the palatine and the medial parts of the maxilla reduced in size (black and white arrowhead, Fig. 4E). The pterygoids (ptg) were smaller and rostrally displaced, contacting two ectopic structures: the 'strut' and the 'palatoquadrate' ('PQ' of Qiu et al. 1995; discussed below). The maxilla, squamosal and jugal each had abnormalities in morphology as the zygomatic arch was highly altered. The squamosal and jugal were 'replaced' by four bones, given the names 'bones 1, 2, 3 and 4', that then variably contributed to the new arch (bone 1 being the most caudodorsal, 2 being caudoventral and often bearing a zygomatic process, 3 being rostradorsal, and 4 being rostroventral and also often bearing a zygomatic process) (os 1–4, Fig. 4E).

With regard to the observed mxBA1-derived ectopic cartilages, each homozygous mutant had an ectopic cartilage interpreted as an atavistic palatoquadrate and an osseous 'strut' extending laterad from the basitrabecular process of the basisphenoid (pq*, strt*, Fig. 4E). (The appellation 'PQ' was chosen by Qiu et al. to reflect the historical size and connectivity of the non-mammalian palatoquadrate; see Figs 2A and 21A–C) Roughly 80% of the mutants had at least one ossified strut. When not ossified, the region of the strut contained fibrous tissues, and it was unclear whether this strut was of splanchnocranial or neurocranial origin. The strut often contacted (fused with) the ectopic PQ* structure. The PQ*, a phenotypically provocative structure, had variable shapes (and was variably continuous as a structure) but had consistent location and topographic relationships to other skeletal elements. These relationships included a rostral process that extended toward the maxilla, a ventromedial process toward the palatine and pterygoid, a caudal ventromedial process often continuous with the strut, a dorsal process contacting the ectopic dermal bones of the sidewall and zygomatic arch, and, finally, an otic process fused to the otic capsule. No alterations of the skull roof, the hyoid, or the malleus, dentary, ectotympanic,

gonial and other distal BA-derived structures were observed. Moreover, no differences between heterozygous and wild-type mice were observed.

Qiu et al. (1995) reached three principal conclusions regarding the *Dlx2*^{−/−} mutant: (1) as no changes were detected in some regions where *Dlx2* is expressed, genetic redundancy was suggested; (2) as there were severe defects in some places it was suggested that each *Dlx* gene had unique functions; and (3) that the ectopias of bone and cartilage generated a skull reminiscent of the basic synapsid skull design found in pre-mammalian terrestrial ancestors.

Although apparently consistent with the hypothesis of a *Dlx* code with regard to abnormal proximal development of the BA in the homozygous mutant, the results did raise the issue of why no phenotypes were observed (1) in heterozygotes or (2) in the distal BA (e.g. mdBA1). Thus, three principal questions arose. First, was the apparent absence of phenotypic change in distal BA-derived structures in the *Dlx2*^{−/−} mutant mice – despite distal expression – due to genetic compensation by other *Dlx* genes, in particular *Dlx1*? Second, was it the case that *Dlx2* actually did not exert a biological, regulatory function in these distal domains? Third, was some aspect of the phenotype missed in the analysis?

Evidence for a genetic interaction of the first-order paralogues, *Dlx1* and *Dlx2*, without evidence of distal BA alterations

To address the notion that another *Dlx* gene was acting genetically to compensate for the loss of *Dlx2*, both a null mutation of *Dlx1* and a compound null allele of *Dlx1/2* were generated by homologous recombination (Qiu et al. 1997). Unlike the *Dlx2*^{−/−} mutants, mice homozygous for the *Dlx1* mutant allele were found to generally be viable at birth (they were small, however, and usually died within a month). No differences between heterozygous mutant and wild-type mice were described. Qiu et al. (1997) reported that elements lateral to the basisphenoid were abnormal, and that the proximal part of the ala temporalis (that portion attached to the basisphenoid) was largely absent whereas the distal component was present (see Fig. 5). They further reported that approximately 50% of the stapes of the *Dlx1*^{−/−} mutants were smaller and lacked stapedia foramina, and that, in the same percentage, the styloid processes lacked a connection to the crista parotica (Fig. 5E). Furthermore, 10% had a small cleft

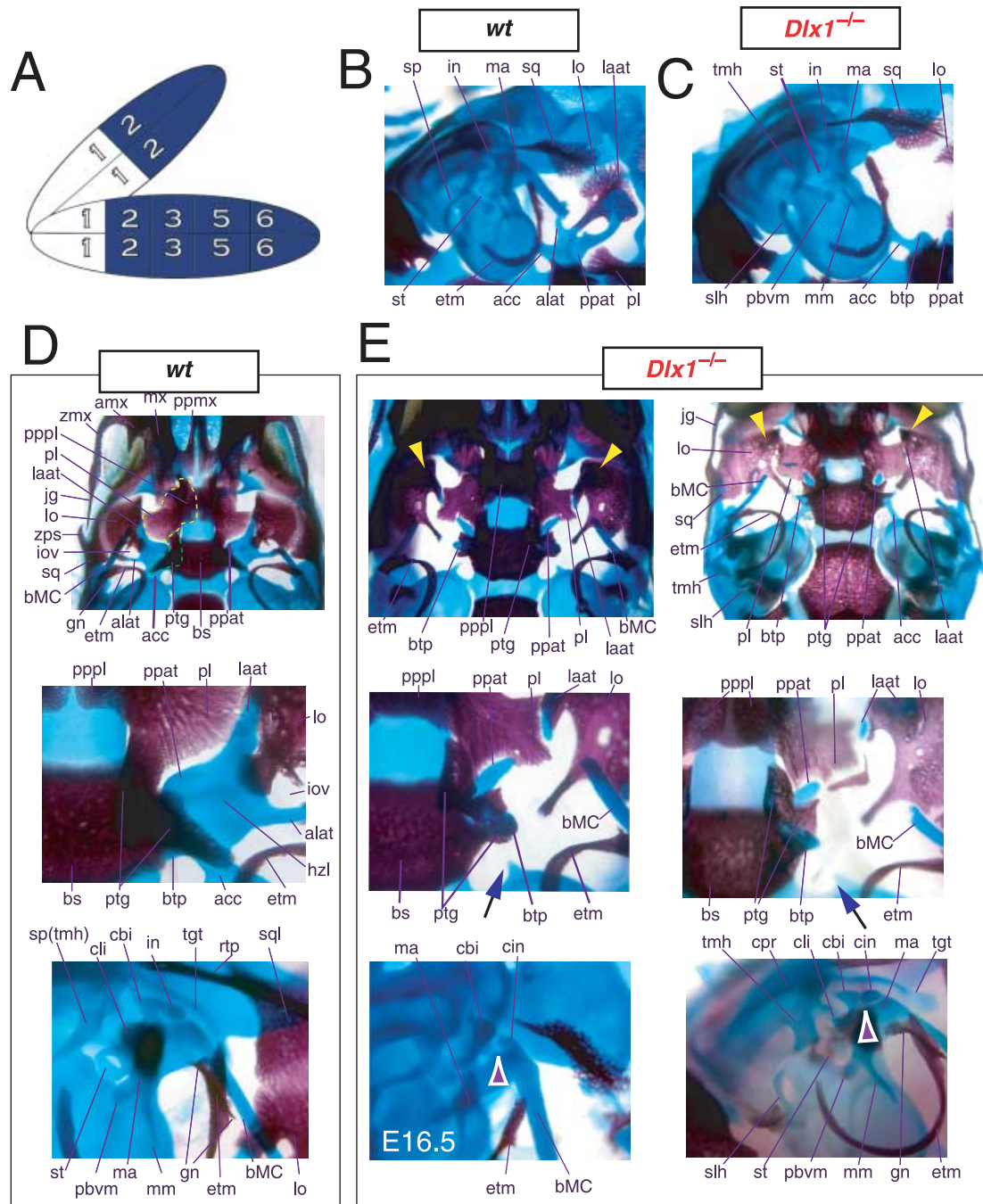


Fig. 5 Skeletal analysis of *Dlx1*^{-/-} mutants through differential staining of bone (alizarin red) and cartilage (alcian blue). (A) Reference schema indicating the loss of two *Dlx1* alleles in BA1. (B) Middle ear and ala temporalis (lo, laa, alat and ppat) region of a wild-type E16.5 skull seen in oblique lateral view. (C) E16.5 *Dlx1*^{-/-} mutant littermate showing the loss of ala temporalis structure. (D) Wild-type P0 skulls highlighting, top to bottom, the palatal region (norma basalis; yellow line outlining the palatine and green line outlining the pterygoid), the ala temporalis and lamina obturans components of the alisphenoid, and the middle ear. (E) P0 (except as noted) *Dlx1*^{-/-} mutant skulls evincing alterations of mxBAl-derived structures. The yellow arrowheads highlight the inability of the lamina obturans to invest the tip of the lamina ascendens of the ala temporalis (laa). The white and purple arrowheads indicate the disassociation of the crus longus and crus brevis of the incus (cli and cbi), while the black and green arrowheads indicate the absence of alicochlear commissures. See text for detailed descriptions and list for abbreviations.

palate, although there was no clear change in the size of the palatines, maxillae or pterygoids. They indicated, however, that the pterygoids were shifted rostrad, causing a slight displacement of the caudal portions of the palatines. Unlike with the *Dlx2*^{-/-} mutants, no ectopic cartilage or dermal bone was observed, and the greater wing of the sphenoid (the alisphenoid: lamina obturans plus ascending lamina), the squamosal and the jugal appeared normal. No mdBA1 or other distal BA defects were noted. Qui et al. concluded: (1) only subsets of elements derived from the proximal portions of the first and second BA were altered; (2) with regard to the lack of a proximal ala temporalis, *Dlx1*^{-/-} mutants were nearly identical to the phenotype seen in the *Dlx2*^{-/-} mutants; and (3) *Dlx1* is involved only in chondrogenic splanchnocranial development and not in dermatocranial development.

Mice homozygous for the compound *Dlx1/2* allele were found to die at birth (Qiu et al. 1997). Although generally similar to the *Dlx2*^{-/-} mutants, it was reported that these compound mutant mice exhibited greater alterations of proximally derived BA skeletal elements, in particular in the palatines, maxillae, lower molars and in the robustness of the ectopic PQ* structures (see Fig. 6). As with the *Dlx2*^{-/-} mutants, the compound *Dlx1/2*^{-/-} mutants were observed to have zygomatic arches that were altered in one of three ways: (1) an inferior temporal arch, composed of bone 2 and the maxillae, formed while bones 3 and 4 formed a postorbital bar that was not connected to the maxilla; (2) no inferior arch developed, while instead a postorbital bar was formed by bones 3 and 4, which articulated with the maxilla, and the rostral, zygomatic process of bone 2 remained unattached; or (3) neither inferior nor postorbital bars formed (Fig. 6E, os 1–4). Unlike in the *Dlx2*^{-/-} mutants, clefting of the secondary palate was reported to be a completely penetrant phenotype (black and white arrowhead, Fig. 6E). The ectopic PQ* was found to be far more robust, generally a continuous structure throughout and the strut contacted the

tegmen tympani of the otic capsule (pq*, laa, Fig. 6E). Perhaps the most significant difference relative to the *Dlx2*^{-/-} single mutants was the loss of all maxillary molars that accompanied the expansion of the PQ* structure.

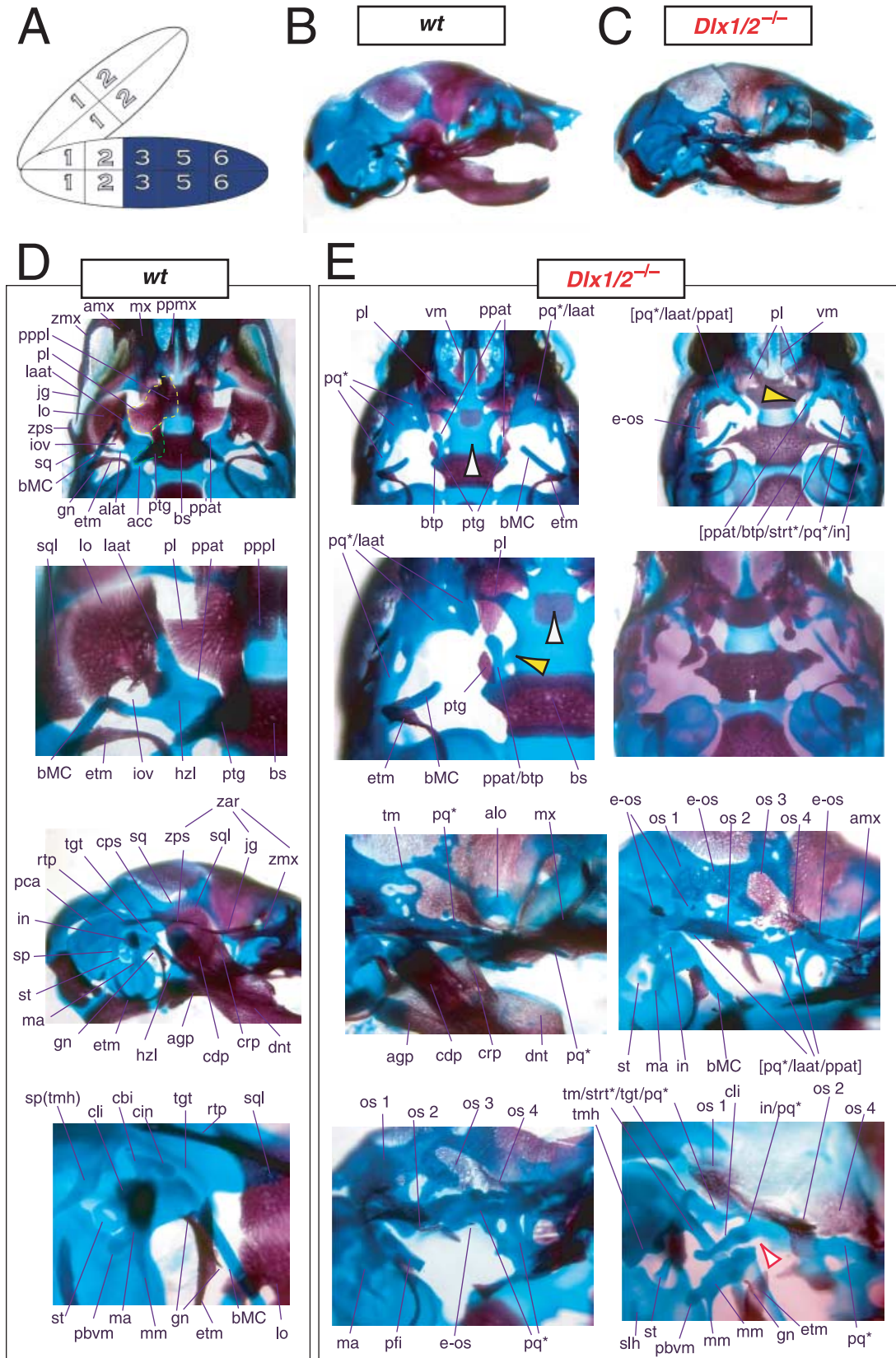
Exacerbation of the phenotype in the compound mutants relative to either single knockout led Qiu et al. (1997) to conclude that a genetic interaction existed between *Dlx1* and *Dlx2* with regard to proximal BA development. No defects were reported for the compound *Dlx1/2*^{+/-} heterozygotes (i.e. *Dlx1*^{+/-}; *Dlx2*^{+/-}), nor were any seen in distally derived elements of BA1 or BA2.

Again, although the genetic interaction evinced was at least consistent with the basic hypothesis of a combinatorial *Dlx* code with regard to the proximal development of the BA, the results of these studies of the genetic interactions of *Dlx1* and *Dlx2* were not clearly constant with regard to the single and compound heterozygous animals or to distal BA development. In essence, the analysis of the loss-of-function of the *Dlx1–Dlx2* second-order paralogues left many questions unanswered: Was the apparent absence of phenotypic change in distal BA-derived structures in the *Dlx1*^{-/-}, *Dlx2*^{-/-} and *Dlx1/2*^{-/-} mutant mice, despite distal expression of *Dlx1* and *Dlx2*, due to genetic compensation by other, distally restricted, *Dlx* genes? Could a distal, nested gene compensate for *Dlx2* in distal domains if *Dlx1* could not? If so, were the compensatory genes second-order genes and/or third-order paralogues? Did any *Dlx* genes regulate the development of the distal BAs, and if so, which and in what way? Did the linked-pair genes *Dlx1* and *Dlx2* actually not exert biological, regulatory functions in these distal domains despite their expression in these domains? Or, was some aspect of the phenotype missed in the published analyses?

Demonstration of *Dlx* regulation of distal BA structure: *Dlx5*^{-/-}

The question of whether any *Dlx* gene played a regulatory role in the development of the distal BA-derived

Fig. 6 Skeletal analysis of compound *Dlx1/2*^{-/-} mutants through differential staining of bone (alizarin red) and cartilage (alcian blue). (A) Reference schema indicating the loss of four *Dlx* alleles, two *Dlx1* and two *Dlx2*, in BA1. (B) Norma lateralis view of a P0 wild-type skull. (C) Norma lateralis view of a P0 *Dlx1/2*^{-/-} mutant skull. (D) Wild-type P0 skulls highlighting, top to bottom, the palatal region (norma basalis; yellow line outlining the palatine and green line outlining the pterygoid), the ala temporalis and lamina obturans components of the alisphenoid, norma lateralis view of the ear region with the primary and secondary jaw articulations and the middle ear. (E) P0 *Dlx1/2*^{-/-} mutant skulls exhibiting alterations of mxBA1-derived structures. The yellow and black arrowheads point to cylindrical cartilages (ppat) running rostrad, parallel to the neurocranial base, toward the medial margins of the PQ*/lamina ascendens (pq*/laa) that have fused to the basitrabecular processes. Black and white arrowheads indicate the clefting of the palate. The red and white arrowhead highlights the loss of the crus brevis of the incus, and the fusion of the remainder of the incus to the ectopic strut (strt*) and palatoquadrate (pq*) structures. See text for detailed descriptions and list for abbreviations.



skeletal morphology was addressed by generating null alleles of *Dlx5*, a nested *Dlx* gene (Depew et al. 1999). *Dlx5* is expressed both in the olfactory and otic placodes, and their derived epithelia, as well as in the ectomesenchyme of the BA (Simeone et al. 1994; Qiu et al. 1997; Yang et al. 1998; Depew et al. 1999; Fig. 3B); and targeted disruption of *Dlx5* leads to craniofacial defects (Fig. 7; Acampora et al. 1999; Depew et al. 1999). *Dlx5*^{-/-} mutants die shortly after birth, approximately one-quarter being exencephalic. Non-exencephalic mutant mice have hypomineralized parietals and interparietals (Fig. 7C), and all mutants have regional defects in their nasal (black and green arrowhead) and otic (black and red arrowhead) capsules (Fig. 7D).

Importantly, *Dlx5*^{-/-} mutants all show dysmorphology in structures derived from the proximal end of their mandibular arch (Fig. 7D,E,G). Meckel's cartilage is shortened and its path back toward the middle ear is disrupted (black and yellow arrowheads, Fig. 7E,G). At a point near the proximocaudal end of the dentary, MC sharply deviates laterad only abruptly to reorientate caudomedially again for a short distance whereupon it splits into two branches. At this split, a medial branch forms (bMC1) a strut toward the pterygoid, basisphenoid and ala temporalis while a lateral branch runs (at the level of the processus folii) to the malleus. By P0, this deviated cartilage is invested by ectopic intramembranous bone, given the appellation 'os paradoxicum', that may also invest, or form a synovial joint with, the pterygoids (ospdx, Fig. 7D,E,G). This ectopic bone also forms a synovial joint with the misshapen gonial, and sutures with the anterior crus of the tympanic. The malleus has a smaller than normal head and is caudally extended and thickened at the level of the manubrium (Fig. 7G). The tympanic is likewise altered, being slightly smaller and thicker. A short and dysmorphic dentary (at the proximal end) develops around the abnormal Meckel's cartilage (Fig. 7D,E,G). The proximal lamina of the coronoid is absent, and the condylar and angular processes are shortened, misshapen and juxtaposed (Fig. 7D,G).

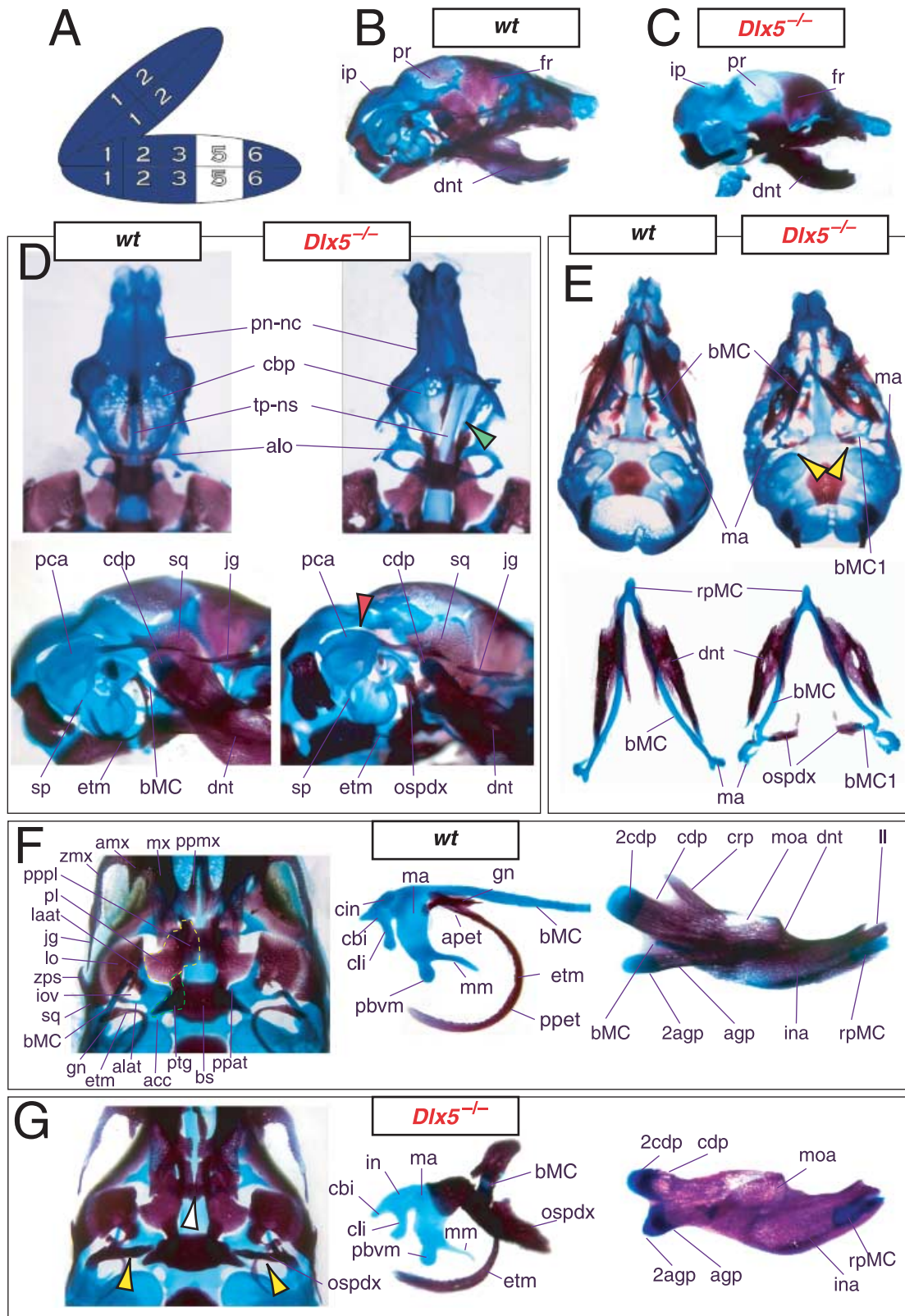
Hence, the result of the loss-of-function of the distally expressed *Dlx5* was an alteration of distal BA (i.e. mdBA1) structures, and was seen to be consistent with a *Dlx* code. Moreover, regardless of whether a distally restricted *Dlx* gene might be capable of genetically compensating for the loss of *Dlx1* and *Dlx2* in distal BA development, apparently neither *Dlx1* nor *Dlx2* were reciprocally capable of a similar genetic compensation for a loss of the nested gene *Dlx5*. As with the initial reports of the *Dlx1*, *Dlx2* and *Dlx1/2* heterozygotes, no change of morphology was seen with the loss of a single *Dlx5* allele.

Testing the notion of a homeotic transformation as a prediction of the nested *Dlx* code hypothesis

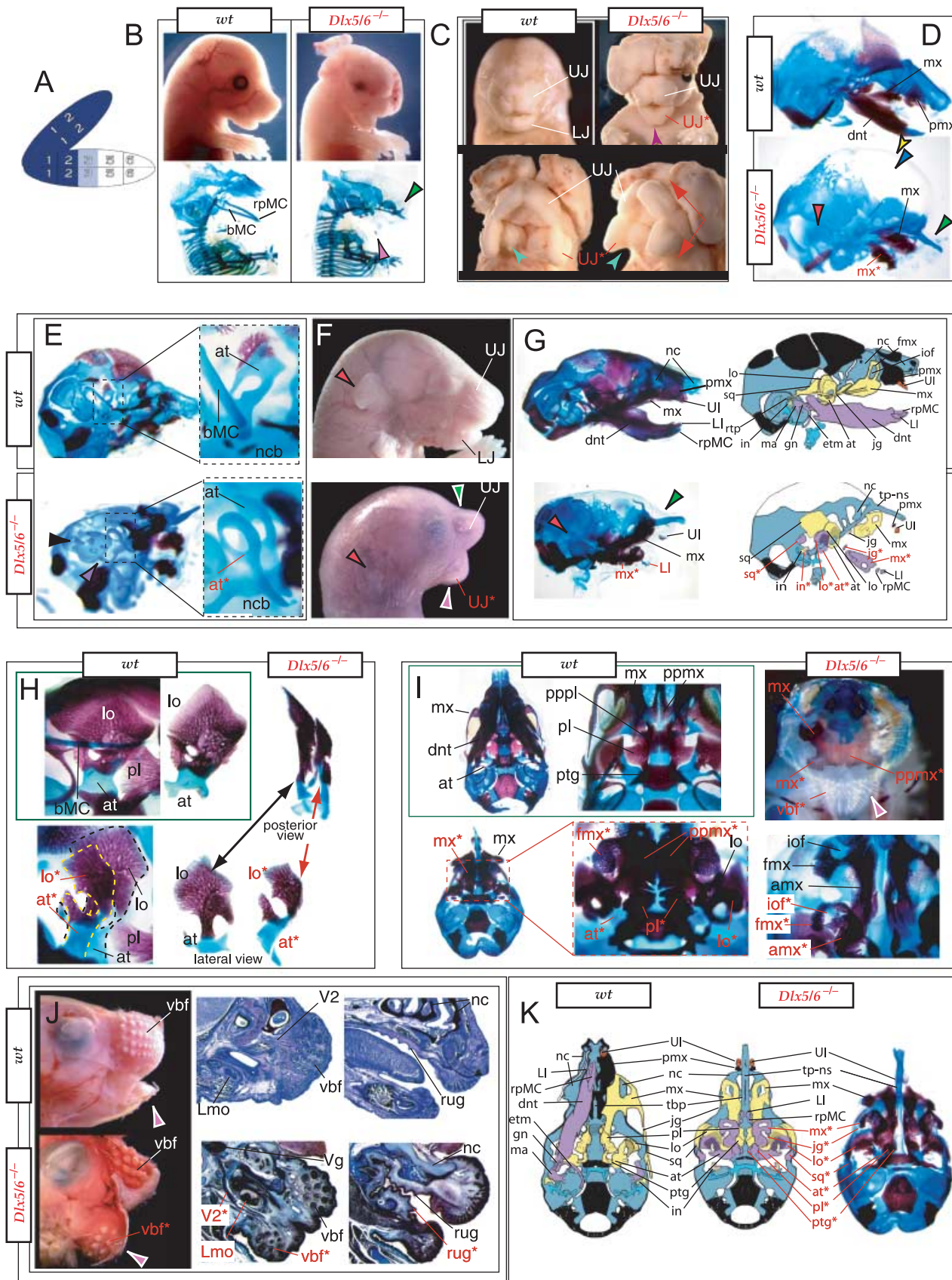
Reflection on the nature of a combinatorial code model led to the conclusion that perhaps a more perspicacious test of the hypothesis would involve the loss-of-function of a distally restricted linked-pair such as *Dlx5/6*. An inherent characteristic of the hypothesized combinatorial code is its regionalization of combination. *Dlx* expression patterns reveal that there are grossly three levels of ectomesenchymal expression nesting: one characterized by the combination of *Dlx1/2*, another by *Dlx1/2/5/6* and a third by *Dlx1/2/5/6/3/4* (Fig. 3B). It might be predicted, then, that regionally replicating the code would result in a regional replication of morphology. Thus, for instance, the loss of the linked gene pair *Dlx5/6* would be predicted to result in the replication of structures coded for solely by *Dlx1/2*.

Such a test of the model was engendered by the generation of a compound null allele of *Dlx5/6* (Beverdam et al. 2002; Depew et al. 2002a; Merlo et al. 2002; Robledo et al. 2002). *Dlx5/6*^{-/-} neonates die just after birth and usually exhibit exencephaly and failure of the distomedial tissues of BA1 to become fully opposed and integrated across the midline (Fig. 8). Whereas skeletal preparations revealed the presence of proximal BA1 skeletal elements, distal BA elements were missing – having instead been replaced by a second set of 'proximal'

Fig. 7 Skeletal analysis of the loss-of-function of the nested gene, *Dlx5*, through differential staining of bone (alizarin red) and cartilage (alcian blue). (A) Reference schema indicating the loss of two *Dlx5* alleles in BA1. (B) Norma lateralis view of a P0 wild-type skull. (C) Norma lateralis view of a P0 *Dlx5*^{-/-} mutant skull. (D) Sensory capsular defects in *Dlx5*^{-/-} mutants. P0 wild-type skulls are on the left and *Dlx5*^{-/-} mutant on the right. Black and green arrowhead indicates the asymmetry that accompanies the greater hypotrophy of the right side nasal capsule and cribriform plate observed in 90% of the *Dlx5*^{-/-} mutants. The black and red arrowhead highlights the loss of semicircular canals in the pars canicularis of the otic capsule. (E) E15.5 wild-type (left) and *Dlx5*^{-/-} mutant (right) skulls showing the deviations of body of Meckel's cartilage (bMC1) and ectopic bone that contributes to the os paradoxicum (ospdx; black and yellow arrowhead). (F) Wild-type P0 skeletal anatomy highlighting the palate, middle ear and



dentary. (G) *Dlx5^{-/-}* mutant palatal, middle ear and dentary bones demonstrating the regulation by *Dlx* of the mdBA1 derivatives. Black and white arrowhead indicates the small, variable clefts of the palate found with some mutants. Black and yellow arrowhead indicates the deviations of body of Meckel's cartilage and ectopic bone that contributes to the os paradoxicum (ospdx). Modified from Depew et al. (1999). See text for detailed descriptions and list for abbreviations.



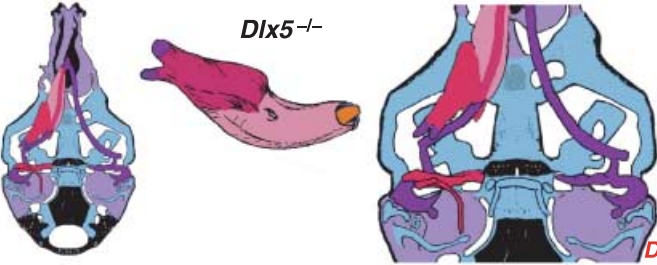
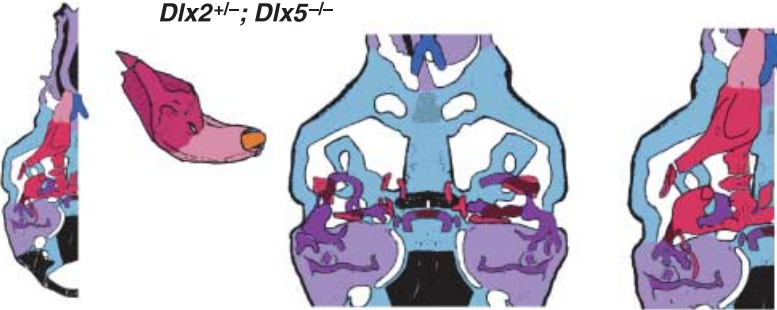
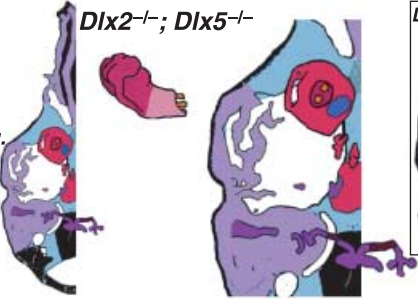

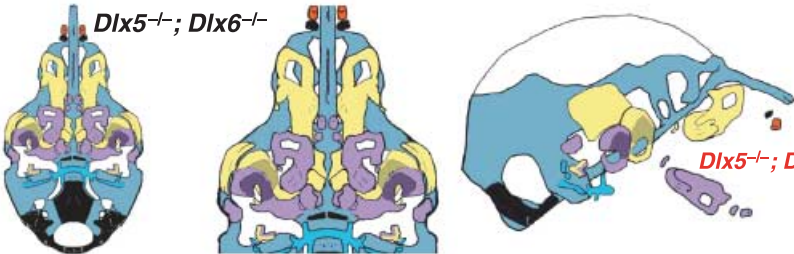
elements. Although affected by aberrant olfactory placodal development and loss of nasal capsular and premaxillary structure (see below), the mxBA1-derived maxilla, palatine, pterygoid, squamosal and, usually, diminutive jugal bones were apparent (Fig. 8D,E,G–I,J). A clearly identifiable ala temporalis and associated lamina obturans were also present in each hemisphere. The body of Meckel's cartilage (bMC), however, was transformed into a second ala temporalis (at*), attached to the neurocranial base (tbp) adjacent to the endogenous mxBA1-derived ala temporalis (Fig. 8E,H). This was accompanied by an ectopic dermal lamina obturans (lo*, Fig. 8H,I).

In addition, mutant mdBA1-derived dematocranial derivatives that developed in the lower jaws appeared to be nearly identical in shape and size to the mxBA1-derived maxillae. These ectopic maxillae (mx*) had frontal processes with infraorbital foramina (iof*), molar alveolae (amx*) and palatal shelves (ppmx*); in mutants without fully cleft mandibles, these extensively abutted, palate-like, at the midline (Fig. 8I).

Ectopic laminar intramembranous bones developed, juxtaposed to the ectopic lamina obturans, which appeared to be duplicated squamosal laminae. Instead of ectotympanic and gonial bones forming, a second set of palatine (pl*) and pterygoid (ptg*) bones developed in conjunction with the ectopic maxillae. The malleus, normally forming the proximal end of MC, appeared to have been transformed into an indistinct cartilaginous structure often fused to a dysmorphic incus; it is plausible that this is an ectopic incal structure. In some cases, the ectopic, lower-jaw maxillae were juxtaposed to free-standing incisors (LI, Fig. 8G), which usually existed without alveolar bone-of-attachment (Fig. 8G). These incisors were not in close association with each other, and were occasionally accompanied by a cartilaginous nodule taken as the remnant of the midline rostral process of MC (e.g. black and purple arrowhead, Fig. 8B). Usually, however, lower incisors failed to form at all (e.g. Fig. 8I). Thus, within the first BA two sets of proximal BA1 skeletal elements developed (shown schematically in Fig. 8G,K and Table 1).

Fig. 8 Homeotic transformation of mdBA1 derivatives into mxBA1-like derivatives due to the loss-of-function of the first-order paralogues, *Dlx5* and *Dlx6*. (A) Reference schema indicating the loss of both alleles of *Dlx5* and *Dlx6* in BA1. *Dlx3* is depicted in light blue as, although the alleles are present, its expression is abrogated in mdBA1. (B) Gross morphology (top) of E14.5 wild-type and exencephalic *Dlx5/6*^{-/-} mutant embryos with lateral views after alcian blue staining (bottom) of the same E14.5 littermates. Note, with the exception of the rostral process (black and purple arrowhead), the absence of Meckel's cartilage (MC) within the mandibular arch tissue and severe reduction of nasal capsules (black and green arrowhead) in the *Dlx5/6*^{-/-} mutants. (C) Morphological transformation of mandibular structure in *Dlx5/6*^{-/-} mutants at E16. Gross anatomy of wild-type (boxed) and exencephalic *Dlx5/6*^{-/-} mutants. In both fused (purple arrowhead, top) and cleft (green arrowhead, bottom) states, the mutant lower jaw (UJ*) is transformed, appearing as a mirror image (red arrows) of the upper jaw (UJ). (D) Norma lateralis views of E16 wild-type (top) and *Dlx5/6*^{-/-} mutant (non-exencephalic) littermates. Despite the loss of MC, dermal bone is seen in the mandibular arch where the dentary is transformed into a maxillae (mx*). The black and green arrowhead points to the remnant of the midline trabecular basal plate–nasal septum, highlighting the loss of the nasal capsules. The black and red arrowhead indicates otic capsular deficiencies. The black and blue arrowhead denotes the lack of ossification in the calvarium. (E) Skeletal staining of E16 wild-type (top) and *Dlx5/6*^{-/-} mutant (exencephalic) littermates, with expanded views, demonstrating the transformation of the body of MC into a second ala temporalis (at*) attached, with the maxillary-derived ala temporalis (at), to the trabecular basal plate (tbp). Note the truncated styloid (black arrowhead), the ectopic projection from the hyoid toward the styloid (black purple arrowhead), and an adjacent stapes. (F) Gross morphology of wild-type (top) and non-exencephalic *Dlx5/6*^{-/-} mutant neonates. Note the transformation of the lower jaw (white and purple arrowhead, UJ*), the loss of nasal capsule elaboration (white and green arrowhead) and the loss of the external ear pinnae (black and red arrowhead). (G) Norma lateralis views after differential bone and cartilage staining of the same littermates with explanatory schemae. The black and green arrowhead highlights the loss of nasal capsular development, while the black and red arrowhead indicates the hypoplasia of the otic capsule. In the schemae, mxBA1 elements are in yellow, mdBA1 in lavender, BA2 in turquoise, the neurocranium in steel blue, premaxillary-derived upper incisors (UI) in orange, and all other ossified elements in black. Transformed elements are labelled in red with an asterisk. (H) Wild-type (boxed) and *Dlx5/6*^{-/-} mutant endogenous and ectopic alisphenoids (ectopic outlined in yellow, endogenous in black) as seen both *in situ* and after dissection. (I) Staining revealing wild-type (boxed in green) and mutant palatal regions. Note the transformation of the dentary in cleft (bottom centre) and non-cleft (right, top and bottom) mandibular states. In the non-cleft state, the ectopic maxillary palatal shelves (ppmx*) and palatine (pl*) reach the midline. (J) Wild-type (top) and *Dlx5/6*^{-/-} mutant (bottom) neonates, minus superficial ectoderm (left) or sectioned (centre, right), reveal concomitant soft tissue transformations and the presence of ectopic vibrissae (compare white and purple arrowheads, vbf*) and rugae (rug*). (K) Norma basalis externa schemas of wild-type and *Dlx5/6*^{-/-} mutant skulls demonstrating the nature of the homeotic transformation in a P0 *Dlx5/6*^{-/-} neonate with a cleft-mandible (left, centre). A stained specimen (right) is included for reference. In the schemae, mxBA1 elements are in yellow, mdBA1 in lavender, BA2 in turquoise, the neurocranium in steel blue, premaxillary-derived upper incisors (UI) in orange, and all other ossified elements in black. Transformed elements are labelled in red with an asterisk. Modified from Depew et al. (2002a). See text for detailed descriptions and list for abbreviations.

TABLE I: Grades of Mandibular Alterations in Compound *Dlx* Mutants

Grade and Phenotype Description	Schemae	Genotypes with Ordered Severity
<div>Grade One</div> <ul style="list-style-type: none">deviated and/or split proximal end of the body of Meckel's cartilagedevelopment of an os paradoxicum, involving the gonial and ectopic ossificationsproximal dentary is represented by juxtaposed condylar and angular processes	<div><i>Dlx5</i>^{-/-}</div> 	<div><i>Dlx1</i>^{-/-}; <i>Dlx5</i>^{+/-} <i>Dlx2</i>^{+/-}; <i>Dlx5/6</i>^{+/-} <i>Dlx1</i>^{+/-}; <i>Dlx2</i>^{+/-}; <i>Dlx5</i>^{+/-}; <i>Dlx6</i>^{+/-} <i>Dlx5</i>^{-/-} <i>Dlx2</i>^{-/-}; <i>Dlx5</i>^{+/-} <i>Dlx1</i>^{-/-}; <i>Dlx2</i>^{-/-}; <i>Dlx5</i>^{+/-} <i>Dlx1</i>^{+/-}; <i>Dlx2</i>^{+/-}; <i>Dlx3</i>^{+/-}; <i>Dlx5</i>^{+/-}; <i>Dlx6</i>^{+/-}</div>
<div>Grade Two</div> <ul style="list-style-type: none">proximal dentary greatly reducedlack of angular and coronoid processesrudimentary condylar process generally with a free floating osseous tipelaborated os paradoxicumproximal body of Meckel's cartilage is bent about itself, reminiscent of an ala temporalisincus and malleus are fusedjaw associated regions of the squamosal, such as the retrotympenic process and the glenoid cavity, are dysmorphic	<div><i>Dlx2</i>^{+/-}; <i>Dlx5</i>^{-/-}</div> 	<div><i>Dlx3</i>^{+/-}; <i>Dlx5</i>^{-/-} <i>Dlx1</i>^{+/-}; <i>Dlx5</i>^{-/-} <i>Dlx2</i>^{+/-}; <i>Dlx5</i>^{-/-} <i>Dlx6</i>^{+/-}; <i>Dlx5</i>^{-/-} <i>Dlx1</i>^{-/-}; <i>Dlx5</i>^{-/-}</div>
<div>Grade Three</div> <ul style="list-style-type: none">catastrophic loss of primary and secondary jawsloss of body of Meckel's cartilage, proximal dentary, gonial, and ectotympanicdentary mainly consisting of distal mandibular structures: e.g. rostral process of Meckel's cartilage, incisors and alveolusa cartilaginous rudiment occupying topography of the incus and malleusdentary-maxillary articulationvibrissae ectopically develop in lower jawdefects of hinge associated upper jaw structures	<div><i>Dlx2</i>^{-/-}; <i>Dlx5</i>^{-/-}</div>  <div><i>Dlx1</i>^{-/-}; <i>Dlx2</i>^{-/-}; <i>Dlx5</i>^{-/-}</div> 	<div><i>Dlx2</i>^{+/-}; <i>Dlx5</i>^{-/-}; <i>Dlx6</i>^{+/-} <i>Dlx1</i>^{+/-}; <i>Dlx2</i>^{+/-}; <i>Dlx5</i>^{-/-}; <i>Dlx6</i>^{+/-} <i>Dlx2</i>^{-/-}; <i>Dlx5</i>^{-/-} <i>Dlx1</i>^{-/-}; <i>Dlx2</i>^{-/-}; <i>Dlx5</i>^{-/-}</div>
<div>Grade Four</div> <ul style="list-style-type: none">comprehensive homeotic transformation of the elements associated with the lower jaw into elements associated with the upper jawsoft tissues structures usually found associated with 'upper' jaws, such as rugae and vibrissae, ectopically develop in 'lower' jawloss of integration of the midlines, including both upper and lower incisor regions, with jaw hinge structures	<div><i>Dlx5</i>^{-/-}; <i>Dlx6</i>^{-/-}</div> 	<div><i>Dlx5</i>^{-/-}; <i>Dlx6</i>^{-/-}</div>

The proximalization of the skeletal structures in BA1 is mirrored by a duplicated set of soft tissue structures normally restricted to the maxillary-premaxillary region (Fig. 8J). For example, a second set of mystacial vibrissae (vbf*) developed out of the soft tissue of mdBA1, while a second set of palatal rugae (rug*) developed in conjunction with the ectopic palatal shelves in the mutant mdBA1-derived lower jaw.

Although more ambiguous in the nature of their transformation, the skeletal derivatives of BA2 and BA3 were also affected. The styloid process was truncated, and the hyoid extended an ectopic process toward it (black and purple arrowhead, Fig. 8E). The lesser horns often projected toward the neurocranial base. Cartilages, taken as stapes, were present (often lacking foramen), as were other associated ectopic cartilages.

As both *Dlx5* and *Dlx6* are expressed in the developing otic and olfactory placodes, it was not surprising that the sensory capsular defects seen in *Dlx5*^{-/-} single mutants were exacerbated with the additional loss of *Dlx6* (Fig. 8). The nasal capsules were severely hypoplastic and the trabecular basal plate was highly truncated (green and black arrowheads, Fig. 8B,D,E,G). The pars canalicularis and cochlearis were highly deficient (red and black arrowhead, Fig. 8B,D,E,G), as was the tegmen tympani that covers the middle ear. Furthermore, the nasal capsule-associated dermal bones, such as the nasals and premaxillae, failed to develop; free-standing incisors, however, were usually observed (Fig. 8G). Exencephalic and non-exencephalic mutants showed the same BA phenotypes.

The structural transformation of the mdBA1-derived lower jaw (and associated structures) into upper-jaw-like structures was found to be presaged by the loss of mdBA1 molecular identity and the acquisition of mxBA1 identity (Beverdam et al. 2002; Depew et al. 2002a). Although *Dlx1* and *Dlx2* expression in the BA ectomesenchyme were maintained, expression of *Dlx3* in the E10.5 mutant BA ectomesenchyme was effectively lost. Likewise, mutant BA expression of *dHAND* and *Alx4* was not observed. Although proximal mdBA1 ectodermal *Bmp7* expression was maintained, expression at the distal midline of mdBA1 was lacking; this was mirrored by the loss of *Dlx2* in the distal-most BA1 midline ectoderm. Mesenchymal *Pitx1* expression was also lost, though ectodermal expression slightly extended further ventrocaudad. Expression of *Msx1* and *Msx2* in mdBA1 was reduced, whereas that of *Prx1*

was slightly expanded. *Barx1* was expanded distad in mdBA1; BA2 and BA3 expression, however, was lost. Therefore, *Dlx5/6*^{-/-} mutants lacked expression domains of several genes implicated in mdBA1 development (such as *Alx4*, *dHAND*, *Dlx3*, *Dlx5/6*, *Bmp7* and *Pitx1*), while they maintained expression of genes also known to participate in mxBA1 development (e.g. *Dlx1*, *Dlx2*, *Msx1*, *Msx2* and *Prx1*). Moreover, examination of the expression of genes (*Wnt5a*, *Meis2* and *Prx2*) that are normally expressed proximodistally in a graded manner within BA1 (higher in proximal BA1 than in distal BA1) suggested that the expression at E10.5 of these genes was more intense and was expanded further lateral and caudal within the mutant mdBA1 relative to the wild type (Depew et al. 2002a). Moreover, the levels of these three genes in the mutant mdBA1 more closely resembled normal mxBA1 than mdBA1.

Thus, loss of the nested *Dlx5/6* linked-pair resulted, as predicted by the code hypothesis, in a homeotic transformation of the lower-jaw structures into upper-jaw structures. Moreover, this transformation occurred around a point set between the upper and lower jaws, and was accompanied by the loss of integration of midline structures with more proximal structures. The relative roles of *Dlx1* and *Dlx2* in the combinatorial code, however, remained obscured.

Reassessing the regulation of *Dlx1* and *Dlx2* in distal BA-derived structures

The analysis of the *Dlx5*^{-/-} and *Dlx5/6*^{-/-} mutant mice addressed one of the salient issues that arose as a result of the analysis of the *Dlx1*^{-/-}, *Dlx2*^{-/-} and *Dlx1/2*^{-/-} mutant mice: consistent with the code hypothesis, *Dlx* genes do regulate distal BA development. Although the related but distinct phenotypes of the *Dlx5*^{-/-} and *Dlx5/6*^{-/-} mutants demonstrated a genetic interaction between these two genes, there was as yet no evidence that either *Dlx1* or *Dlx2* was capable of genetic compensation for the loss of either nested gene. With regard to the relative roles of *Dlx1* and *Dlx2* in distal BA development, then, the same questions remained, including: Was the apparent absence of phenotypic change in distal BA-derived structures in the *Dlx1*^{-/-}, *Dlx2*^{-/-} and *Dlx1/2*^{-/-} mutant mice (despite distal expression of *Dlx1* and *Dlx2*) due to genetic compensation by other, distally restricted, *Dlx* genes? Could a distal, nested gene compensate for *Dlx2* in distal domains if *Dlx1* could not? If so, was the compensatory gene a second-order and/or

a third-order gene? Did the linked-pair genes *Dlx1* and *Dlx2* actually not exert biological, regulatory functions in these distal domains despite their expression there? Or, was it possible that some aspect of the *Dlx1*^{+/−}, *Dlx2*^{+/−} and *Dlx1/2*^{+/−} mutant phenotype was missed in the initial analysis? To address this last question, we re-examined the *Dlx1*^{+/−}, *Dlx2*^{+/−} and *Dlx1/2*^{+/−} mutant mice. In the following four sections, of necessity we reiterate some of the known phenotypes, but augment their descriptions in some significant ways with regard to the code and heterozygous states.

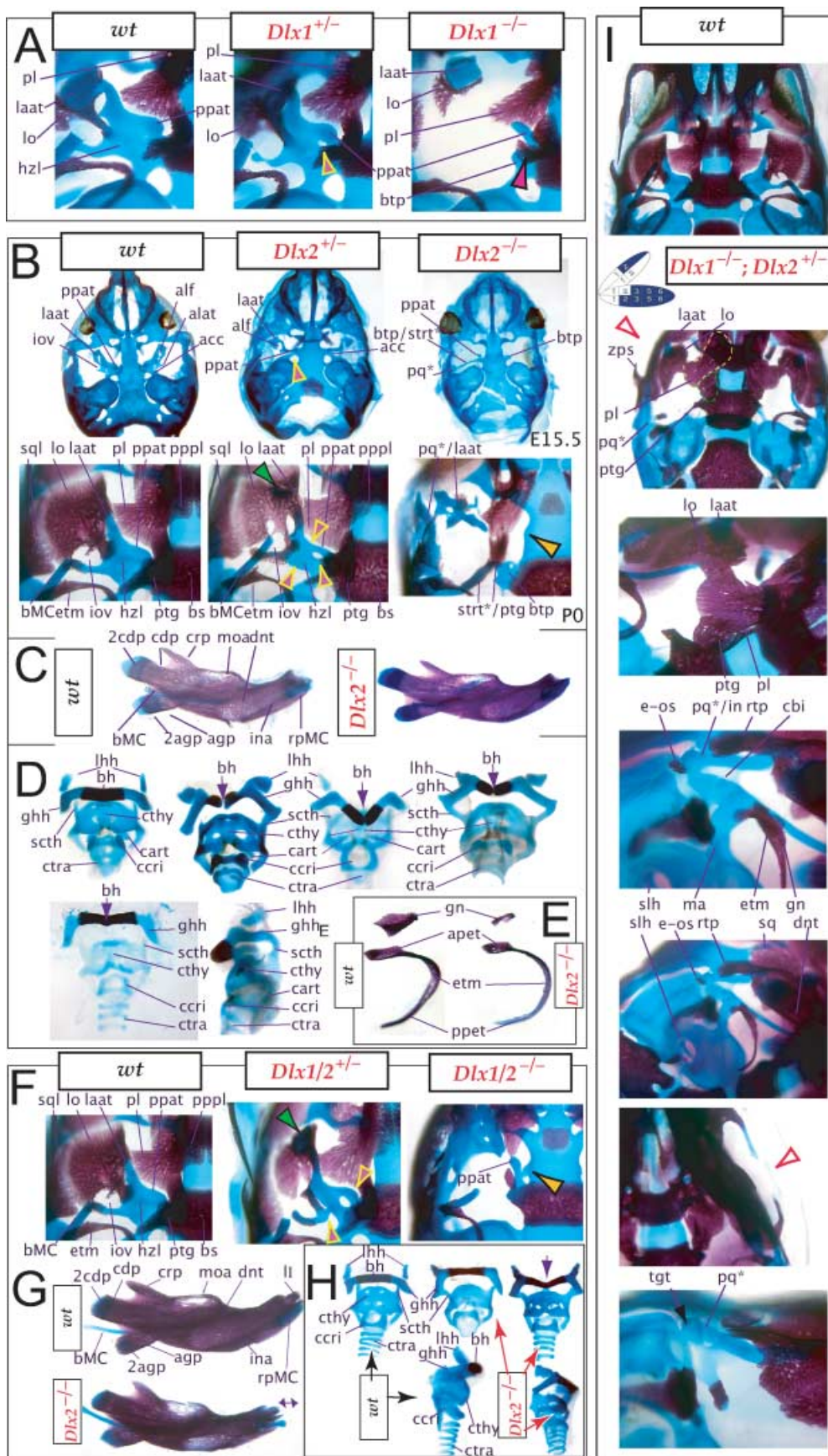
Augmenting the phenotypic descriptions of mice carrying *Dlx1* mutant alleles

The descriptions of Qiu et al. (1997) regarding the *Dlx1*^{+/−} mutants appear to be correct in general principle. Alterations of BA-derived skeletal tissues occur in the *Dlx1*^{+/−} mutants, although these appeared to be restricted to structures derived from regions where only *Dlx1* and *Dlx2* are expressed (Figs 5 and 9). Alterations in structures derived from the distal BA domains where nested *Dlx* genes are expressed (including MC, the dentary, ectotympanic, gonial, lesser horns and body of the hyoid, and portions of the thyroid and cricoid cartilages) were not noted on re-examination of *Dlx1*^{+/−} mutants from E15 to P8.

In accord with Qiu et al. we find that the tissues lateral to the basisphenoid are indeed altered and that the proximal ala temporalis is 'largely' absent in the *Dlx1*^{+/−} mutants (Figs 5E and 9). As is implied, the entire

proximal ala temporalis is not absent. Significantly, the cartilaginous pterygoid process of the ala temporalis remains distinct, running rostralaterad, but unattached (contrary to wild-types) to the neurocranial base (ppat, Fig. 9A). Qiu et al. are correct to note that the pterygoids are pushed rostrad, but they do not mention that the pterygoids are also smaller and that their palatine and basitrabecular laminae wrap around (medially and caudally) the remnant of the detached pterygoid process of the ala temporalis (see 'ptg' and 'ppat' of Figs 5E and 9). Moreover, the basitrabecular processes (btp) of the basisphenoid are present but are un-ossified (remaining cartilaginous) and only contact the alicochlear commissures (acc, which, contrary to the initial descriptions, are not universally present; green and black arrowheads, Fig. 5E) emanating from the otic capsules. The caudal palatines are altered in position and size, although this may not be secondary to the position of the pterygoids, as suggested by Qiu et al., but due to the same primary reorganization of structure affecting the pterygoids. In fact, the caudal palatine (pl) laminae are also pushed laterad and appear to separate the pterygoid processes of the ala temporalis from the dorsal tips of each lamina ascendens of the ala temporalis as the rest of the lamina ascendens fails to form (Fig. 5E). These dorsal tips appear to develop in a relatively normal position, and, as noted by Qiu et al., are accompanied by dermal bone (Fig. 9A). This dermal bone develops, as described by Qiu et al., into the dermal portion, or lamina obturans, of the alisphenoid. Contrary to Qiu et al., we have

Fig. 9 Re-evaluation of the morphological consequence of the loss-of-function of *Dlx1*, *Dlx2* and *Dlx1/2* in mice. (A) Skeletal analysis of wild-type, *Dlx1*^{+/−} and *Dlx1*^{−/−} mutants demonstrates that the loss of a single *Dlx1* allele affects the development of the ala temporalis (yellow and pink arrowhead pointing to an ectopic foramen). (B–E) Skeletal analysis of wild-type, *Dlx2*^{+/−} and *Dlx2*^{−/−} mutants. (B) E15.5 (top) and P0 (bottom) wild-type (left), *Dlx2*^{+/−} (centre) and *Dlx2*^{−/−} (right) mutants exhibiting transformations of the ala temporalis. Yellow and pink arrowheads point to the alterations of the horizontal lamina (hzi) of the ala temporalis evinced in the *Dlx2*^{+/−} heterozygotes. Black and yellow arrowhead points to the ectopic lateral projection from the trabecular basal plate between the presphenoid and the basisphenoid. (C) Wild-type and *Dlx2*^{+/−} mutant dentaries. (D) Hyoid and thyroid cartilages of wild-type and *Dlx2*^{+/−} mutant neonates. The cleft hyoid bodies (hb, purple arrows) and fusions of the greater horns (ghh) to the thyroid cartilages (cthy) of the mutants suggest that distal BA elements are altered with the loss of *Dlx2*. (E) Dissected gonial (gn) and ectotympanic (etm) bones of wild-type and *Dlx2*^{+/−} mutant neonates. (F–H) Skeletal analysis of wild-type, *Dlx1/2*^{+/−} and *Dlx1/2*^{−/−} mutants. (F) P0 wild-type, *Dlx1/2*^{+/−} and *Dlx1/2*^{−/−} mutants exhibiting transformations of the ala temporalis greater in scope than those seen in the comparable single mutants. Yellow and pink arrowheads point to the alterations of the horizontal lamina of the ala temporalis evinced in the *Dlx1/2*^{+/−} heterozygotes. Black and yellow arrowhead points to the ectopic projection from the trabecular basal plate, between the presphenoid and the basisphenoid, that connects to a cartilage taken as a transformed pterygoid process of the ala temporalis (ppat). Green arrowhead indicates the distal tip of the lamina ascendens of the *Dlx1/2*^{+/−} heterozygote that has not been properly invested by the lamina obturans. (G) P0 wild-type and *Dlx1/2*^{+/−} mutant dentaries. The double-headed arrow highlights the slight truncation in length seen in the mutant. (H) Wild-type (black arrows) and *Dlx1/2*^{+/−} mutant (red arrows) hyoid and thyroid cartilages. Note cleft of the hyoid body (bh, purple arrow). (I) Skeletal staining of *Dlx1*^{+/−}, *Dlx2*^{+/−} neonates that exhibit a distinct phenotype. Green and purple arrow points out the lack of a jugal. The black and purple arrow indicates the formation of an ectopic pq* cartilage fused to the tegmen tympani (tgt). The yellow line outlines the palatine, and the green line outlines the pterygoid. See text for detailed descriptions and list for abbreviations.



found that it does not develop normally. Usually by P0 (natal day), there is no discontinuity between the portion of the alisphenoid that arises from dermal investment around the dorsal tip of the lamina ascendens and the dermal bone lateral to this. In the *Dlx1*^{-/-} mutants, however, a discontinuity is apparent and the dorsal tip fails to be properly invested; instead, it remains as a cartilaginous remnant surrounded by dermal bone (yellow arrowheads, Fig. 5E). Thus, at this location, the normal programme of cellular differentiation and subsequent morphogenesis is altered.

Moreover, Qiu et al. failed to note that the caudal processus brevis and processus longus of the incus can form unattached to the remainder of the corpus of the incus (white and purple arrowheads, Fig. 5E), which is of note as this position is also greatly affected in the *Dlx2*^{-/-} and *Dlx1/2*^{-/-} mutants. Although the stapes often fails to form a stapedia foramen, we note that when one does develop it is usually asymmetrically placed.

A final point of discord with the analysis of Qiu et al. involves the *Dlx1*^{+/-} mice, which were reported as having no abnormalities. We find that the basal horizontal lamina of the ala temporalis of the heterozygous mice foreshadows the homozygous condition: the pterygoid process is elevated, although it maintains continuity with the lamina ascendens, and the anterolateral process of the ala temporalis develops more independently and less robustly (yellow and pink arrowheads, Fig. 9A). The end effect of this is the development of a foramen at the conjunction of these substructures along the horizontal lamina of the ala temporalis. This then suggests that each *Dlx1* allele contributes to the code.

Augmenting the phenotypic descriptions of mice carrying *Dlx2* mutant alleles

The descriptions of Qiu et al. (1995, 1997) regarding the *Dlx2*^{-/-} mutants appear to be, with some notable exceptions, correct in principle. As in the *Dlx1*^{-/-} mutants, the proximal ala temporalis is generally lacking (Figs 4E and 9B). Unlike the *Dlx1*^{-/-} mutants, however, which consistently have a detached pterygoid process, the *Dlx2*^{-/-} mutants may or may not have this remnant (which is not noted by Qiu et al.; see 'ppat' in Figs 4E and 9B). When present, a cartilaginous pterygoid process exists rather lateral and rostral to its usual position next to the basitrabecular process. Moreover, unlike the generally cylindrical, rod-like pterygoid

process of the *Dlx1*^{-/-} mutants, those found in the *Dlx2*^{-/-} may vary greatly in shape and size. Qiu et al. reported, moreover, that the pterygoid bones are small and rostrally placed. Indeed, residual dermal pterygoids may be found in association with the cartilaginous pterygoid processes; pterygoid bones, however, do not always form (e.g. purple arrowhead, Fig. 4E), and when they do they may consist of more than one ossification centre. As detailed by Qiu et al., they may also contact a number of ectopic structures (see below; Fig. 4E). Additionally, the aliochlear commissures are, as detailed, frequently lacking (blue and black arrow, Fig. 4E).

Clefting of the secondary palate is the norm, as reported, and the morphology and topology of the palatine and maxillary bones are affected; more than just the caudal end of the palatine bones is affected, however, as the entire bones are diminished in size, rostrally placed and lack palatal shelves (black and white arrowhead, Fig. 4E). As with their counterparts in the *Dlx1*^{-/-} mutants, the caudal aspects of the palatines may be found between the pterygoid process remnants and those of the dorsal tips of the lamina ascendens (see below). The portions of the maxillae that develop around the nasal capsules are in most respects normal (Fig. 4C). The caudal molar alveolus, however, is diminished and may contain ectopic dermal ossifications (not shown). Unnoted by Qiu et al., the alveolus also often develops in association with a number of cartilaginous ectopias, particularly one that develops ventral to the infraorbital foramen along the crista facialis (not shown).

Qiu et al. correctly point out that the cranial sidewalls of the *Dlx2*^{-/-} mutants are greatly modified. Normally, the sidewalls are dominated by the laminae of the squamosals (dorso-caudally) and the greater wings of the sphenoids (rostrally-medially) formed of the combined ala temporalis and lamina obturans (Fig. 4D). The lateral aspect of the skull is further normally dominated by the zygomatic arch, which underlies the orbit of the eye. The arch is composed caudally of the rostrally orientated zygomatic process of the squamosal, the jugal (which stands entirely free of the neurocranium) and the caudally orientated zygomatic process of the maxilla. Qiu et al. reported that the sidewall in the mutants is dominated by a number of dermal bones that they suggest replace the squamosal and the jugal. We concur that these bones are probably composed of cells which, if in a wild-type skull, would have been fated to contribute to the squamosal and jugal; there

are, however, generally more than four ossifications in this region (os 1–4, e-os; Fig. 4E). Moreover, perhaps the most striking detail of this region is the duplicate (rostral-caudal) nature of the major ossifications, especially as several bones may have rostrally orientated zygomatic projections without actually contributing to the orbital arch.

Similar to the *Dlx1*^{-/-} mutants, a cartilage (the AT* of Qiu et al.) is generally found in the region of the dorsal tip of the lamina ascendens of the ala temporalis. Unlike the *Dlx1*^{-/-} mutants, in which the morphology is otherwise strikingly similar to the wild-type, the cartilage here has various sizes, shapes and orientations, often existing both within the normal plane of the side wall and outside of it underlying the caudal orbit ('pq*/laat' of Figs 4E and 9B). As reported by Qiu et al., this cartilaginous structure is associated with dermal bone. In fact, there is often more than one dermal bone associated with the cartilage occupying the position normally held by the dorsal tip of the lamina ascendens (Fig. 4E); in contrast to the condition seen in the *Dlx1*^{-/-} mutants, this dermal bone never comes close to taking the form of the wild-type morphology of the lamina obturans.

Moreover, the cartilaginous remnants of the lamina ascendens may be in continuity with an ectopic cartilage (the 'PQ*' of Qiu et al.) emanating from the region of the tegmen tympani overlying the middle ear (pq*, black and green arrowhead in Fig. 4E). Indeed, the tegmen tympani is transformed and incorporated into a neomorphic structure that generally has four processes: (1) one that extends rostrad and which may contact the cartilage at the dorsal tip of the lamina ascendens or even contribute to the ventral orbit; (2) one that extends back to the otic capsule and may fuse with it; (3) one that takes a lateroventral tack toward the region of the basisphenoid; and (4) one that takes a medioventral tack toward the region of the basisphenoid (Fig. 4E). Each process is usually present but may vary to some extent in the length of projection from the region of the tegmen tympani. As described by Qiu et al., this complex cartilaginous structure may contact another ectopia of the *Dlx2*^{-/-} mutants, the 'strut' that extends from the basitrabecular process (Fig. 4E). When present, this endochondral structure extends laterad to meet one or the other of the ventral PQ* projections. Moreover, the incus has often lost its independence and is fused to it. As unreported by Qiu et al., however, the incus may be split. In accord with Qiu et al. we find the sidewall and arch are regions in

which structures derived from the BA have lost their normal structure, size and shape, and have acquired new ones.

In further agreement with Qiu et al. we find that proximal BA2-derived structures were also abnormal. The stapes and the styloid process are altered in size, shape and connection (Fig. 4E). The stapes contains no foramen and it does not articulate with the incus. It is also generally smaller than the stapes of the *Dlx1*^{-/-} mutants. Moreover, the styloid process is truncated, lacks a connection between the tympanohyal and stylohyal portions, and barely covers the fenestra rotunda of the otic capsule.

In discord with Qiu et al., however, we observe that the entire hyoid apparatus is altered (Fig. 9D). The body (which arises from both distal BA2 and BA3) is typically (but not always) cleft at the midline and projects caudoventrally (purple arrows, Fig. 9D). The lesser horns are smaller and placed in the proximodistal plane of the cleft body. The greater horns make their connection to the body but are also generally laterally orientated; they are also fused to the superior cornu of the thyroid cartilages, which also aberrantly extended laterad.

Our re-examination of the *Dlx2* mutants reveals three additional significant differences with the analysis of Qiu et al. (1995, 1997). First, although we observe that the dentary and MC appear grossly normal (though perhaps slightly smaller overall) in the *Dlx2*^{-/-} mutants (Fig. 9C), we find that the gonial and the ectotympanic are not (Fig. 9E). Typically, the gonial is diminished in size (although it appears to continue to invest the process folii of the malleus) and the anterior process of the ectotympanic is slightly truncated. Second, the ala temporalis of the *Dlx2*^{+/-} heterozygous skulls are altered (e.g. yellow and purple arrowheads, Fig. 9B). As with the *Dlx1*^{-/-} mutants, the coalescence of the parts of the ala that form the horizontal lamina is incomplete and a foramen develops. And third, the neurocranial base between the basisphenoid and presphenoid extends ectopic projections, of unknown significance, laterad (black and yellow arrowheads, Figs 4E and 9B).

Augmenting the phenotypic descriptions of mice carrying compound *Dlx1/2* mutant alleles

As was initially reported, we observe that the *Dlx1/2*^{-/-} mutants do exhibit a more robust chondrification of

the ectopic PQ* element at the expense of the maxillary molar field and alveolar bone (pq*, laa, Fig. 6E). This increase in the phenotypic alteration seen in the PQ* structure, however, is symptomatic of the trend in morphological transformations seen in the *Dlx1/2*^{-/-} mutants in general. For example, the pterygoid processes of the ala temporalis, which present as small, detached cylindrical rods running rostralaterad in the *Dlx1*^{-/-} mutants, and as less consistently shaped but generally rostrally orientated structures in the *Dlx2*^{-/-} mutants, are usually found as elongated, cylindrical cartilages running rostrad, parallel to the neurocranial base, toward the medial margins of the pq*/lamina ascendens (see below) and often fused to the basitrabecular processes (ppat, yellow arrowheads, Figs 6E and 9F).

Moreover, the lateral projections between the basisphenoid and the presphenoid that are seen in the trabecular basal plate of *Dlx2*^{-/-} mutants are more prominent in the *Dlx1/2*^{-/-} mutants (compare black and yellow arrowheads, Figs 4E, 6E and 9F). These projections may end abruptly; alternatively, they may extend caudad to contact the basitrabecular processes, laterad to contact the rostrally orientated pterygoid process cartilage, rostrad to contact the large lamina ascendens (laa) of the PQ*, or some combination of all three. Pterygoid bones are frequently missing altogether, but may form as small isolated ossifications adjacent to the basitrabecular processes (ptg, Fig. 6E). The cartilage that forms in the position of the dorsal tip of the lamina ascendens is greatly expanded and usually connects to the rostral processes of the ectopic cartilage to form a large PQ* structure. A number of small dermal ossifications not described by Qiu et al. are found in association, but a lamina obturans *per se* is not (e-os, Fig. 6E). These ossifications may be investing the associated cartilage.

Again, as with the *Dlx2*^{-/-} mutants, and in accord with Qiu et al., we find the sidewalls and zygomatic arches greatly transformed. The PQ*, however, makes a greater contribution to the ventral orbit in the *Dlx1/2*^{-/-} mutants (Fig. 6E). The alterations of the tegmen tympani are accompanied by changes of the taenia marginalis, which is variably fused to the ectopic PQ* cartilage. Moreover, the incus does not form its usual close relationship with the mdBA1-derived malleus, but instead is fused to the enlarged PQ* structure (see red and white arrowhead, Fig. 6E).

Other changes of BA structures found in the *Dlx2*^{-/-} mutants, but not reported by Qiu et al., are similarly

found in the *Dlx1/2*^{-/-} mutants. For example, the body of the hyoid may be cleft (purple arrow, Fig. 9H) and the greater horns fused to the superior cornu of the thyroid cartilage. Perhaps importantly, however, fewer hyoids are found cleft and more are found elongated mediolaterally with a slight bend at the midline. In either case, the lesser horns are reorientated laterad. The gonial and anterior process of the ectotympanic are also smaller than normal (not shown). MC appears to be grossly normal; the dentary, however, is clearly smaller, its coronoid process diminished, and the gap between the condylar process and the angular process is shortened (Fig. 9G). The styloid processes are disconnected and the tympanohyal portion that attaches to the crista parotica is truncated even more than in the *Dlx2*^{-/-} mice (not shown).

Significantly, the alterations of the ala temporalis seen in the *Dlx1* and *Dlx2* heterozygous skulls are greatly compounded in the *Dlx1/2*^{+/-} skulls, where separation of the components of the horizontal lamina of the ala temporalis is the norm (yellow and pink arrowheads, Fig. 9F). The lamina ascendens is maintained as a cartilage longer, akin to the situation in the *Dlx1*^{-/-} mutants (green arrowhead, Fig. 9F).

The *Dlx1*, *Dlx2* and *Dlx1/2* mutant phenotypes in relation to the hypothesized combinatorial *Dlx* code and the nature of heterozygous phenotypes

The generation of null alleles of *Dlx1* and *Dlx2* allows for a loss-of-*Dlx*-level test of the hypothesized combinatorial *Dlx* code regulation of BA skeletal development, pattern and morphogenesis. Animals in the heterozygous state provide perhaps the simplest tests of the results of modified combinatorial *Dlx* codes. Although not reported by Qiu et al. (1995, 1997), we have shown that *Dlx1*^{+/-}, *Dlx2*^{+/-} and *Dlx1/2*^{+/-} skulls each exhibit alterations of the BA-derived ala temporalis morphology. With regard to mBA1 derivatives, the ala temporalis appears most sensitive to reductions in *Dlx* dosage. Hence, the alterations of morphology found in these heterozygotes are consistent with the hypothesis of a combinatorial *Dlx* code, and at its simplest the combination (and therefore the code) might be defined by the total number of functional alleles.

The transformation of morphology of the *Dlx1/2*^{+/-} ala temporalis, moreover, is greater in scope than that seen in either the *Dlx1*^{+/-} or the *Dlx2*^{+/-} ala temporalis (compare yellow and pink arrowheads in Fig. 9A,B,F),

suggesting synergy between single alleles of *Dlx1* and *Dlx2* in the development of this structure. This transformation of morphology is not, however, as significant in scope as that of either the *Dlx1*^{-/-} or the *Dlx2*^{-/-} mutants (compare Fig. 9A and 9B). When considering the combinatorial code, the contribution of each individual allele is not therefore strictly additive nor proportional to the total number of expressed alleles: one *Dlx1* plus one *Dlx2* (i.e. two in total) is not functionally equivalent to two *Dlx1* or two *Dlx2* alleles.

The interaction between *Dlx1* and *Dlx2* further revealed by the exacerbated phenotypes apparent in the *Dlx1/2*^{-/-} mutants is also consistent with the combinatorial code hypothesis. To test further the combination *per se*, we generated *Dlx1*^{-/-}; *Dlx2*^{+/-} mice. The skulls of *Dlx1*^{-/-}; *Dlx2*^{+/-} mice exhibit transformations of BA morphology distinct from either the *Dlx1*^{-/-}; *Dlx2*^{+/-}, the *Dlx1*^{+/-}; *Dlx2*^{-/-} or the *Dlx1*^{-/-}; *Dlx2*^{-/-} mice (Fig. 9I). For example, they lack jugal bones (see green and purple arrow, Fig. 9I), possess uniquely shaped ectopic PQ*-associated cartilages (pq*), have diminished lamina obturans (lo) and broadened squamosals (sq) with shortened (but thickened) retrotympanic processes (rtp, Fig. 9I).

Reassessing the code: regulation of distal BA morphology and rationale for further examining the loss-of-function of distal *Dlx* genes

Testing genetic interactions: utilizing the loss of a nested *Dlx* gene to further address the code

Although it was initially reported that structures derived from the distal regions of the BA were unaltered by the functional loss of *Dlx1* and/or *Dlx2*, our re-evaluation of the *Dlx2*^{-/-} and *Dlx1/2*^{-/-} mutants reveals a small number of transformations in structures derived from the proximal parts of mdBA1 and from BA2. These include smaller gonials, truncated anterior processes of the ectotympanics, clefting of the bodies of the hyoids, and fusions of the greater horns of the hyoids to the superior cornu of the thyroid cartilages (Fig. 9). With the exception of the slightly smaller dentaries, the alterations of structure seen in the *Dlx1/2*^{-/-} mutants do not vary significantly from those seen in *Dlx2*^{-/-} mutants; distal transformations do, however, provide some evidence for a contribution of *Dlx1* and *Dlx2* to the hypothesized combinatorial regulation of distal BA

morphology. Importantly, however, as distal defects are as a rule not significant in scope overall in the *Dlx1/2*^{-/-} mutants, *Dlx1* and *Dlx2* do not appear to compensate overly for each other with regard to distal BA development.

Moreover, these transformations of distal morphology appear minor (so much so as to be missed in the initial descriptions), especially when one considers: (1) the apparent levels of expression of *Dlx1* and *Dlx2* in the distal BA primordia (e.g. see Fig. 3); (2) the degree of transformation seen in proximally derived structures in the *Dlx1*^{-/-}, *Dlx2*^{-/-} and *Dlx1/2*^{-/-} mutants; and (3) the fact that the most prominent distal BA structures – the dentary and MC of BA1 – appear relatively unaffected. There are various hypotheses that may explain this general dearth of phenotypic change distally in the BAs of the *Dlx1*^{-/-}, *Dlx2*^{-/-} and *Dlx1/2*^{-/-} mutant mice, including: (1) that the lack of alteration is due to genetic compensation by other, distally restricted (nested), *Dlx* genes (i.e. *Dlx3*, *Dlx4*, *Dlx5* and/or *Dlx6*); and (2) that the *Dlx1* and *Dlx2* linked-pair do not exert significant biological, regulatory functions in these distal domains.

If this first hypothesis were to be correct, and genetic compensation explains why there are no significant alterations of distal structures, it begged the questions: Was it reasonable to expect that a distally restricted *Dlx* gene would be able to compensate for the loss of *Dlx2* when *Dlx1* was essentially unable to do so (and vice versa)? Conversely, might one not have reasonably expected that the loss of functional alleles of a distal *Dlx* gene, such as *Dlx5*, would likewise be compensated by the presence of *Dlx1* or *Dlx2* (which was clearly not the case)? If there was genetic redundancy in the code for the distal BA morphology, might this be revealed by the loss of both (or more) of the redundant genes? Would *Dlx2*^{-/-}; *Dlx5*^{-/-} mice, for example, exhibit transformations of distal BA structures and thus suggest some redundancy? However, if no transformations were to occur in such a compound mutant mouse, then might additional genes be compensating? For instance, could the linked-pair gene *Dlx1* be additionally compensating distally for *Dlx2* function (which could then be unmasked in *Dlx1/2*^{-/-}; *Dlx5*^{-/-} mice)? Alternatively, as suggested by the second hypothesis above, it was possible that these genes might not have significant functions distally (which would be a severe counter to the combinatorial code hypothesis).

Thus, key issues remained from the initial tests of the *Dlx* code hypothesis. It was clear, however, that the

Dlx5 mutant mice, as representative of the loss of *nested* genes, could be utilized to: (1) test for genetic interactions between *Dlx1*, *Dlx2* and *Dlx3* with regard to distal BA development; and, if found, (2) test the nature of the interactions relative to first-order (e.g. *Dlx5* and *Dlx6*), second-order (e.g. *Dlx5* and *Dlx2* or *Dlx3*) and third-order paralogues (e.g. *Dlx5* and *Dlx1*). We therefore utilized *Dlx5* mutants to test the hypothesis of a genetic compensation for *Dlx1* and *Dlx2* with regard to distal development.

Evidence of a genetic interaction between second-order paralogues: *Dlx2*^{-/-}; *Dlx5*^{-/-} mutants have extensively altered BA derivatives, including cleft mandibles

Compound *Dlx2*^{+/-}; *Dlx5*^{+/-} heterozygotes are viable and fertile, and when crossed generate the expected genotypes: [*Dlx2*^{+/+}; *Dlx5*^{+/+}], [*Dlx2*^{+/-}; *Dlx5*^{+/+}], [*Dlx2*^{+/+}; *Dlx5*^{+/-}], [*Dlx2*^{+/-}; *Dlx5*^{+/-}], [*Dlx2*^{-/-}; *Dlx5*^{+/+}], [*Dlx2*^{+/-}; *Dlx5*^{-/-}], [*Dlx2*^{-/-}; *Dlx5*^{-/-}] and [*Dlx2*^{-/-}; *Dlx5*^{-/-}]. Beyond those alterations of the ala temporalis already noted for the *Dlx2*^{+/-} heterozygotes, transformations of BA skeletal structures were not observed in the compound *Dlx2*^{+/-}; *Dlx5*^{+/-} heterozygotes. However, significant and sometimes drastic BA alterations are found in the [*Dlx2*^{+/-}; *Dlx5*^{-/-}], [*Dlx2*^{-/-}; *Dlx5*^{+/-}] and [*Dlx2*^{-/-}; *Dlx5*^{-/-}] mutants.

As with the *Dlx5/6*^{-/-} mutants, the *Dlx2*^{-/-}; *Dlx5*^{-/-} mutants are striking at birth, having small domed heads and, usually, cleft mandibles (Fig. 10). The *Dlx2*^{-/-}; *Dlx5*^{-/-} mandible is severely truncated, appearing as a small projection subjacent to the eye, and is shorter than that of the *Dlx5/6*^{-/-} mutant mandible (Figs 10 and 11; compare with Fig. 8). The ectoderm covering the eye either fails to cover the eye or does so without benefit of eyelids (black and light blue arrows, Fig. 10F,G,J). The external auditory pinnae, which usually develop out of, and around, the first pharyngeal cleft between BA1 and BA2, are nearly absent and are represented by the barest of a hillock (black arrows, Fig. 10F,J). Moreover, those glands developing in and around the BA appear to be absent (e.g. the parotid and submandibular glands; black and green arrows, Fig. 10G).

Dlx2^{-/-}; *Dlx5*^{-/-} mutants fail to develop a normal oral opening (Fig. 10C,E,H,I). Significantly, they develop a small patch of vibrissae on the outer mandibular surface (see 'LJ'-associated purple arrowheads, Fig. 10F,H,J) and ectopic rugae in the oral ectoderm near, but not

on, the oral surface of the truncated mandible (black and orange arrows, Fig. 10H,I). In both respects, these ectopias do not appear to be as robust as those seen with the *Dlx5/6*^{-/-} mutants (compare Figs 8 and 10). The tongue, an organ of both BA and non-BA origins, is also cleft and highly truncated, each half ending at the point where the mandible juts from the head (yellow and black arrows, Fig. 10H,I).

The distinct changes of head morphology in evidence at birth are clearly distinctive at E10 and beyond (Fig. 10A–F). Additionally, a wide range of defects in limb development also occurs, including truncation below the humerus or femur, further details of which will appear in a separate manuscript (Depew and Rubenstein, unpublished), as well as rib defects (data not shown).

Although compound *Dlx2*^{-/-}; *Dlx5*^{-/-} mutants have a number of phenotypes distinct from the single mutants (see below), alterations specific to either the *Dlx2*^{-/-} or the *Dlx5*^{-/-} single mutants are in evidence; this includes the loss of most of the alisphenoid and the presence of altered side-wall dermal ossifications, an ectopic palatoquadrate (PQ*) structure, and lateral projections from the basitrabecular plate rostral to the basisphenoid (as seen in the *Dlx2*^{-/-} mutants), as well as occasional exencephaly and otic and (asymmetric) nasal capsular defects (as seen with the *Dlx5*^{-/-} mutants) (Fig. 11G). However, these phenotypic alterations are not all essentially identical to those presented by the single mutants. For instance, the palatoquadrate structure does not project medially, and it has a greater degree of fusion to the taenia marginalis and otic capsule where the tegmen tympani would have been (red and blue arrowhead, Fig. 11G). That portion of the PQ* element that forms in the region where the ascending lamina of the ala temporalis normally would be found is less robust and may exist solely as a number of small cartilaginous bodies (pq*, laa, Fig. 11G). Ectopic 'struts' (as seen in the *Dlx2*^{-/-} mice) were not seen in any of the *Dlx2*^{-/-}; *Dlx5*^{-/-} mutants, although basitrabecular processes (btp) were occasionally in evidence. Where present, dermal ossifications of the lamina obturans are smaller than those in the *Dlx2*^{-/-} single mutants.

In regions derived from where both *Dlx2* and *Dlx5* are extensively expressed – that is, the distal BAs – the greatest alterations and transformations have taken place (Fig. 11). Meckel's cartilage, except for the rostral process (rpMC), is essentially absent (Fig. 11C,G,H). Clearly identifiable incudes and mallei are not present; however, diminutive cartilaginous bodies found in the

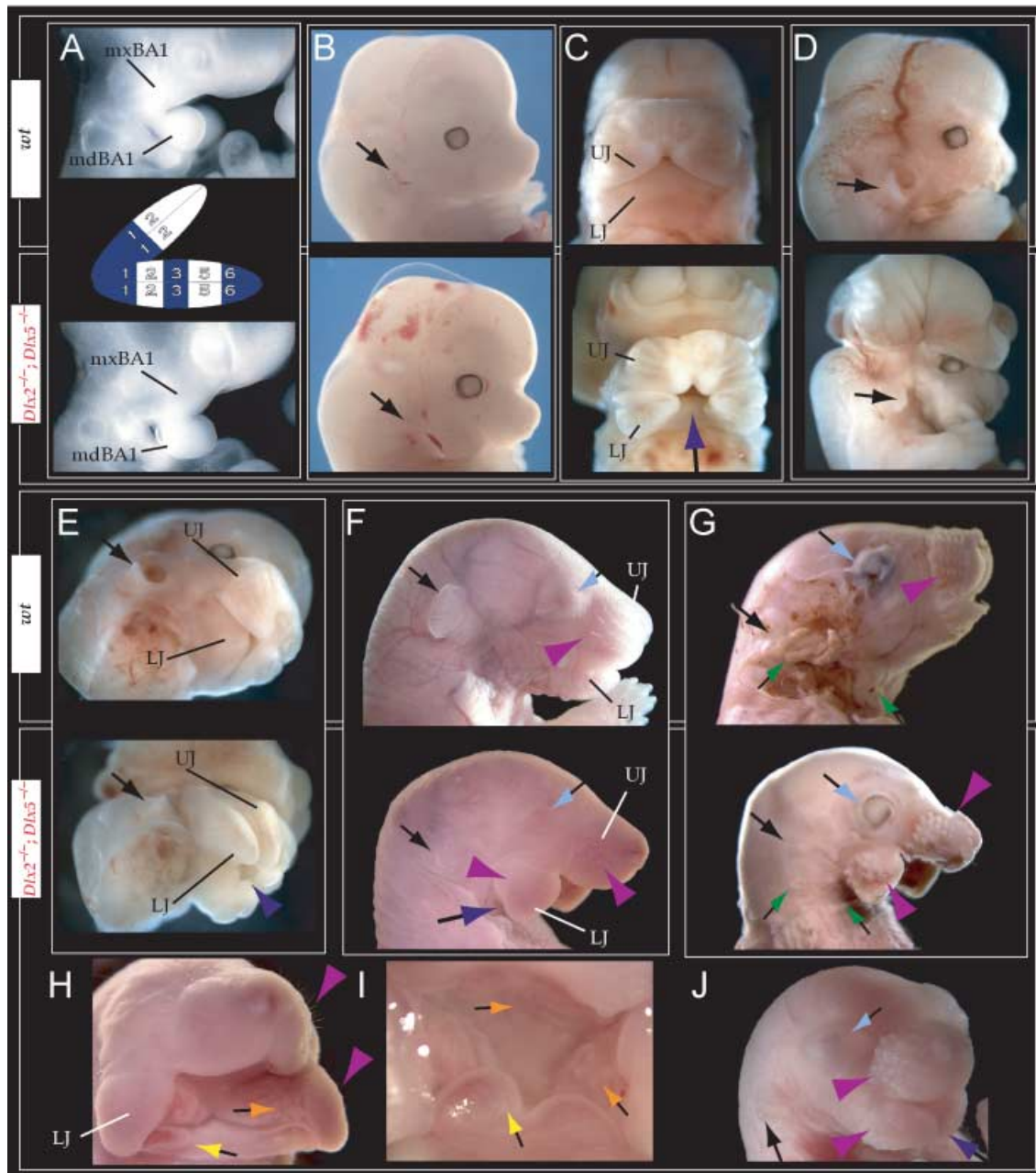
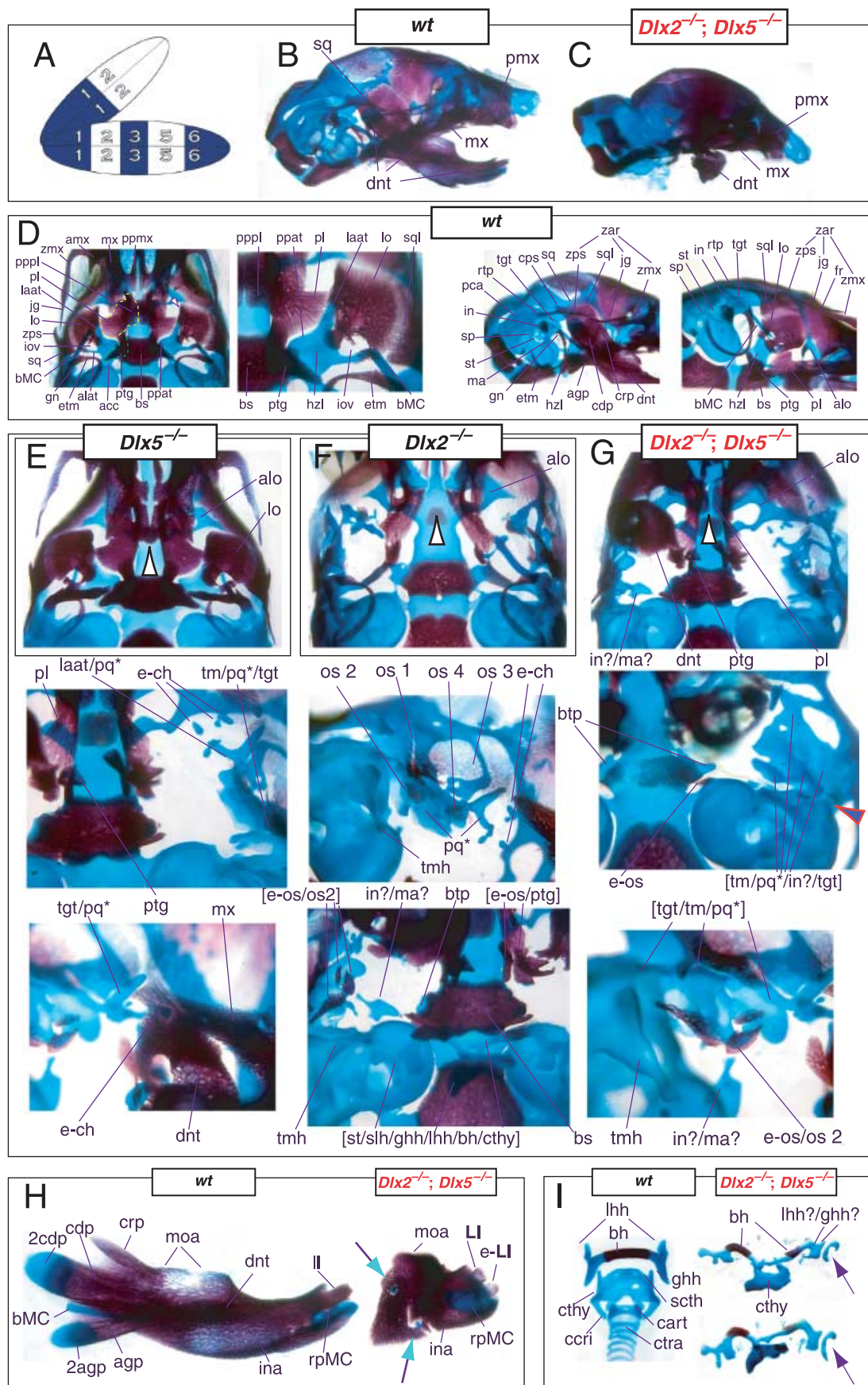


Fig. 10 Gross anatomy of *Dlx2*^{-/-}; *Dlx5*^{-/-} mutants revealing a genetic interaction between these two second-order paralogues. (A) E10 wild-type (top) and *Dlx2*^{-/-}; *Dlx5*^{-/-} mutant (bottom) embryos clearly showing differences at this age in the elaboration and development of mdBA1 and mxBA1. Reference schema indicating the loss of both alleles of *Dlx2* and *Dlx5* in BA1 is included. (B) E13.75 wild-type (top) and *Dlx2*^{-/-}; *Dlx5*^{-/-} mutant (bottom) embryos. Black arrow indicates ear region. (C–E) Gross anatomy of an E15.5 wild-type embryo (top) and an exencephalic *Dlx2*^{-/-}; *Dlx5*^{-/-} mutant (bottom) littermate. The exencephaly rate in the compound mutant is roughly the same as with the single *Dlx5*^{-/-} mutant. (C) Norma frontalis view of E15.5 wild-type (top) and *Dlx2*^{-/-}; *Dlx5*^{-/-} mutant (bottom) embryos. The blue and black arrow points to the left mandible. Note the ridges of the lower jaw (LJ) indicating incipient vibrissae development. (D, E) Norma lateralis (D) and oblique (E) views of the same E15.5 wild-type (top) and *Dlx2*^{-/-}; *Dlx5*^{-/-} mutant (bottom) embryos. Black arrows highlight the lack of integration of the lower jaw with the ear region, while the blue and black arrow points to the left mandible. (F, G) Unaltered (F) and skinned (G) gross anatomy of wild-type (top) and *Dlx2*^{-/-}; *Dlx5*^{-/-} neonates. The blue and black arrow points to the left mandible. Light blue and black arrows emphasize the abnormality of the ectoderm over the eye. The *Dlx2*^{-/-}; *Dlx5*^{-/-} mutants essentially lack ear pinnae (black arrows) and possess ectopic vibrissae on their lower jaws (purple arrowheads). Green and black arrows highlight the loss of BA-associated glands. (H, I) Oral region of the *Dlx2*^{-/-}; *Dlx5*^{-/-} mutants. Yellow and black arrows point to the cleft tongue, while orange and black arrows point to ectopic rugae. Purple arrowheads indicate vibrissae. (J) Example of a *Dlx2*^{-/-}; *Dlx5*^{-/-} mutant without a fully cleft lower jaw. Arrows as above. See text for detailed descriptions and list for abbreviations.



appropriate region may represent a fusion of what would have been both ('in?/ma?' in Fig. 11G). Moreover, a cartilage (possibly representing a residual portion of the incus as based on position) may be found fused to the palatoquadrate. Hence, the primary jaw articulation has disappeared.

The greatly truncated dentary develops a closely apposed, abnormal articulation with the truncated molar alveolus of the maxilla (dnt, Fig. 11C,G); thus, the dentary–squamosal secondary jaw articulation is lost. The dentary is represented only by the barest remnant of a molar alveolus, a diminished incisive alveolus, a stand-alone rostral process of Meckel's cartilage, and one or two aberrant incisors (Fig. 11C,G,H). Indeed, 40% of the examined dentaries housed duplicate (oral–aboral), rounded incisors ('e-II' of Fig. 11H). Neither a gonial nor a definitive ectotympanic are ever observed.

Inserted between the apposed dentary and maxilla may occasionally be found an extension of the palatoquadrate element; a partial contribution to this insertion from residual portions of the body of Meckel's cartilage cannot be definitively ruled out ('bMC/pq*', Fig. 11G). The entire zygomatic process and ventral optic support is of maxillary (mx) origin, and consists of a short but robust caudal process and a similarly short and robust ectopic rostral projection. Proximal and medial to the dentary, small ectopic ossifications, including what may be considered a small residual pterygoid (ptg), are found (Fig. 11G). Palatal clefting is seen, but it is not as extensive as is seen with the *Dlx2*^{-/-} single mutants (black and white arrowhead, Fig. 11G).

Additionally, the otic capsule does not contain an oval window, and a stapes (as such) is not in evidence (Fig. 11G). The tympanohyal (tmh) portion of the styloid projects from the otic capsule, but is rostrally displaced (Fig. 11G); a definitive crista parotica fails to develop on the capsule. An ectopic cartilage occasionally devel-

ops at the distal tip of the tympanohyal and may represent a stylohyal or perhaps a transdifferentiated ectotympanic; moreover, a thin connection may occasionally be seen to the lateral edges of the dysmorphic hyoid cartilages. The tympanohyal, however, is distinctly different in morphology and position from that seen in the *Dlx2*^{-/-} mutants.

The distal BA2 derivatives are likewise extensively altered. The hyoid body is split with two widely separated centres of endochondral ossification (bh, Fig. 11G,I). Chondrogenic extensions from these two centres meet at the midline, and are fused to a highly dysmorphic thyroid cartilage remnant (cthy, Fig. 11I). There are no typical lesser or greater hyoid horns. Instead, lateral to the hyoid bodies, a number of cartilaginous projections develop; occasionally, one will project to the basisphenoidal neurocranial basal plate. Although there are no discernible stapes, the lateral tips of this compound hyoid–thyroid structure may comprise cells that would otherwise have been allocated to a forming stapes. Oddly, there is a consistent asymmetry in the hyoid structures that do develop (see purple arrows, Fig. 11I).

Clearly, then, the combined loss of *Dlx2* and *Dlx5* has resulted in a drastic alteration and transformation of BA skeletal development, pattern and morphology. This is highlighted by the loss of both the primary (malleo-incal) and the secondary (dentary–squamosal) jaw articulations. Thus, this genetic interaction reveals a role for *Dlx2* in the development of the distal BA *Dlx* code.

***Dlx2*^{-/-}; *Dlx5*^{+/-} mutants: phenotypic similarity to, but not identity with, the distal BA transformations seen in *Dlx5*^{-/-} mutants**

Examination of *Dlx2*^{-/-}; *Dlx5*^{+/-} mutants provides further evidence for a genetic interaction. Moreover, it provides

Fig. 11 Skeletal analysis of the loss-of-function of the second-order paralogues, *Dlx2*^{-/-}; *Dlx5*^{+/-}, revealing a genetic interaction between the two. (A) Reference schema indicating the loss of two *Dlx2* and two *Dlx5* alleles in BA1. (B) Norma lateralis view of a P0 wild-type skull. (C) Norma lateralis view of a P0 *Dlx2*^{-/-}; *Dlx5*^{+/-} mutant skull. Note the rostral displacement, apposition, and articulation of the truncated dentary (dnt) with the maxilla (mx) and not with the squamosal. (D) Wild-type P0 skulls highlighting, left to right, the palatal region (norma basalis; yellow line outlining the palatine and green line outlining the pterygoid), the ala temporalis and lamina obturans components of the alisphenoid, the ear region with the primary and secondary jaw articulations, and the middle ear without the dentary attached. (E, F) Norma basalis views of the *Dlx5*^{+/-} (E) and *Dlx2*^{-/-} (F) single mutants for comparison. (G) Skeletal staining of compound *Dlx2*^{-/-}; *Dlx5*^{+/-} neonate mutants emphasizing the drastic loss of BA structure. (H) Wild-type and *Dlx2*^{-/-}; *Dlx5*^{+/-} neonate PO dentaries. The mutant dentary is represented mainly by structures associated with the distal midline, such as the rostral process of Meckel's cartilage (rpMC). Mutant dentaries often possess an ectopic second incisor (e-II). Green and black arrows point to miniscule cartilages associated with the proximal end of the truncated dentary. (I) Wild-type (left) and mutant (right) hyoid and thyroid cartilages. These caudal BA elements are also severely affected by the loss of both *Dlx2* and *Dlx5*. The purple arrows are to highlight the asymmetric nature of the hyoids of these mutants. See text for detailed descriptions and list for abbreviations.

the opportunity to compare the phenotypes of a number of mutants that present distinct combinations of *Dlx* genes – and therefore distinct *Dlx* codes. For example, in a combination otherwise devoid of *Dlx2*, a comparison can be made of the relative contribution of two, one or no wild-type *Dlx5* alleles. We have already seen in a *Dlx2* null background that when both wild-type *Dlx5* alleles are present, minor changes to the gonial and ectotympanic bones are seen, as well as a clefting of the hyoid body; otherwise, distal-BA1 structures such as Meckel's cartilage and the dentary are, in general, unaffected. We have also seen that when neither wild-type *Dlx5* allele is present in a *Dlx2* null background, the dentary is severely truncated (represented mainly by the incisive region) and Meckel's cartilage is mostly absent. Here, we show that the presence of a single wild-type *Dlx5* gene rescues much of the dentary and Meckel's cartilage (Fig. 12).

Dlx2^{-/-}; *Dlx5*^{+/-} mutants exhibit the range of proximal BA alterations of skeletal morphology seen in the *Dlx2*^{-/-} mutants [e.g. an ectopic pq* and side-wall ossifications (os 1–4); Fig. 12F,G]. Distal BA derivatives are, however, also affected. In a manner similar to, but not identical with, the *Dlx5*^{-/-} mutants, the dentaries are truncated at their proximal ends (Fig. 12F,I). They lack coronoid processes, and the angular and condylar processes are juxtaposed and compressed (as well as being slightly smaller than those of the *Dlx5*^{-/-} mutants). Unlike the *Dlx5*^{-/-} mutants, moreover, ectopic secondary cartilage develops on the buccal surface of the dentary between the angular and condylar processes (black and green arrows, Fig. 12I).

Whereas Meckel's cartilage in the *Dlx5*^{-/-} mutants deviates medially to contribute to the ectopic os paradoxicum before continuing toward the malleus,

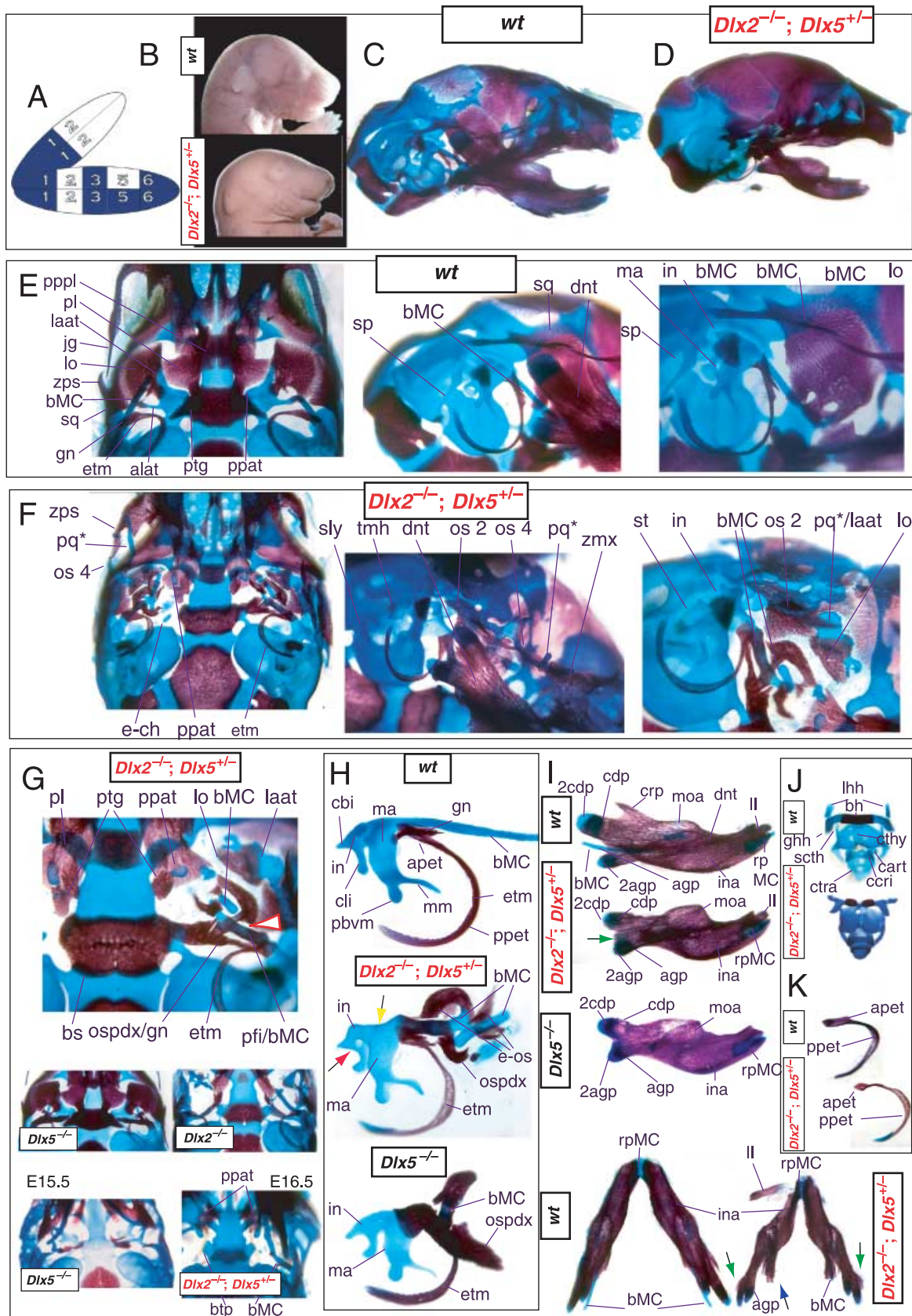
Meckel's cartilage in the *Dlx2*^{-/-}; *Dlx5*^{+/-} mutants is generally discontinuous distal to the malleus (bMC, Fig. 12F,G,H). The distal part (representing the central portion of the body of Meckel's cartilage) continues toward the body of the dentary, and is surrounded by a number of ectopic ossifications (e-os, Fig. 12F–H). The portion continuous with the malleus (pfi) is invested by the residual gonial, and is highly ossified (Fig. 12F–H). Its distal tip is also invested by an ectopic dermal bone; the gonial also contributes to an os paradoxicum (ospdx), which is variably fused to the laterally displaced pterygoids (Fig. 12G).

Distinct from the situation seen in the *Dlx2*^{-/-} mutants, the incus does not contact the ectopic palatoquadrate cartilage; rather, the corpus is fused to the malleus (yellow and black arrow, Fig. 12H). Furthermore, its body is invariably pierced by a single foramen (red and black arrow, Fig. 12H). The malleus is smaller and the manubrium shorter, thicker and more caudally reflected toward the ectotympanic. The ectotympanic itself (in particular the anterior process) is smaller than in the wild type (Fig. 12H,K). Lastly, the hyoid resembles, though is not identical to, that of the *Dlx2*^{-/-} mutants (Fig. 12J). The uniqueness of this phenotype suggests that once under a particular threshold of general *Dlx* expression levels, each allele of particular a *Dlx* gene makes a contribution to the combination forming the code.

***Dlx2*^{+/-}; *Dlx5*^{-/-}: exacerbation of the *Dlx5*^{-/-} phenotype with transformation of the body of Meckel's cartilage to a morphology reminiscent of an ala temporalis**

We have seen how, in a *Dlx2*-compromised background, each allele of *Dlx5* contributes to the overall

Fig. 12 Skeletal analysis of the *Dlx2*^{-/-}; *Dlx5*^{+/-} mutant through differential staining of bone (alizarin red) and cartilage (alcian blue). (A) Reference schema indicating the loss of two *Dlx2* alleles and one *Dlx5* allele in BA1. (B) Gross anatomy of wild-type and *Dlx2*^{-/-}; *Dlx5*^{+/-} neonates. (C) Norma lateralis view of a P0 wild-type skull. (D) Norma lateralis view of a *Dlx2*^{-/-}; *Dlx5*^{+/-} neonatal skull. (E) Wild-type P0 skulls highlighting, left to right, the palatal region (norma basalis), the ear region with the primary and secondary jaw articulations, and the middle ear with the dentary detached. (F) *Dlx2*^{-/-}; *Dlx5*^{+/-} neonatal skulls evincing an alteration of proximal BA1 derivatives in addition to defects usually seen in the *Dlx2*^{-/-} single mutant; left to right: the palatal region (norma basalis) and the middle ear with, and without, the dentary attached. (G) Magnified norma basalis view of the palatal region of a *Dlx2*^{-/-}; *Dlx5*^{+/-} neonate showing the disruption of the body of Meckel's cartilage and ectopic dermal bones contributing to an os paradoxicum. For comparison, P0 and late fetal skulls of the single mutants are included. (H) Dissected middle ear bones and body of Meckel's cartilage from (top to bottom) wild-type, *Dlx5*^{+/-} and *Dlx2*^{-/-}; *Dlx5*^{+/-} neonates. (I) Comparison of wild-type and mutant dentaries. Above: from top to bottom – wild-type, *Dlx2*^{-/-}; *Dlx5*^{+/-} and *Dlx5*^{-/-} elements. At bottom, norma basalis externa views of a wild-type (left) and a *Dlx2*^{-/-}; *Dlx5*^{+/-} mutant (right) dentary. Green and black arrows indicate the ossification on the lateral aspect of the condylar process. Blue and black arrows highlight the segregation of the buccal and lingual halves of the mutant dentary. The mutant incisor has been extracted from the alveolus. (J) Hyoid and thyroid development in the mutant. Note the cleft in the hyoid body (bh) of the mutant. (K) Relative ectotympanic development. See text for further descriptions and list for abbreviations.



code and therefore to the subsequent morphology of a BA. This principle applies in the converse as well: in a *Dlx5*-compromised background, each allele of *Dlx2* contributes to the overall code and therefore the subsequent morphology of the BA.

With the loss of one wild-type allele of *Dlx2*, the already truncated proximal dentary of the *Dlx5*^{-/-} mutants is further altered in the *Dlx2*^{+/-}; *Dlx5*^{-/-} mutants (Fig. 13). In addition to the coronoid process already missing in the *Dlx5*^{+/-} mutants, the angular process is lost, and the condylar process is severely hypoplastic (Fig. 13G). The condyle is represented only by a small projection toward the squamosal, the tip of which is a distinct, self-contained ossification (black arrow, Fig. 13F,G). The caudolingual aspect of the dentary is significantly dissociated from the caudobuccal aspect, and projects toward the pterygoids at the neurocranial base (blue and black arrow, Fig. 13G). The distal-most portions of the dentary, as represented by the rostral process of Meckel's cartilage, incisors and incisive alveolus, remain. They do not reach their usual caudal extension, however (Fig. 13G).

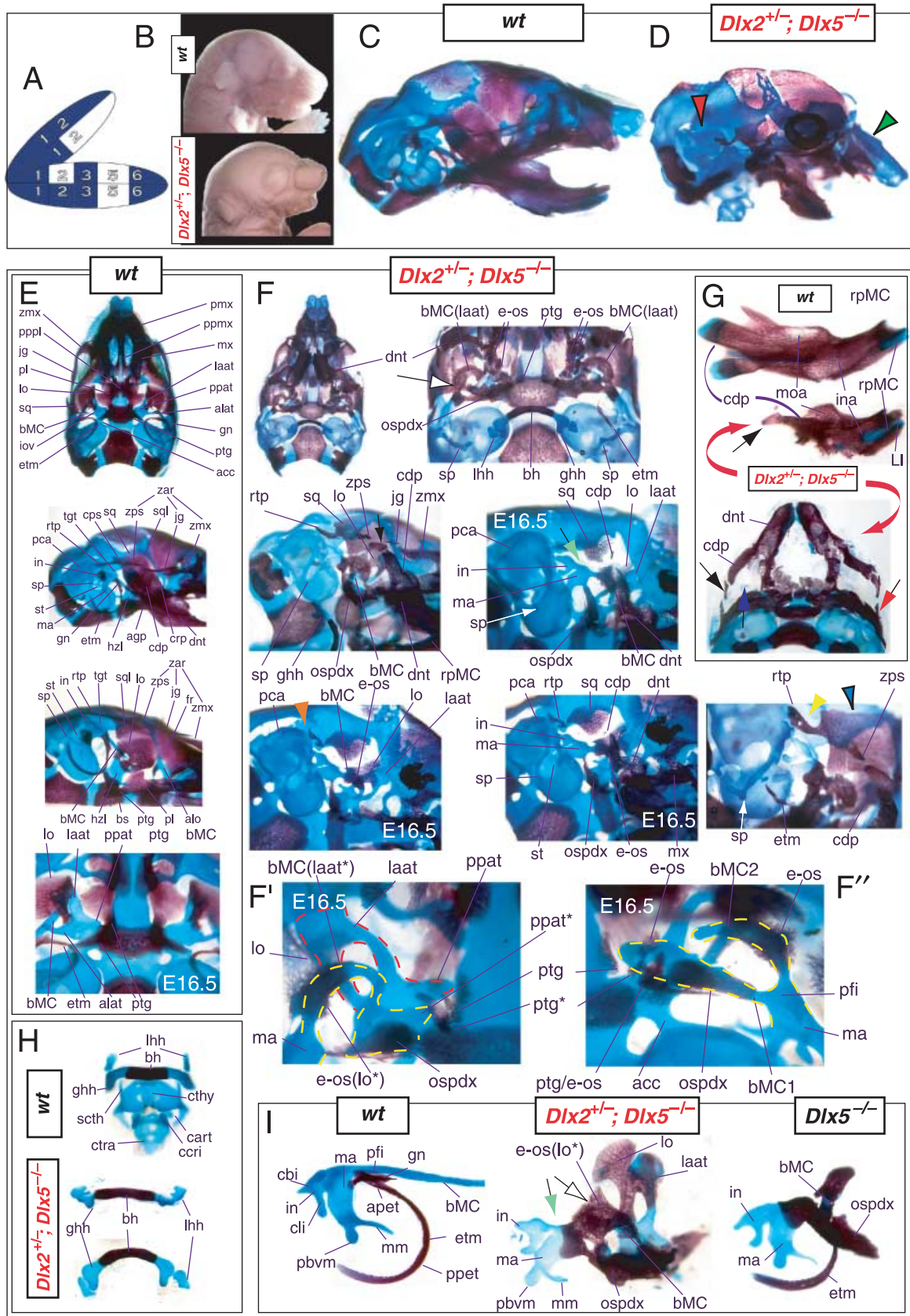
As with the *Dlx2*^{+/-}; *Dlx5*^{+/-} mutants, the corpus of the incus is fused to the malleus (black and green arrow, Fig. 13F,I). The manubrium is slightly truncated and reflected rostrad (as opposed to the other mutants thus far described). Additionally, the os paradoxicum and body of Meckel's cartilage are greatly transformed. (Fig. 13F,H). Distal to the point of fusion between the incus and the malleus (at the processus folii), the body of Meckel's cartilage is relatively broadened but flattened. Distal to this point, the cartilage is found in one of two patterns (outlined in yellow, Fig. 13F', F''): (1) it makes a loop, extending slightly rostralaterad, then rostromedial, then back both caudolaterad and

caudomedial toward the basitrabecular process where the endogenous ala temporalis fuses (Fig. 13F'); or (2) it extends two processes, one that extends rostralaterad (bMC2) and then medial and another rostromedial toward the basitrabecular process (often fusing with it) (bMC1, Fig. 13F''). These two shapes are variations of a common form. When not split, their morphologies are strikingly similar to the lamina ascendens, pterygoid process and associated alisphenoid foramen of the ala temporalis.

Furthermore, four ectopic centres of ossification (e-os) are clearly seen in association with this transformed body of Meckel's cartilage: (1) a dermal ossification surrounding and investing the rostralateral projection; (2) a dermal ossification surrounding the medial projection; (3) a second dermal ossification caudal to the one projecting around the medial projection, but distinct from it, and often fused to the ectopic pterygoid (see below) or the medial projection; and (4) an ectopic pterygoid (ptg*) – or the caudal end of the pterygoid that has been completely separated from the rostral portion – that surrounds the ectopic pterygoid process of the medial projection (e-os, Fig. 13F,H). The os paradoxicum is then made of the medial projection and associated dermal ossifications. These ossifications invest the cartilage of the transformed bodies of Meckel's cartilage much in same manner as the lamina obturans and gonial invest the lamina ascendens and processus folii, respectively.

It should be noted that although clearly recognizable in its morphology, portions of the endogenous ala temporalis itself are transformed; this is particularly true of the pterygoid process (ppat), which is elevated and parallels the medial projection (compare 'ppat' and 'ppat*', Fig. 13F',F''). Moreover, the invested ossification

Fig. 13 Skeletal analysis of the *Dlx2*^{+/-}; *Dlx5*^{-/-} mutant through differential staining of bone (alizarin red) and cartilage (alcian blue). (A) Reference schema indicating the loss of one *Dlx2* allele and two *Dlx5* alleles in BA1. (B) Gross anatomy of wild-type (top) and the *Dlx2*^{+/-}; *Dlx5*^{-/-} neonates. (C) Norma lateralis view of a P0 wild-type skull. (D) Norma lateralis view of the *Dlx2*^{+/-}; *Dlx5*^{-/-} neonatal skull. The red and black arrowhead denotes the otic capsular deficiencies associated with the loss of *Dlx5*, while the green and black arrowhead highlights the nasal capsular defects. (E) Wild-type skulls highlighting, top to bottom, norma basalis view of a P0 skull minus the dentary, the middle ear with, and without, the dentary attached, and the palatal region minus the dentary of an E16.5 skull. (F) P0 and E16.5 skulls of *Dlx2*^{+/-}; *Dlx5*^{-/-} mutants. The black and green arrow points to the fusion of the incus and malleus, while the yellow arrowhead indicates the foramen in the retrotympenic process. The black and white arrow points to the edge of the transformed osseous body of Meckel's cartilage that articulates with the squamosal, while the orange arrowhead highlights the deficiency of the tegmen tympani. The transformed Meckel's cartilage is outlined in broken yellow lines; the endogenous ala temporalis is outlined in red. The black and blue arrowhead highlights the loss of normal dorsal squamosal architecture. (G) Dentary development in the *Dlx2*^{+/-}; *Dlx5*^{-/-} mutant. (H) Hyoid development in the *Dlx2*^{+/-}; *Dlx5*^{-/-} mutant. (I) Development of the middle ear and os paradoxicum in the *Dlx2*^{+/-}; *Dlx5*^{-/-} mutant, with a wild-type (left) and *Dlx5*^{-/-} mutant (right) structures for comparison. Note that the endogenous alisphenoid has been included with the *Dlx2*^{+/-}; *Dlx5*^{-/-} mutant. See text for further descriptions and list for abbreviations.



associated with the rostrolateral projection may make small articulations with both the squamosal (dorsad; black and white arrow, Figs 13F,I) and lamina obturans (rostrad). The lamina of the squamosal is broadened both dorsally and ventrally (Fig. 13F). The zygomatic process of the squamosal (zps) is truncated (red and black arrows, Fig. 13F) and does not meet the jugal itself – but rather a diminutive ossification orientated toward the distal ossification of the condylar process of the dentary. The retrotympanic process (rtp) is shortened, thickened, often contains a foramen (yellow arrowhead, Fig. 13F) and is frequently separated from the remainder of the squamosal. As there is little remaining of the tegmen tympani or fossa incudi (orange arrowhead, Fig. 13F), it fails to act as a bridging cover. Furthermore, there is no clear morphological distinction between the caudal process and the dorsal lamina of the squamosal (black and blue arrowhead, Fig. 13F).

The ectotympanic does not reach the malleus and body of Meckel's cartilage, and does not extend fully to the styloid process (etm, Fig. 13F). The styloid is extended distad, but is dysmorphic along its rostral and caudal borders. The distal tip is either reflected rostrad or caudad (white arrow, Fig. 13F). It seems that this may be, at least in part, plietropic to the other regional alterations of morphology.

Unlike the hyoid of the *Dlx5*^{-/-} mutants, which (although slightly smaller) is fairly normal, the hyoid body of the *Dlx2*^{+/-}; *Dlx5*^{-/-} mutants is slightly stretched mediolaterally and its centre of ossification more extensive (Fig. 13H). The lesser and greater horns are truncated, giving the hyoid more of a horseshoe shape than in wild-types. Lastly, the otic (red and black arrowhead) and nasal (green and black arrowhead) capsules are hypoplastic as in the *Dlx5*^{-/-} mutants (Fig. 13D).

Thus, in the absence of both wild-type alleles of *Dlx5* and in the presence of just a single copy of *Dlx2*, distal BA derivatives are greatly transformed. The nature of this alteration is particularly noteworthy as the body of Meckel's cartilage resembles in some respects an ala temporalis, the dentary loses much of the ossification of its proximal end, and ectopic ossifications develop around the modified body of Meckel's cartilage that extend, like the lamina obturans, to the squamosal. It is also important to note that this transformation is not of the magnitude seen with the *Dlx5/6*^{-/-} mutant's transformation of a lower jaw to an upper jaw. It does appear, however, that the greater relative loss of the

nested gene, *Dlx5*, compared with the proximodistally extended gene, *Dlx2*, has resulted in the loss of some mandibular/distal identity and the gain of some maxillary/proximal identity (discussed further below).

Genetic interaction of the third-order paralogues, *Dlx1* and *Dlx5*: evidence that *Dlx1*^{-/-}; *Dlx5*^{+/-} mutants are phenotypically more similar to *Dlx2*^{+/-}; *Dlx5*^{+/-} mutants than to *Dlx2*^{-/-}; *Dlx5*^{-/-} mutants

Phenotypic evidence of a genetic interaction between *Dlx2* and *Dlx5* demonstrates that *Dlx2* contributes to patterning of distal parts of BA1 (mdBA1) and BA2, supporting the hypothesis of a genetic redundancy, or compensation, in the *Dlx* code. *Dlx2* and *Dlx5* are second-order paralogous genes, sharing a greater degree of similarity outside of the homeodomain than either of their linked-pair genes, *Dlx1* and *Dlx6*, respectively (Stock et al. 1996; Panganiban & Rubenstein, 2002; Stock, 2005). This is suggestive of the possibility that second-order paralogous genes may uniquely share a set of interacting partners (i.e. ones not shared with first- or third-order paralogous genes). To test the degree to which third-order paralogues genetically interact, we examined the phenotypes of compound *Dlx1*^{-/-}; *Dlx5*^{-/-} mutants.

As with the *Dlx2*^{+/-}; *Dlx5*^{+/-} compound heterozygotes, compound *Dlx1*^{+/-}; *Dlx5*^{+/-} heterozygotes are viable and fertile, and produce offspring of the expected genotypes. No transformations of BA morphology (beyond those of the variety already noted for *Dlx1*^{+/-} mutants) were observed in the compound heterozygotes. However, distinct transformations are found in the [*Dlx1*^{+/-}; *Dlx5*^{-/-}], [*Dlx1*^{-/-}; *Dlx5*^{+/-}] and [*Dlx1*^{-/-}; *Dlx5*^{-/-}] mutants (Fig. 14).

We find that there is a strong interaction between the *Dlx1* and *Dlx5* null alleles that affects the morphogenesis of mandibular skeletal structures from regions where *Dlx1* and *Dlx5* expression overlaps. However, the phenotypes of the *Dlx1*^{-/-}; *Dlx5*^{+/-} mutants are less severe than those of the *Dlx2*^{-/-}; *Dlx5*^{+/-} mutants, and in several ways more resemble the *Dlx2*^{+/-}; *Dlx5*^{+/-} mutants (Fig. 14E; compare with Figs 11 and 13). The external morphology of the *Dlx1*^{-/-}; *Dlx5*^{+/-} mutants clearly identifies them as such but is not as striking as that of the *Dlx2*^{-/-}; *Dlx5*^{+/-} mutants: for example, the external ear is more developed, and the mandible is not cleft (not shown).

The proximal dentaries of the mutants are mostly represented by truncated condylar processes with

miniscule unattached tips (black arrow, Fig. 14E); they are, however, slightly smaller than those of the *Dlx2^{+/-}*; *Dlx5^{-/-}* mutants (compare with Fig. 13G). Each condylar process runs toward (without reaching) a squamosal, which lacks a fully extended zygomatic process (red and black arrow, Fig. 14E). Ectopic ossifications are also associated with the proximolingual aspects of the dentaries and pterygoids, and the caudolingual aspect of the dentary is significantly dissociated from the caudobuccal aspect. However, unlike with the *Dlx2^{+/-}*; *Dlx5^{-/-}* mutant, jugals are never observed (Fig. 14E). Overall, the dentary is anteriorly placed and closely apposed to the maxilla (Fig. 14B). Each maxilla has a diminished molar alveolus. Similar to what is seen in the *Dlx2^{+/-}*; *Dlx5^{-/-}* mutant, the entire zygomatic process and ventral optic support is of maxillary origin, and consists of a short but robust caudal process and a similarly short and robust ectopic rostral projection (see mx, Fig. 14E).

However, as in the *Dlx2^{+/-}*; *Dlx5^{-/-}* mutants, the body of Meckel's cartilage in the *Dlx1^{-/-}*; *Dlx5^{-/-}* mutants is present but deviated: one part projects toward the squamosal and resembles the alisphenoid, while another projects toward the basitrabecular process (with the os paradoxicum) (Fig. 14E); each portion is associated, moreover, with greater degrees of ossification than are encountered in the *Dlx2^{+/-}*; *Dlx5^{-/-}* mutants. A well-developed, though aberrant, articulation by this ossified portion of the bMC with the ventral squamosal develops (black and white arrow, Fig. 14E). The squamosals are likewise similar to those seen in the *Dlx2^{+/-}*; *Dlx5^{-/-}* mutants: they contain retrotympanic processes with a foramen (yellow arrowhead, Fig. 14E), have no distinguished caudal processes (orange arrowhead, Fig. 14E), and possess expanded laminar and sphenotic processes. The incudes and mallei are fused, and although the processes of each are present, they are thicker and more dysmorphic than with the *Dlx2^{+/-}*; *Dlx5^{-/-}* mutants (compare Figs 13F, 13H and 14E). Moreover, both the crus brevis and the crus longus of each incus is uniquely bent caudad toward the tympanohyal in an inverted 'C' shape (Fig. 14E). The ectotympanic is probably represented by the small centre of ossification that forms near the processus brevis of the malleus ('etm' of Fig. 14E). A distinct gonial is absent, and probably has been subsumed into the os paradoxicum and/or the ossifying body of Meckel's cartilage. Moreover, the body of the hyoid, although not cleft, has two centres of ossification (red and white arrow-

heads, Fig. 14E), and the horns are truncated and fused to the body; the thyroid cartilage generally only lacks superior cornu. The styloid process is represented by a tympanohyal (tmh) rostrally displaced on the otic capsule; a separate, disconnected stylohyal forms at its distal tip (much like with the *Dlx2^{+/-}*; *Dlx5^{-/-}* mutants).

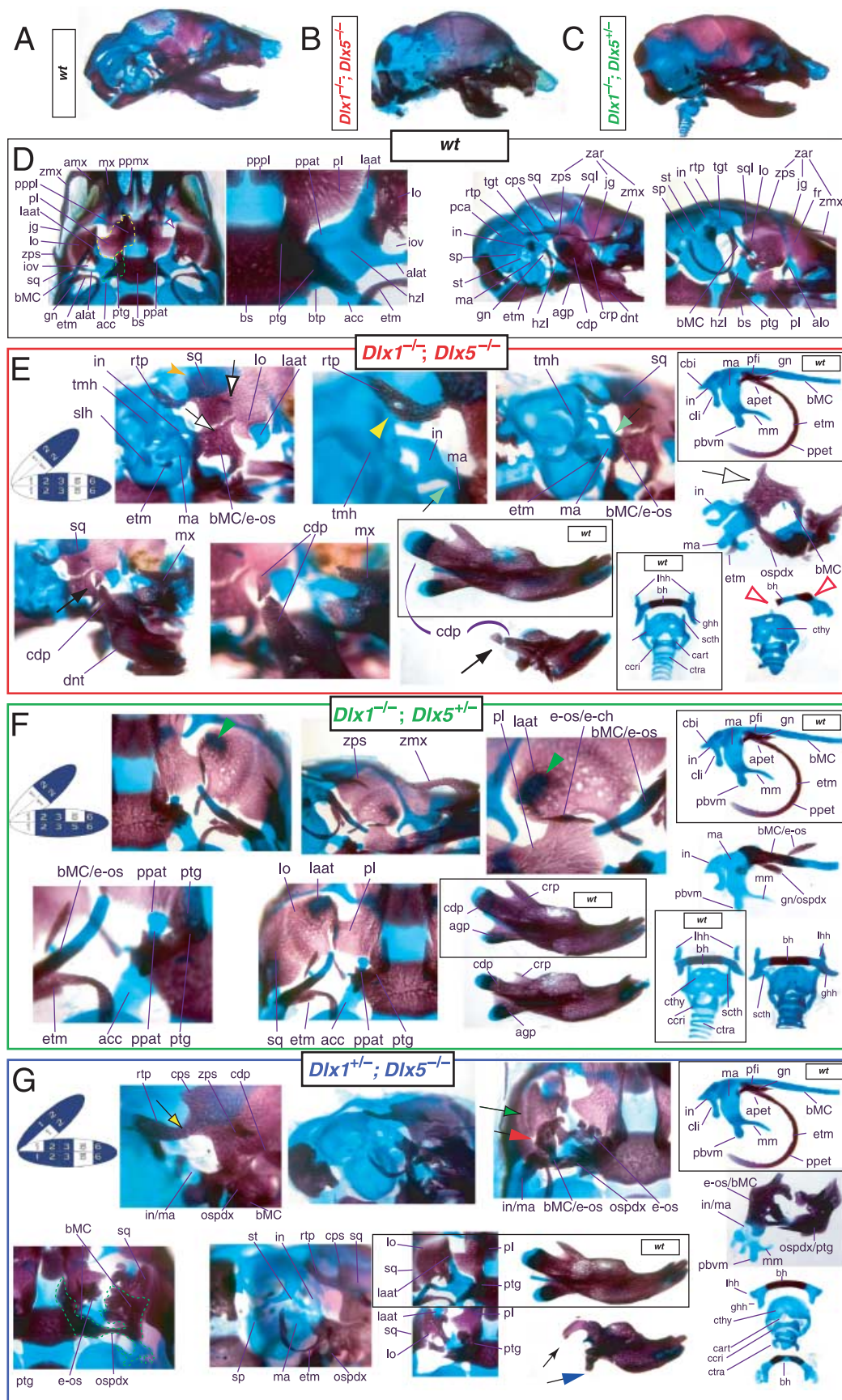
It is worth noting that characteristics associated with the *Dlx1* and *Dlx5* single mutants are, in general, present in the *Dlx1^{-/-}*; *Dlx5^{-/-}* mutants. The sensory capsules are modified (as with the *Dlx5^{-/-}* mutants), and the ala temporalis is represented principally by the dorsal tip of the ascending lamina and associated dermal lamina obturans (lo, laat, Fig. 14E). The dermal bone, however, is associated only with the cartilage of the dorsal tip, and, unlike the *Dlx1^{-/-}* mutants, does not extend toward the basitrabecular process. Moreover, the palate is cleft (not shown).

We have found, then, that the compound homozygous *Dlx1^{-/-}*; *Dlx5^{-/-}* mutants phenotypically resemble more the *Dlx2^{+/-}*; *Dlx5^{-/-}* mutants in some respects (e.g. the deviation and ossification of the body of Meckel's cartilage and the state of the proximal dentary) than they do the *Dlx2^{+/-}*; *Dlx5^{-/-}* mutants (which, for example, have no clear incus or malleus to be fused or a condylar process of the dentary). Thus, in a *Dlx5* null background, the less drastic phenotypic transformations seen in the *Dlx1^{-/-}* mutants, relative to the *Dlx2^{+/-}* mutants, are replicated in the more distal BA derivatives. This relative and comparative trend is also seen with the *Dlx1^{-/-}*; *Dlx5^{+/-}* mutants and the *Dlx1^{+/-}*; *Dlx5^{-/-}* mutants (Fig. 14F,G). In summary, these morphological transformations demonstrate a dosage-dependent genetic interaction between the third-order paralogous *Dlx* genes, *Dlx1* and *Dlx5*, in regulating distal BA1 and BA2 development.

Evidence for a role for *Dlx3* in BA development: genetic interaction of *Dlx3* and *Dlx5*

Having seen that first-, second- and third-order *Dlx* genes interact in regulating BA development, we sought evidence that this was not specific to *Dlx1*, *Dlx2*, *Dlx5* and *Dlx6*. Therefore, we tested the interaction between the nested second-order paralogues, *Dlx3* and *Dlx5*. As *Dlx3^{-/-}* mutants die around E10.5 due to placental failure (Morasso et al. 1999), we studied *Dlx3^{+/-}*; *Dlx5^{-/-}* mutants.

Compound *Dlx3^{+/-}*; *Dlx5^{-/-}* mutants have distinct skeletal transformations relative to *Dlx5^{-/-}* mutants



(Fig. 15). Of note, whereas the proportion of *Dlx5*^{-/-} mutants that are exencephalic is closer to 1 in 4, 80% of the compound *Dlx3*^{+/-}; *Dlx5*^{-/-} mutants examined were exencephalic (see Fig. 15D). Furthermore, uncharacteristic of the exencephaly in other Dlx mutants, this neural tube defect may have affected the distal BA morphology as the exencephalic and non-exencephalic dentaries are slightly different at their proximal ends (though neither resembles the *Dlx5*^{-/-} dentary; Fig. 15F,G). In both states, the condylar and angular processes are diminished and little secondary cartilage is seen. Although a well-formed jugal is present, it is orientated toward the dentary, and the squamosal of the non-exencephalic mutants, in most other respects similar to that of the *Dlx1*^{+/-}; *Dlx5*^{-/-} and *Dlx1*^{-/-}; *Dlx5*^{-/-} mutants, has no zygomatic process to come out to meet it (red and black arrowhead, Fig. 15F).

A thickened corpus of the incus is fused to the malleal head (green arrowhead, Fig. 15F). The crus brevis of the incus, moreover, is uniquely fused caudally to the otic capsule (red arrowhead, Fig. 15F). As with the *Dlx1*^{+/-}; *Dlx5*^{-/-} and *Dlx2*^{+/-}; *Dlx5*^{-/-} mutants, the body of Meckel's cartilage is split, with an ossified branch running rostrad; an extensive os paradoxicum is also in evidence. Although these structures are similar in the three mutants, they are clearly distinct; for instance, the ossification that runs to the squamosal is relatively smaller and that running to the midline is relatively larger in the *Dlx3*^{+/-}; *Dlx5*^{-/-} mutants than in the *Dlx2*^{+/-}; *Dlx5*^{-/-} mutants (compare Figs 13F, 14E and 15F). The

ectotympanics are variably truncated, often with a split between diminutive anterior and posterior processes (Fig. 15H).

Such evidence of a genetic interaction leads to the conclusion that, like all other murine *Dlx* genes thus far tested, *Dlx3* participates in the development of the BA skeleton. We have seen therefore that *Dlx1*, *Dlx2*, *Dlx3*, *Dlx5* and *Dlx6* each make a contribution to BA skeletal development, consistent with a combinatorial *Dlx* code model.

***Dlx1/2*^{-/-}; *Dlx5*^{-/-} mutants: BA development in light of the loss of both a linked-pair partner and a paralogous partner**

Thus far, we have presented evidence that the loss-of-function of one or two *Dlx* genes leads to transformations of BA pattern and morphogenesis. The evidence for genetic interactions has been, however, either between two linked-pair first-order paralogous genes or two second-order paralogous genes. To evaluate BA development with a further reduction in *Dlx* dosage, we generated mice lacking *Dlx1*, *Dlx2* and *Dlx5* (i.e. a linked-pair plus second-order paralogues) (Fig. 16).

The characteristics of the proximal BA transformations of the *Dlx1/2*^{-/-}; *Dlx5*^{-/-} mutant are, perhaps surprisingly, not identical to those of the *Dlx1/2*^{-/-} mutants, further demonstrating that nested genes such as *Dlx5* can affect mxBA1 development in a compromised background. For example, the palatal and maxillary

Fig. 14 Skeletal analysis of the [*Dlx1*^{+/-}; *Dlx5*^{-/-}], [*Dlx1*^{-/-}; *Dlx5*^{+/-}] and [*Dlx1*^{+/-}; *Dlx5*^{+/-}] mutants through differential staining of bone (alizarin red) and cartilage (alcian blue). (A) Norma lateralis view of a P0 wild-type skull. (B) Norma lateralis view of a *Dlx1*^{+/-}; *Dlx5*^{-/-} neonatal skull. (C) Norma lateralis view of a *Dlx1*^{-/-}; *Dlx5*^{+/-} neonatal skull. (D) Wild-type P0 skulls highlighting, left to right, the palatal region (norma basalis; yellow line outlining the palatine and green line outlining the pterygoid), the ala temporalis and lamina obturans components of the alisphenoid, norma lateralis view of the ear region with the primary and secondary jaw articulations, and the middle ear without the dentary attached. (E) P0 skulls of *Dlx1*^{+/-}; *Dlx5*^{-/-} mutants. The yellow arrowhead indicates the foramen in the retrotympenic process of the squamosal. The black and green arrow points to the fusion of the incus and malleus. The black and white arrow points to the edge of the transformed osseous body of Meckel's cartilage that articulates with the squamosal. The orange arrowhead highlights the loss of normal dorsal squamosal architecture, while the red and black arrow indicates the truncation of the zygomatic process of the squamosal, the black arrow highlights the diminished condylar process of the dentary. The two centres of ossification in the aberrant hyoid are indicated by the red and white arrowheads. A reference schema indicating the loss of two *Dlx1* alleles and two *Dlx5* alleles in BA1 is included. (F) P0 skulls of *Dlx1*^{+/-}; *Dlx5*^{+/-} mutants. The green arrowhead indicates the remnant of the distal tip of the ascending lamina that remains cartilaginous, a feature associated with the loss of *Dlx1*. A reference schema indicating the loss of two *Dlx1* alleles and one *Dlx5* allele in BA1 is included. (G) P0 skulls of *Dlx1*^{+/-}; *Dlx5*^{-/-} mutants. The black and green arrow indicates the dysmorphic ala temporalis and the red and black arrow indicates the transformation of the body of Meckel's cartilage, while the black arrow points to the dysmorphic condylar processes. The yellow and black arrow indicates the dysmorphology of the squamosal, and the black and blue arrow points to the dysmorphic angular process that is associated with the proximolingual aspect of the dentary. A reference schema indicating the loss of one *Dlx1* allele and two *Dlx5* alleles in BA1 is included. See text for further descriptions and list for abbreviations.

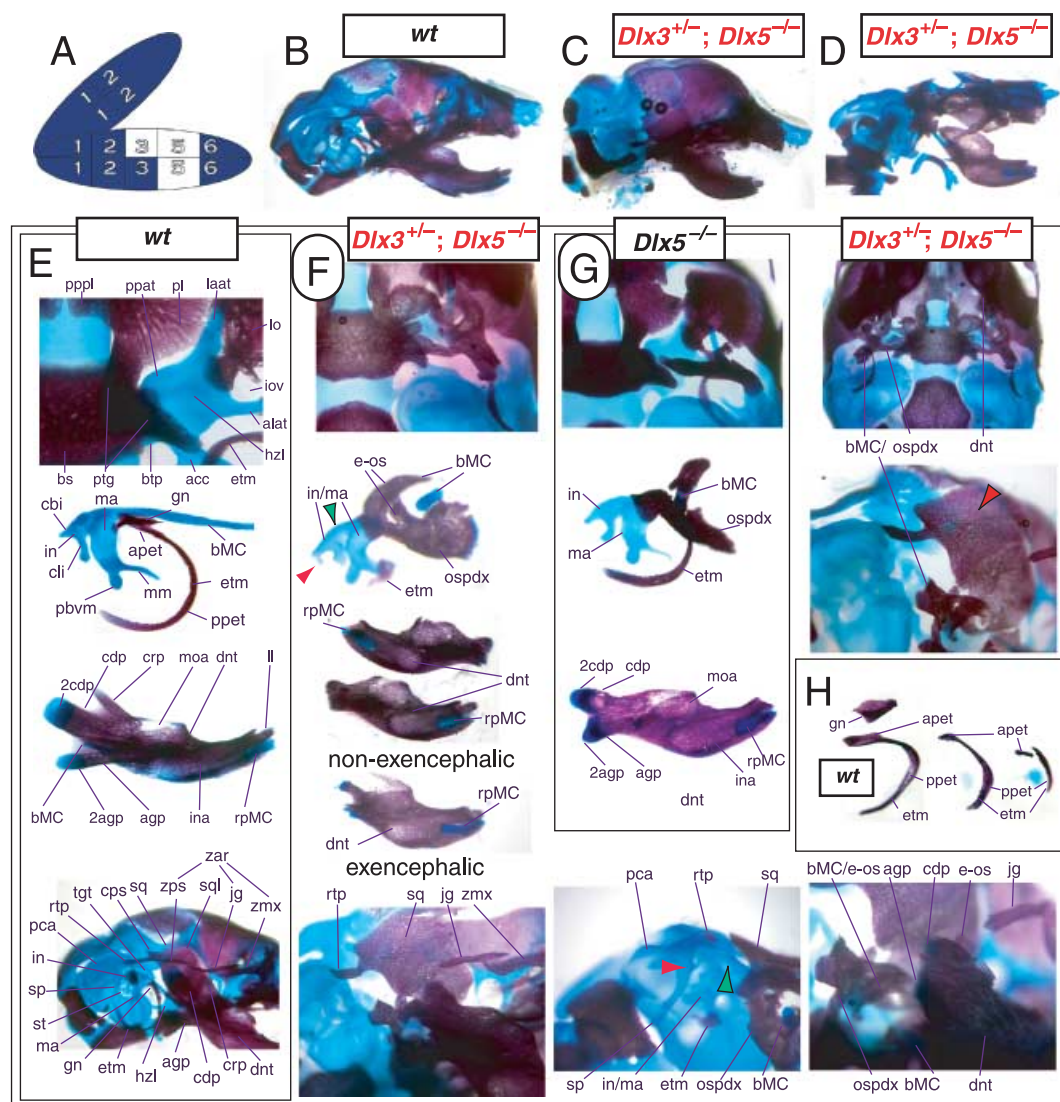


Fig. 15 Skeletal analysis of the *Dlx3*^{+/-}; *Dlx5*^{-/-} mutant. (A) Reference schema indicating the loss of one *Dlx3* allele and two *Dlx5* alleles in BA1. (B) Norma lateralis view of a P0 wild-type skull. (C) Non-exencephalic and (D) exencephalic norma lateralis views of P0 *Dlx3*^{+/-}; *Dlx5*^{-/-} mutant skulls. (E) Wild-type P0 skulls highlighting, top to bottom, norma basalis view of the ala temporalis and lamina obturans components of the alisphenoid, middle ear structures, and norma lateralis views of a wild-type mandible, and middle ear with the dentary attached. (F) P0 skulls of *Dlx3*^{+/-}; *Dlx5*^{-/-} mutants. The red arrowheads indicate the points of fusion between the head of the incus and the otic capsule, while the green arrows point to the fusion between the malleus and the crus brevis of the incus. The red and black arrowhead indicates the complete loss of the zygomatic process of the squamosal. (G) *Dlx5*^{-/-} mutant middle ear structures and mandible for comparison. (H) Comparisons of wild-type and *Dlx3*^{+/-}; *Dlx5*^{-/-} ectotympanic development. See text for further descriptions and list for abbreviations.

palatal shelves are not completely cleft (black and white arrowhead, Fig. 16B), the transformed side walls have fewer and smaller centres of ossification (os 1–4), and both the palatoquadrate (pq*) and the lamina ascendens (laat) cartilages are considerably less robust (Fig. 16B).

Furthermore, although they are similar to the compound *Dlx2*^{-/-}; *Dlx5*^{-/-} mutants, the compound *Dlx1/2*^{-/-}; *Dlx5*^{-/-} mutants are not identical and present a distinct

phenotype. Occasionally, amorphic cartilages are found topographically in place of definitive mallei and incudes (e-ch, Fig. 16B); otherwise, there is no evidence of either. Ectotympanics and gonials are also lacking. Two processes extend from the basisphenoid (strt*), but they are distinctly less robust than the struts seen in the *Dlx1/2*^{-/-} mutants. The larger is cartilaginous, with an endochondral centre of ossification (orange arrowhead, Fig. 16B), and extends toward the rostral otic

capsule. Its tip is bifurcated, and runs caudad toward the dysmorphic styloid process (green arrowhead, Fig. 16B), which is represented by a tympanohyal (tmh) element. As with the *Dlx2^{-/-}*; *Dlx5^{-/-}* mutants, the palatoquadrate cartilage (pq*) is fused to the taenia marginalis and the otic capsule (red and blue arrowhead, Fig. 16B). While the tympanohyal of the *Dlx2^{-/-}*; *Dlx5^{-/-}* mutants is truncated with an ectopic cartilage at its tip, the tympanohyal of the *Dlx1/2^{-/-}*; *Dlx5^{-/-}* mutants is even shorter and runs caudad at its tip. This tip may be crescent shaped. No evidence of a stapes or a round window is observed. The second process mentioned above is a shorter osseous spicule caudal to, and parallel with, the first (black and yellow arrowhead, Fig. 16B). The body of the hyoid, moreover, is cleft (Fig. 16B), and the associated, hypoplastic thyroid cartilage is even less developed than that of the *Dlx2^{-/-}*; *Dlx5^{-/-}* mutants.

Each dentary is severely truncated, having lost most of its proximal, articular end, but certainly not so much more so than in the *Dlx2^{-/-}*; *Dlx5^{-/-}* mutants (Fig. 16B). Each is represented by a diminished incisive alveolus, one or two incisors (one-quarter of the dentaries contain duplicated incisors) and the rostral process of Meckel's cartilage; unlike with the *Dlx2^{-/-}*; *Dlx5^{-/-}* mutants, a molar alveolus does not appear. The caudal borders of the dentary may contain a miniscule free-standing cartilaginous nodule (blue and black arrow, Fig. 16B). The dentary, moreover, articulates with the maxilla but has no coronoid, angular or condylar process (Fig. 16B); rather (perhaps surprisingly), it has some similarity to the endogenous maxilla in that it extends laterad, to articulate with the maxilla, an osseous process with an extensive foramen (green and black arrow, Fig. 16). This process and foramen also bears a superficial similarity to the frontal process and infraorbital foramen of the transformed *Dlx5/6^{-/-}* lower jaw maxilla (mx*, Fig. 8): with the *Dlx5/6^{-/-}* mutant, however, the process and foramen forms at the distal extremity of the neomorphic maxilla, and is associated with a molar alveolus caudo-proximal to it, whereas in the *Dlx1/2^{-/-}*; *Dlx5^{-/-}* mutant, this process and its foramen itself lies caudo-proximal to the more antero-distal extending incisive alveolus and incisors.

***Dlx1/2^{-/-}*; *Dlx5^{-/-}* and *Dlx1/2^{-/-}*; *Dlx5^{-/-}* mutants**

The distinctiveness of the phenotype of the compound *Dlx1/2^{-/-}*; *Dlx5^{-/-}* mutants suggests that a genetic inter-

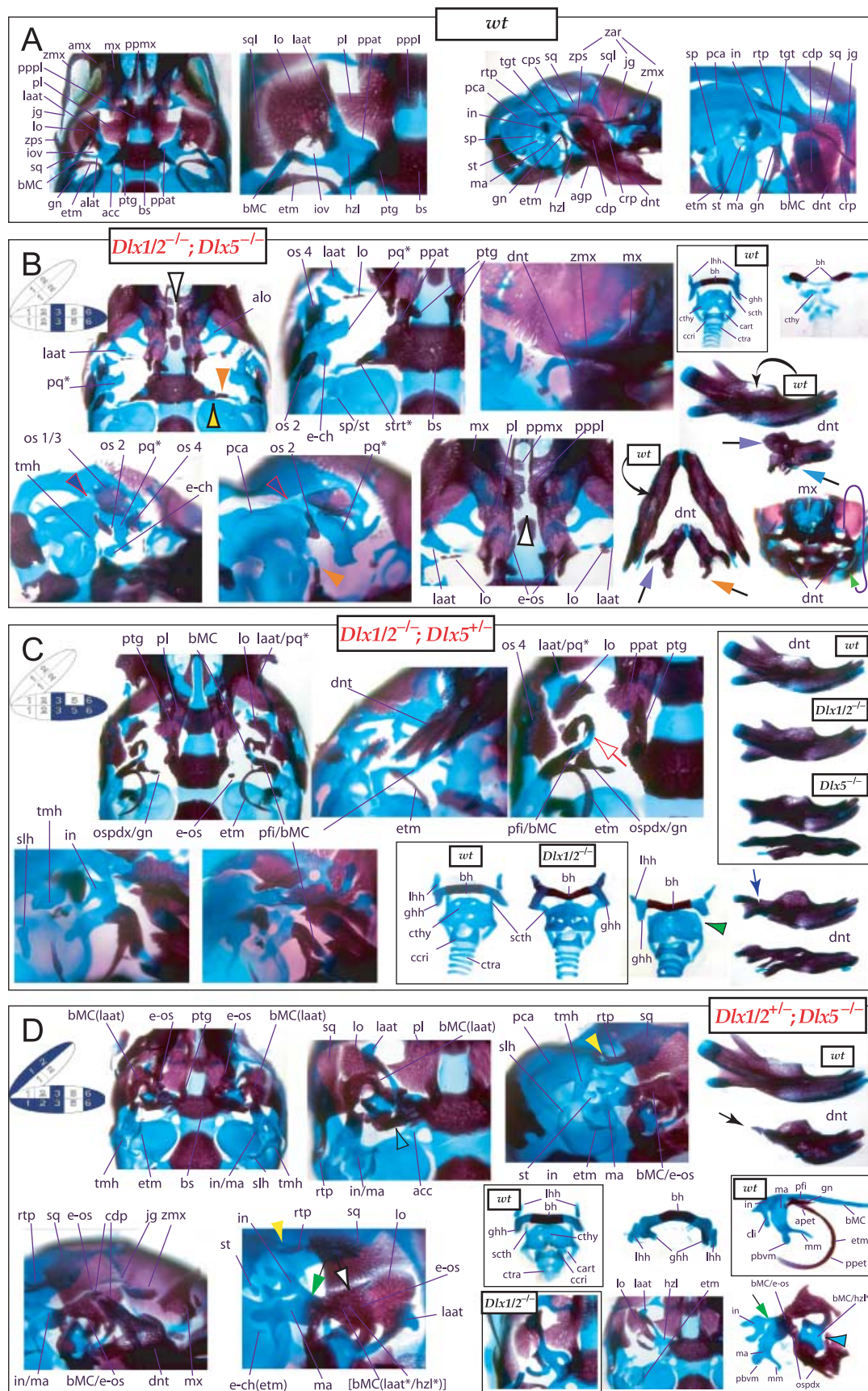
action occurs between these three genes. This is further in evidence when examining the compound [*Dlx1/2^{-/-}*; *Dlx5^{-/-}*] and [*Dlx1/2^{-/-}*; *Dlx5^{-/-}*] mutants (Fig. 16C,D).

As [*Dlx1/2^{-/-}*; *Dlx5^{-/-}*] and [*Dlx1/2^{-/-}*; *Dlx5^{-/-}*] mutants have phenotypes that are related to but somewhat augmented compared with *Dlx2^{-/-}*; *Dlx5^{-/-}* and *Dlx2^{-/-}*; *Dlx5^{-/-}* mutants, respectively, we make only a few points here. For example, in the *Dlx1/2^{-/-}*; *Dlx5^{-/-}* mutants, the body of Meckel's cartilage is clearly split; the rostral tip extending from the processus folii of the malleus is ossified and bends back caudolaterad (red and white arrow, Fig. 16C). An unarticulated os paradoxicum/gonial is also seen. The dentary lacks a coronoid process, and the angular and condylar processes are more juxtaposed and smaller than in the *Dlx2^{-/-}*; *Dlx5^{-/-}* mutants (blue arrow, Fig. 16C). Although the body of the hyoid is cleft as with the *Dlx1/2^{-/-}* mutants, the greater horns are shortened and do not fuse with the superior cornu of the thyroid cartilage (green and black arrowhead, Fig. 16C).

The dentary of the *Dlx1/2^{-/-}*; *Dlx5^{-/-}* mutants has a condylar process, including the disarticulated tip, but it is distinctly smaller than those seen in either the *Dlx1^{-/-}*; *Dlx5^{-/-}* or the *Dlx2^{-/-}*; *Dlx5^{-/-}* mutants (black arrow, Fig. 16D). Meckel's cartilage makes a loop, and actually has a large un-ossified region parallel to the horizontal lamina of the ala temporalis with which it has great similarity (black and turquoise arrowhead, Fig. 16D). The os paradoxicum is extensive, and may be found fused to an ectopic pterygoid bone. In a number of respects, the features of the transformed region of Meckel's cartilage and malleus are similar to the *Dlx3^{-/-}*; *Dlx5^{-/-}* mutants. For example, whereas the malleus and incus are fused, the incus is more crescent shaped, and bent back toward the otic capsule (Fig. 16D). In addition, the ectotympanic is usually a spicule of bone (etm, Fig. 16D), although its position may be marked by a single small ectopic cartilaginous nodule as well.

Minimal transformation of the BA in the *Dlx3^{-/-}*; *Dlx1/2^{-/-}* mutants

We have presented evidence of a distinct genetic interaction between the linked-pair genes *Dlx1* and *Dlx2* and the nested gene, *Dlx5*. Likewise, we have demonstrated that the nested gene, *Dlx3*, interacts genetically with *Dlx5*. This suggested the possibility that *Dlx3* might also genetically interact with the *Dlx1* and *Dlx2* linked-pair. We therefore generated *Dlx3^{-/-}*; *Dlx1/2^{-/-}*



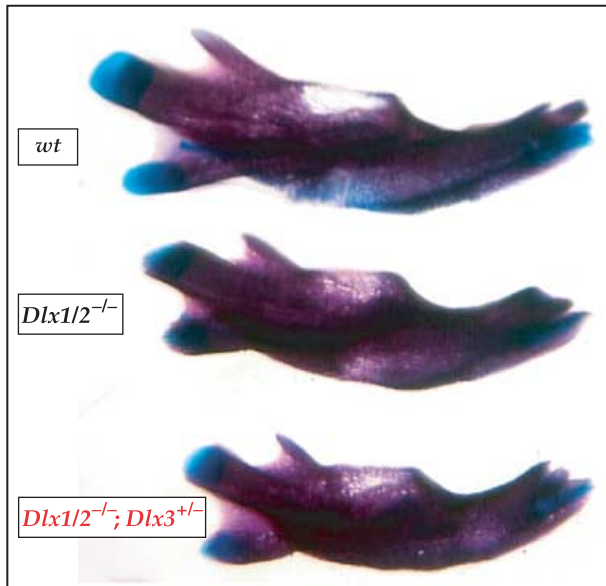


Fig. 17 Dentary of compound a *Dlx1/2^{-/-}; Dlx3^{+/-}* mutant (bottom) as compared with a wild-type (top) and a *Dlx1/2^{-/-}* single mutant (middle). Note the decrease in size of the proximal end of the dentary, in particular of the three processes, of the *Dlx1/2^{-/-}* mutant and the exacerbation of this decrease in the *Dlx1/2^{-/-}; Dlx3^{+/-}* mutant.

mutants. Unlike the *Dlx5^{+/-}; Dlx1/2^{-/-}* mutants, in the *Dlx3^{+/-}; Dlx1/2^{-/-}* mutants we found only minimal transformations of BA skeletal elements not already seen in the *Dlx1/2^{-/-}* mutants (Fig. 17). The main difference is in the smaller overall size of the dentaries (relative to both wild-type and *Dlx1/2^{-/-}* mutant) and the presence of a germinal os paradoxicum (not shown).

Transformations resulting from the compound loss of single *Dlx* gene alleles

Neonatal lethality with phenotypic similarity to *Dlx5^{-/-}* mutants in compound *Dlx1/2^{+/-}; Dlx5/6^{+/-}* heterozygotes

We have seen that the replication of regional *Dlx* expression resulted in the replication of regional skeletal identity, pattern, and morphogenesis: loss of both *Dlx5* and *Dlx6* resulted in two regions solely expressing *Dlx1* and *Dlx2*, the subsequent result of which was the transformation of the lower jaw into an upper jaw. We hypothesized that the combined loss of *Dlx1*, *Dlx2*, *Dlx5* and *Dlx6* would have a similar result, namely that the transformations of proximal BA elements seen in the *Dlx1/2^{-/-}* mutants would be replicated in the distal elements.

We were unable to test this possibility because compound *Dlx1/2^{+/-}; Dlx5/6^{+/-}* heterozygotes die as neonates, probably as a result of a transformation of the pharyngeal region rather similar to that of the *Dlx5^{-/-}* mutants (Fig. 18). They exhibited the alteration of the ala temporalis characteristic of the *Dlx1/2^{+/-}* heterozygotes. As with the *Dlx5^{-/-}* mutants, *Dlx1/2^{+/-}; Dlx5/6^{+/-}* heterozygotes had a deviated Meckel's cartilage and an extensive os paradoxicum (Fig. 18E, E', E''). The proximal dentary is likewise modified similar to that of the *Dlx5^{-/-}* mutants: a coronoid process is not present, and the angular and condylar processes are truncated and juxtaposed (Fig. 18G). The dentary, however, is slightly larger than that of the *Dlx5^{-/-}* mutants (compare

Fig. 16 Skeletal analysis of compound *Dlx1; Dlx2; Dlx5* mutants. (A) Wild-type P0 skulls highlighting, left to right, the palatal region (norma basalis), the ala temporalis and lamina obturans components of the alisphenoid, and the primary and secondary jaw articulations, and the middle ear with the dentary associated. (B) P0 and E16.5 skulls of *Dlx1/2^{-/-}; Dlx5^{-/-}* mutants and a reference schema indicating the loss of two *Dlx1* alleles, two *Dlx2* alleles and two *Dlx5* alleles. The orange arrowhead points to the cartilaginous strut that extends from the basisphenoid toward the rostral otic capsule, while the black and yellow arrowhead indicates the associated parallel dermal ossification. The red and blue arrowhead points to the extensive fusion of the remnant of the pars canicularis of the otic capsule to the taenia marginalis and parietal plate. The black and green arrow indicates the extensive foramen (infraorbital?) that develops in a lateral process (black and purple arrow) emanating from the caudal end of the incisive canal. The orange and black arrow points to the lingual aspect of the truncated dentary. Note the absence of a molar alveolus. The blue and black arrow highlights a cartilaginous nodule often associated with the proximal end of the dentary. The black and white arrowhead brings attention to the nature of the palate: while still cleft, the palatal development progresses further than in the *Dlx1/2^{-/-}* single mutants. (C) P0 and skulls of *Dlx1/2^{-/-}; Dlx5^{+/-}* mutants. A reference schema indicating the loss of two *Dlx1* alleles, two *Dlx2* alleles and one *Dlx5* allele is included. The blue arrow indicates the exacerbated deficiency in proximal dentary development exhibited by the *Dlx1/2^{-/-}; Dlx5^{+/-}* mutants relative to the *Dlx2^{-/-}; Dlx5^{+/-}* mutants. The red and white arrow indicates the disruption of Meckel's cartilage, while the green and black arrowhead points to the loss of the superior cornu of the thyroid cartilage. (D) P0 skulls of *Dlx1/2^{+/-}; Dlx5^{-/-}* mutants. A reference schema indicating the loss of one *Dlx1* allele, one *Dlx2* allele and two *Dlx5* alleles is included. The yellow arrowhead indicates the foramen in the retrotympenic process of the squamosal. The black and green arrow points to the fusion of the incus and malleus, and the black and white arrow points to the edge of the transformed osseous body of Meckel's cartilage that articulates with the squamosal. The black and turquoise arrowhead indicates the expanded, un-ossified lamina formed from the medial projection of the transformed body of Meckel's cartilage. The black arrow points to the deficiencies of the dentary. See text for further descriptions and list for abbreviations.

Fig. 18B,E). Moreover, the thyroid cartilage lacks extended superior cornu (not shown).

Similar neonatal lethality in *Dlx2*^{+/-}; *Dlx5/6*^{+/-} heterozygotes

Owing to the size and nature of the distal BA transformations observed with the *Dlx1/2*^{+/-}; *Dlx5/6*^{+/-} heterozygotes, we hypothesized that *Dlx2*^{+/-}; *Dlx5/6*^{+/-} heterozygotes would likewise develop an os paradoxicum and truncated dentary. Therefore, we generated compound *Dlx2*^{+/-}; *Dlx5/6*^{+/-} heterozygote neonates; these also died at birth. Indeed, they too had a truncated dentary and an os paradoxicum, though the transformations were not as extensive as with those seen in the *Dlx1/2*^{+/-}; *Dlx5/6*^{+/-} compound heterozygotes (Fig. 18C).

Extensive heterozygosity: [*Dlx1*^{+/-}; *Dlx2*^{+/-}; *Dlx3*^{+/-}; *Dlx5*^{+/-}; *Dlx6*^{+/-}] mutants

We have seen evidence above that each allele of a *Dlx* gene is significant with regard to the development and pattern of the BA skeleton. As a last presentation of evidence for this point, we show here the phenotype

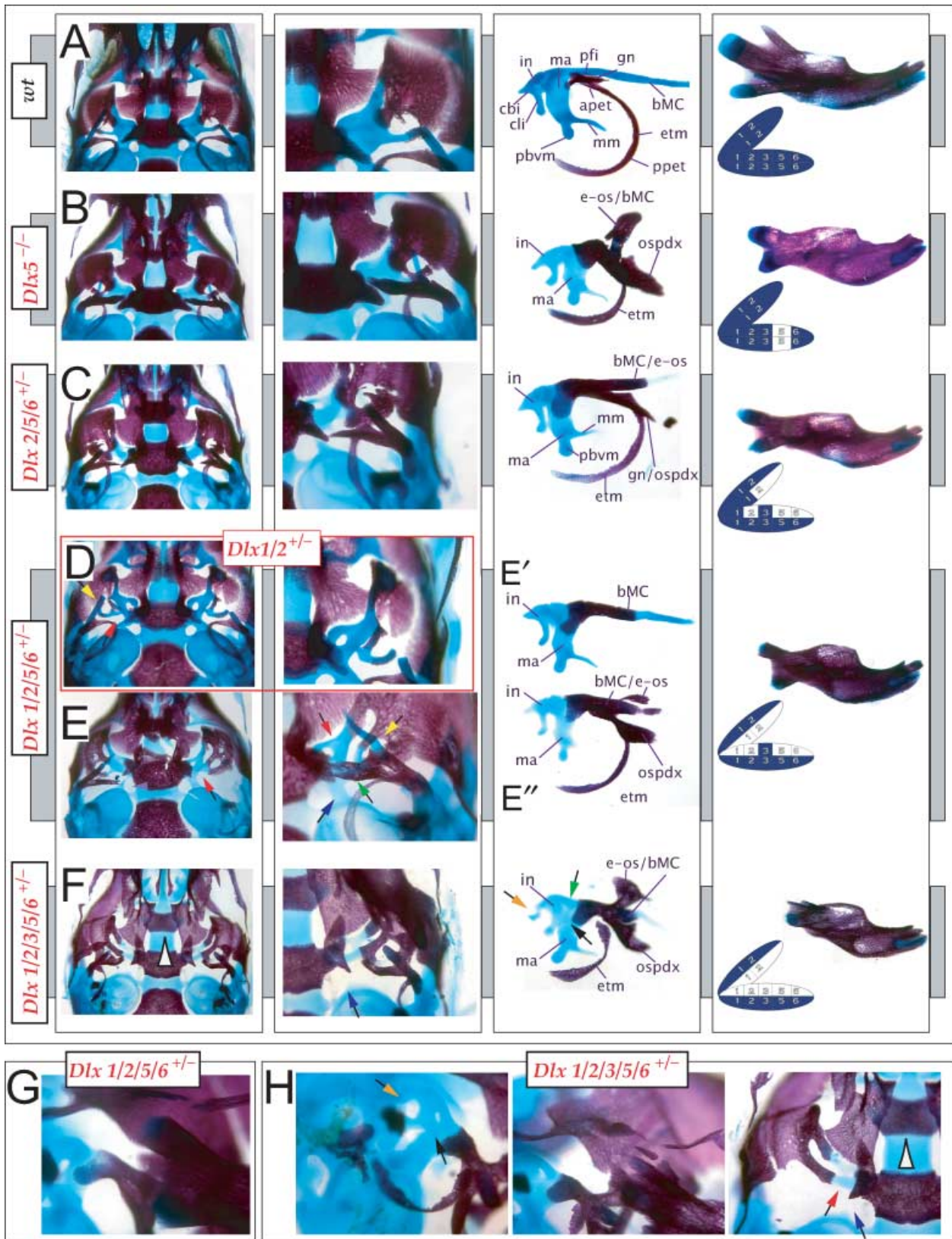
of mice heterozygous for five of the six known *Dlx* genes, i.e. [*Dlx1*^{+/-}; *Dlx2*^{+/-}; *Dlx3*^{+/-}; *Dlx5*^{+/-}; *Dlx6*^{+/-}] mutants (Fig. 18F,H). As one would now expect these mutants have truncated proximal dentaries and ectotympanics, possess ectopic os paradoxicums and have bodies of Meckel's cartilage that are split. The ala temporalis is diminished (black and red arrows, Fig. 18H), the alicochlear commissure is lacking (blue and black arrow, Fig. 18F,H) and the palate is extensively cleft (black and white arrowheads, Fig. 18F,G). Moreover, the incus is fused both with the crista parotica (orange and black arrows, Fig. 18F,H) and with the malleus (black arrow, Fig. 18F,H).

Testing Equivalents: comparing first-, second- and third order paralogues and comparing unique combinations and numbers of *Dlx* alleles

Dlx6^{+/-}; *Dlx5*^{+/-} mutants: phenotypic similarity to, but not identity with, *Dlx2*^{+/-}; *Dlx5*^{+/-} and *Dlx1*^{+/-}; *Dlx5*^{+/-} mutants

We have seen above that distal BA derivatives are extensively modified in a *Dlx5* null background. This is

Fig. 18 Comparison of *Dlx5*^{+/-} mutants with compound [*Dlx2*^{+/-}; *Dlx5/6*^{+/-}], [*Dlx1/2*^{+/-}; *Dlx5/6*^{+/-}] and [*Dlx1/2*^{+/-}; *Dlx3*^{+/-}; *Dlx5/6*^{+/-}] heterozygous mutant mice. (A) Wild-type structures of a neonate for comparison. Left to right: cranial base (norma basalis) minus dentaries; alisphenoid; incus, malleus, proximal body of Meckel's cartilage, ectotympanic and gonial; dentary and wild-type allele diagram. (B) Similar panel of *Dlx5*^{+/-} mutant neonatal phenotypes for comparison. (C) Compound *Dlx2*^{+/-}; *Dlx5/6*^{+/-} heterozygous mutant neonatal skulls. Note the similarity to the *Dlx5*^{+/-} neonate in the development of the proximal mdBA1 structures, including the loss of the coronoid process of the dentary, juxtaposition of the condylar process and angular processes, and the presence of an ectopic os paradoxicum (ospdx). (D) Views of the *Dlx1/2*^{+/-} neonatal cranial base (boxed in red, norma basalis) minus dentaries and magnified view of the alisphenoid highlighting the degradation of the horizontal lamina of the ala temporalis (red and black arrow) but normal body of Meckel's cartilage (yellow and black arrow). (E,E',E'') Panel of *Dlx1/2*^{+/-}; *Dlx5/6*^{+/-} neonatal cranial structures. (E) Views of the *Dlx1/2*^{+/-}; *Dlx5/6*^{+/-} neonatal cranial base (norma basalis) minus dentaries, magnified view of the alisphenoid, dissected middle ear elements and dentary. Note the similarity to the loss of both alleles of *Dlx5* and exacerbation of phenotype, due to the loss of a single allele of *Dlx1*, compared with the *Dlx2*^{+/-}; *Dlx5/6*^{+/-} compound heterozygous mutant. Red and black arrows point to the horizontal lamina of the ala temporalis, whose development is slightly more disrupted than that of the *Dlx1/2*^{+/-} neonate. The yellow and black arrow indicates the remnant of the body of Meckel's cartilage, while the green and black arrow points to the developing os paradoxicum. The purple and black arrow indicates the variable development of the alicochlear commissure. (E') Dissected incus, malleus and precociously ossified proximal body of Meckel's cartilage. (E'') Dissected incus, malleus and proximal body of Meckel's cartilage along with associated ectotympanic, os paradoxicum and ectopic dermal ossification. (F) Views of the compound [*Dlx1/2*^{+/-}; *Dlx3*^{+/-}; *Dlx5/6*^{+/-}] heterozygous mutant neonatal cranial base (norma basalis) minus dentaries, magnified view of the alisphenoid, dissected middle ear elements and dentary. Note the exacerbation of phenotype, due to the additional loss of a single allele of *Dlx3*, as compared with the *Dlx1/2*^{+/-}; *Dlx5/6*^{+/-} compound heterozygous mutant. The white and black arrow indicates the cleft palate found in this mutant. Red and black arrows point to the horizontal lamina of the ala temporalis, whose development is slightly more disrupted than that of the *Dlx1/2*^{+/-}; *Dlx5/6*^{+/-} neonate. The yellow and black arrowhead indicates the remnant of the body of Meckel's cartilage, while the green and black arrow points to the developing os paradoxicum. The purple and black arrow indicates the lack of the alicochlear commissure. (G) Secondary (functional) jaw joint of the *Dlx1/2*^{+/-}; *Dlx5/6*^{+/-} compound heterozygous mutant. (H) Additional views of the BA derivatives of compound *Dlx1/2*^{+/-}; *Dlx3*^{+/-}; *Dlx5/6*^{+/-} heterozygous mutant neonates. Left: middle ear bones *in situ*. Orange and black arrow points to the fusion of the incus to the crista parotica of the otic capsule. Light blue and black arrows indicate the points of fusion of the incus to the malleus. Centre: secondary (functional) jaw joint. Right: neurocranial base highlighting the exacerbated degradation of the horizontal lamina (red and black arrow) of the ala temporalis, loss of the alicochlear commissure (purple and black arrow), and cleft palate (white and black arrow).



pronounced with the additional loss of single alleles of its second-order paralogous genes, *Dlx2* and *Dlx3*. We have already seen that the additional loss of both alleles of the linked-pair gene, *Dlx6*, leads to a homeotic transformation within the BA skeleton, including an ectopic ala temporalis in place of Meckel's cartilage. We therefore generated *Dlx6^{-/-}*; *Dlx5^{+/-}* mutants in order to compare the result of *Dlx6* heterozygosity in a *Dlx5* null background with that observed with *Dlx2* and *Dlx3* heterozygosity (Fig. 19). Similar to [*Dlx2^{+/-}*; *Dlx5^{-/-}*], [*Dlx1^{-/-}*; *Dlx5^{-/-}*] and [*Dlx3^{+/-}*; *Dlx5^{-/-}*] mutants, *Dlx6^{-/-}*; *Dlx5^{+/-}* mutants possess dentaries that are severely truncated at their proximal ends. What remains of the dentary primarily comprises structures from the incisive region (the most distal mandible); a truncated condylar process, an os paradoxicum and a deviated body of Meckel's cartilage reminiscent of an alisphenoid also form (Fig. 19B,D,F). Moreover, the hyoid horns are also shortened (Fig. 19E). Although similar in nature, each of the above mutants has a distinct phenotype when the specific details are compared (compare Figs 13–15 and 19). It might be suggested therefore that when the BA are developmentally compromised by loss of *Dlx* alleles, each remaining *Dlx* allele makes both general and specific contributions to BA development and pattern.

Comparisons of [*Dlx2^{+/-}*; *Dlx5^{-/-}*; *Dlx6^{+/-}*], [*Dlx3^{+/-}*; *Dlx5^{-/-}*; *Dlx6^{+/-}*], [*Dlx1^{+/-}*; *Dlx2^{+/-}*; *Dlx5^{-/-}*; *Dlx6^{+/-}*] and [*Dlx5^{-/-}*; *Dlx6^{-/-}*] mutants

To evaluate further the notion that each allele makes a specific genetic contribution to BA development and pattern, we compared the loss of wild-type alleles of *Dlx2*, *Dlx3* and *Dlx6* in a background that was already compromised by the loss of both wild-type alleles of *Dlx5* as well as one allele of *Dlx6*. That is, we compared the following phenotypes: [*Dlx2^{+/-}*; *Dlx5^{-/-}*; *Dlx6^{+/-}*], [*Dlx3^{+/-}*; *Dlx5^{-/-}*; *Dlx6^{+/-}*], [*Dlx1^{+/-}*; *Dlx2^{+/-}*; *Dlx5^{-/-}*; *Dlx6^{+/-}*] and [*Dlx5^{-/-}*; *Dlx6^{-/-}*] (Figs 8 and 20).

[*Dlx2^{+/-}*; *Dlx5^{-/-}*; *Dlx6^{+/-}*] mutants die at birth. They have diminished ear pinnae relative to *Dlx5^{-/-}*; *Dlx6^{+/-}* mutants [but larger than with the *Dlx2^{-/-}*; *Dlx5^{-/-}* mutants (black arrows, Fig. 20A)]. The frontal aspect of the mutants exhibits a symmetrical jaw architecture of four roughly equivalent quadrants similar to, but distinct from, that of a non-exencephalic *Dlx5/6^{-/-}* mutant (Fig. 20A). As with the *Dlx1/2^{-/-}*; *Dlx5^{-/-}* mutants, a cartilaginous rod, with a centre of endochondral

ossification, extends from the basitrabecular process of the basisphenoid toward the parietal plate (green and black arrows, Fig. 20). Parallel and caudal to this is a dermal bone (larger than the similar ossification seen in the *Dlx1/2^{-/-}*; *Dlx5^{-/-}* mutants; yellow arrowhead, Fig. 20B). The basitrabecular process takes on a bifurcated appearance, as the ala temporalis is represented only by a thin ascending process (Fig. 20B). This is associated with a small lamina obturans (blue arrowhead, Fig. 20B). Hence, proximal BA derivatives have also been transformed. Furthermore, an ectopic lamina obturans is present, rather similar to the corrupted endogenous one, that invests an unattached cartilage with a projection toward the basitrabecular process (red arrowhead); this we have taken as the remnant of the deviated Meckel's cartilage seen in *Dlx5^{-/-}*; *Dlx6^{+/-}* mutants and is similar in nature to the endogenous ascending lamina of the ala temporalis (black arrowhead, Fig. 20B). A single pterygoid sits superficial to the connection of the cartilaginous rod and the ascending lamina. Two ectopic cartilaginous bodies (possibly incal and malleal remnants?) lie superficial to the rod near the short tympanohyal remainder of the styloid process. Neither a stapes nor a developed round window are observed (see below). The dentary is extremely small and has the barest of condylar processes orientated toward the squamosal (Fig. 20C). Moreover, there are neither ectotympanics nor gonials. The body of the hyoid is a straight ossified rod transversing the width of the pharynx; greater and lesser horns are severely hypoplastic and fused (not shown).

[*Dlx3^{+/-}*; *Dlx5^{-/-}*; *Dlx6^{+/-}*] mutants present yet another distinct phenotype (Fig. 20C, and data not shown). Although there is no cartilaginous rod extending laterad from the basitrabecular process (as is observed in the [*Dlx2^{+/-}*; *Dlx5^{-/-}*; *Dlx6^{+/-}*] mutants), greatly expanded pterygoids are present; moreover, they extend a lamina toward the malleus. The incus and malleus are fused; unlike other mutants, however, the malleus bears neither a processus brevis nor a manubrium. The body of Meckel's cartilage loops and is ossified.

We further examined [*Dlx1^{+/-}*; *Dlx2^{+/-}*; *Dlx5^{-/-}*; *Dlx6^{+/-}*] mutants. Although in general aspect these mutants are similar to the *Dlx2^{+/-}*; *Dlx5^{-/-}*; *Dlx6^{+/-}* mutants, in external appearance, these mutants bear the greatest similarity to the external appearance of the *Dlx5/6^{-/-}* mutants (Fig. 20A). They appear to have a greater degree of symmetry between the upper (maxillary and premaxillary)

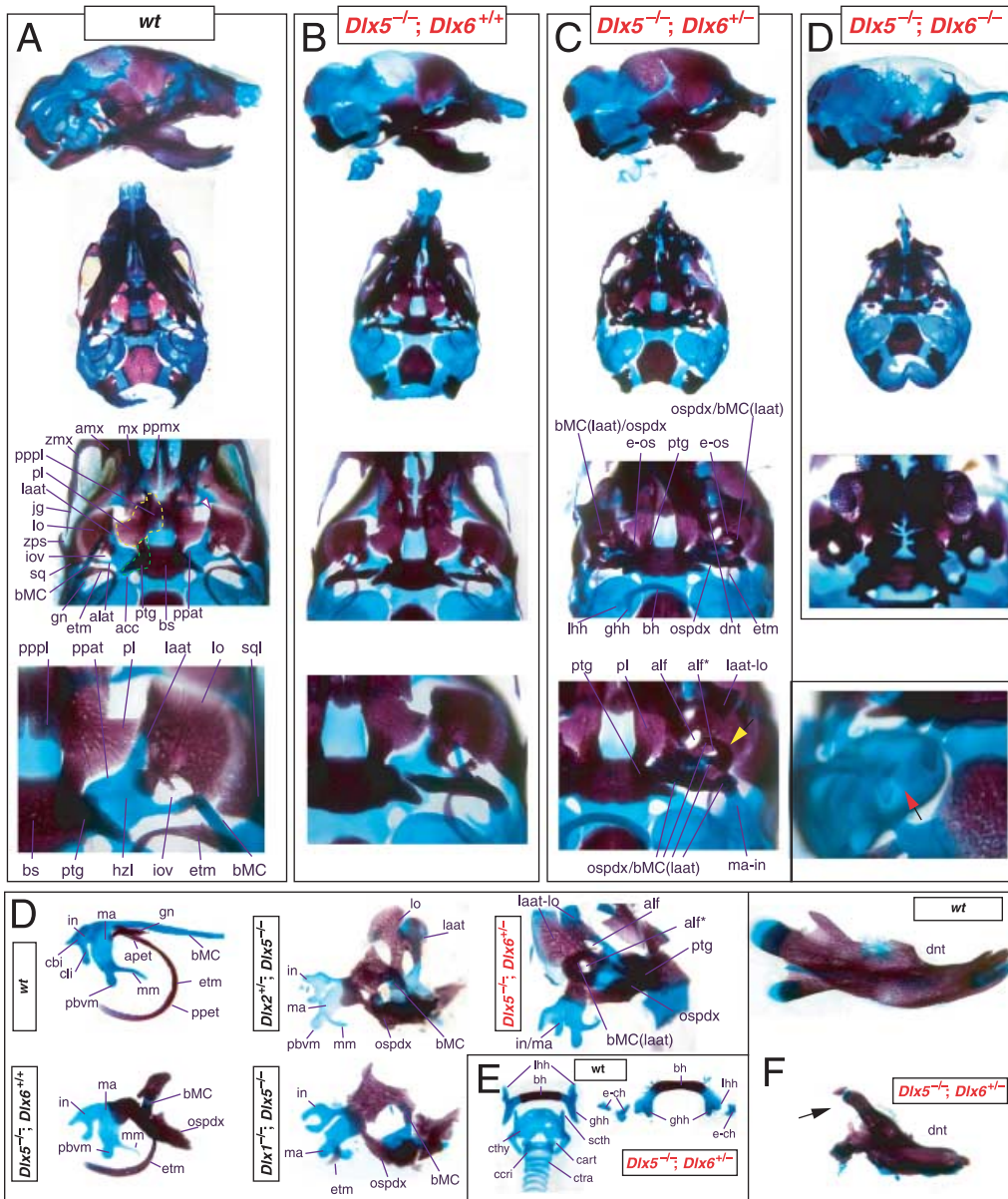


Fig. 19 Skeletal analysis of *Dlx5*^{−/−}; *Dlx6*^{+/−} mutants. (A–D) *Dlx5*^{−/−}; *Dlx6*^{+/−} mutant skulls (C), with comparisons with wild-type (A), *Dlx5*^{−/−} mutant (B) and *Dlx5*^{−/−}; *Dlx6*^{+/−} compound homozygous mutants (D). The yellow and black arrow in C points to the looped structure derived from the body of Meckel's cartilage of the mutant that is reminiscent of an ala temporalis. The red and black arrow indicates the disruption of the styloid process of the mutant. (D) Comparison of the middle ear and associated structures of wild-type, *Dlx5*^{−/−}, [*Dlx2*^{+/−}; *Dlx5*^{−/−}] compound, [*Dlx1*^{+/−}; *Dlx5*^{−/−}] compound, and [*Dlx5*^{−/−}; *Dlx6*^{+/−}] compound mutants. The *in situ* endogenous alisphenoidal structures of the [*Dlx2*^{+/−}; *Dlx5*^{−/−}] and [*Dlx5*^{−/−}; *Dlx6*^{+/−}] mutants are included for reference. (E) Wild-type (left) and *Dlx5*^{−/−}; *Dlx6*^{+/−} compound mutant hyoid structures. (F) A comparison of a wild-type and a [*Dlx5*^{−/−}; *Dlx6*^{+/−}] compound mutant dentary.

jaws and the lower (mandibular) jaws (Fig. 20A). The cartilaginous rod extending from the basitrabecular process, however, is thicker and more ossified; the ectopic, parallel dermal ossification is likewise thicker (Fig. 20B). The tympanohyal is small and, surprisingly, runs toward a nodule of cartilage (not shown). The

hyoid body is elongated across the pharynx (Fig. 20). The phenotypes of the [*Dlx2*^{+/-}; *Dlx5*^{+/-}; *Dlx6*^{+/-}], [*Dlx3*^{+/-}; *Dlx5*^{+/-}; *Dlx6*^{+/-}], [*Dlx1*^{+/-}; *Dlx2*^{+/-}; *Dlx5*^{+/-}; *Dlx6*^{+/-}] and [*Dlx5*^{+/-}; *Dlx6*^{+/-}] are thus distinct, adding further support to the hypothesis that each gene has unique functions in a combinatorial code.

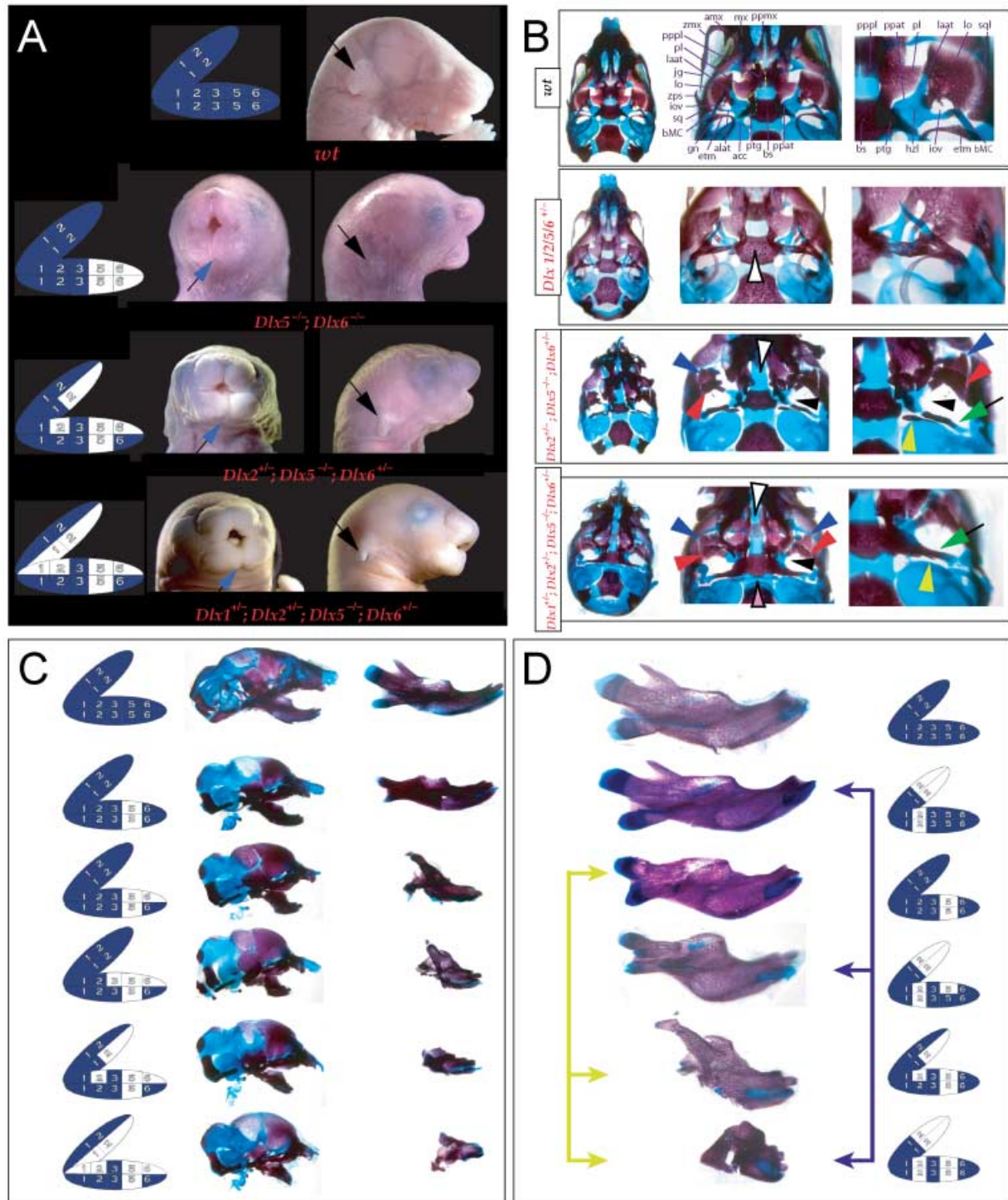


Fig. 20 Comparisons of the relative ramifications of the loss of function of *Dlx1*, *Dlx2*, *Dlx3*, *Dlx1/2* and *Dlx6* alleles in a *Dlx5* null background, and the relative interactions of *Dlx2* and *Dlx5*. (A) Gross anatomy of, top-to-bottom, wild-type, *Dlx5*^{-/-}; *Dlx6*^{+/+}, *[Dlx2*^{+/+}; *Dlx5*^{-/-}; *Dlx6*^{+/+}] and *[Dlx1*^{+/+}; *Dlx2*^{+/+}; *Dlx5*^{-/-}; *Dlx6*^{+/+}] compound mutant neonates. Black arrows highlight the defects in the development of the external auditory pinnae (microtia). Note that the *Dlx5*^{-/-} mutant has aural atresia and further essentially lacks a pinnae while the *[Dlx2*^{+/+}; *Dlx5*^{-/-}; *Dlx6*^{+/+}] mutant develops a nypoplastic pinnae; thus, in a *Dlx5*^{-/-}; *Dlx6*^{+/+} background, the loss of a *Dlx2* allele is not equivalent to the loss of another *Dlx6* allele. The blue and black arrow indicates the relative mandibular clefting associated with each of these mutants; in the case of the *Dlx5*^{-/-} mutant, a non-fully cleft specimen is shown. (B) Norma basalis views of neonatal skulls, top-to-bottom, of wild-type, *[Dlx1*^{+/+}; *Dlx2*^{+/+}; *Dlx5*^{-/-}; *Dlx6*^{+/+}], *[Dlx2*^{+/+}; *Dlx5*^{-/-}; *Dlx6*^{+/+}] and *[Dlx1*^{+/+}; *Dlx2*^{+/+}; *Dlx5*^{-/-}; *Dlx6*^{+/+}] compound mutants differentially stained for bone (red) and cartilage (blue). White and black arrows indicate the cleft palates. The red arrowheads and black arrowheads highlight the combined ramifications of distinct trends seen in disparate

Denouement – getting your head on straight in a *Dlx* world

Insights into the nature of the *Dlx* functions in patterning of the branchial arch-derived skeleton

Based upon the correlation of a nested pattern of *Dlx* gene expression in the BA ectomesenchyme with the subsequent development of a proximodistal series of skeletal elements therefrom, we have previously hypothesized that a combinatorial *Dlx* code regulates the identity and development of BA-derived skeletal elements. A corollary to this hypothesis is that a change of the combination of *Dlx* genes, either by loss or gain, would result in a change of identity and in the subsequent development of the skeletal elements. We have confirmed and extended this model through the morphological analysis of branchial arch-derived skeletal structures that are formed in mice with varying dosages of *Dlx1*, *Dlx2*, *Dlx3*, *Dlx5* and *Dlx6*.

How might this combinatorial code work? It is possible that the code operates through a quantitative mechanism, a qualitative mechanism or both. With a quantitative mechanism, the code would depend on the concentration of all active Dlx proteins in a given nucleus, and any change of Dlx concentration above or below a critical threshold would alter the fate of affected cells. At its extreme, the quantitative model postulates that each active Dlx protein is equivalent (e.g. *Dlx1* and *Dlx2* would have equivalent functions), and only the total concentration of Dlx proteins determines the gene expression readout. By contrast, the qualitative model postulates that the code would depend on the concentration of specific Dlx proteins in a given nucleus (e.g. *Dlx1* and *Dlx2* would have some unique functions) and distinct phenotypes would appear depending upon which Dlx proteins are expressed and where. Thus, the code – and the resulting morphology – might be defined by the number and type of functional *Dlx* alleles that are expressed in any particular portion of a BA, and hence, at its simplest, the combination is the code.

The fundamental question of the relative balance of qualitative vs. quantitative modes in the mechanism of operation of the *Dlx* code cannot ultimately be answered by the genetic studies presented here. Although these studies adequately address levels of alleles, they do not address levels of protein within individual cells or tissues. Thus, to begin to distinguish between these modes one needs to measure the concentrations of active Dlx proteins at different parts of the branchial arch ectomesenchyme as a function of *Dlx* gene dosage. This is a particularly important distinction as cross-regulation of *Dlx* gene expression, where protein from one *Dlx* gene regulates expression of a second *Dlx* gene, has been demonstrated (Anderson et al. 1997; Depew et al. 2002a). Although we are currently quantitatively assaying levels of *Dlx* transcript and protein at various ages in the relevant tissues in this allelic series, these studies may also not be definitive as, for example, we do not know a priori that the operation of the code requires that each cell act in the same mode. We are also acting on a number of strategies to understand further the qualitative nature of the code, including the generation of transgenic mice that ectopically express *Dlx* genes through the *in situ* replacement (knock-in) of another *Dlx* gene. Again, these studies may not, however, be entirely definitive. For instance, while an animal harbouring *Dlx5* in place of *Dlx2* that was phenotypically wild-type might argue against a qualitative mode of operation of the code, it does not strictly provide definitive proof against it; it is possible, for example, that the code requires second-order paralogues to act quantitatively, and first-order or third-order paralogues to act qualitatively.

To set the stage for this level of analysis, however, we have here systematically reduced the dosage of functional, wild-type *Dlx* alleles and described the phenotypes of the BA skeleton. A requisite test of the combination, as such, comes with the forced replication of the code, as results, for instance, with the loss of a nested gene pair such as *Dlx5/6*. To determine whether the expression of *Dlx1* and *Dlx2* alone is

mutants: the red arrowheads indicate the trend of a bent BMC transformed into an ala-temporalis-like structure seen in the [*Dlx5*^{-/-}; *Dlx6*^{+/-}] mutant (and fully realized as a homeotic transformation in the *Dlx5/6*^{-/-}), while the black arrowheads indicate the degradation of the horizontal lamina of the ala temporalis that accompanies the *Dlx1/2*^{+/-}; *Dlx5/6*^{+/-} mutant. The green and black arrows indicate the restructuring of the os paradoxicum and body of Meckel's cartilage that characterizes the [*Dlx2*^{+/-}; *Dlx5*^{-/-}; *Dlx6*^{+/-}] and [*Dlx1*^{+/-}; *Dlx2*^{+/-}; *Dlx5*^{-/-}; *Dlx6*^{+/-}] compound mutants. (C) Comparison of the variable loss of *Dlx* alleles in an otherwise *Dlx5*-null background. Left: schemae of corresponding allele distribution. Centre: norma lateralis view of neonatal skulls. Right: dissected dentaries. (D) Dissected dentaries demonstrating the nature of the genetic interaction of *Dlx2* and *Dlx5* in the development of mdBA1-derived structures. Yellow arrows indicate relative loss of *Dlx2* in a *Dlx5*-null background, while the blue arrows indicate the converse. Right: schemae of corresponding allele distribution.

sufficient to define 'maxillary arch', we (and others) previously examined the phenotype of the *Dlx5/6*^{-/-} mice. In these mutants, the mandibular arch loses expression of *Dlx3*, *Dlx5* and *Dlx6* (the expression of *Dlx4* remains ambiguous), maintains expression of *Dlx1* and *Dlx2*, and generates a homeotic transformation of lower jaws into upper jaws (Beverdam et al. 2002; Depew et al. 2002a). This is the clearest demonstration that *Dlx* dosage defines regional identity. Although this replication of identity demonstrates that the first branchial arch is homeomeric (i.e. capable of homeotic transformation) within, it does not distinguish between the quantitative or the qualitative models. Furthermore, the *Dlx5/6*^{-/-} mutant shows that there is cross-regulation between the *Dlx* genes: *Dlx5*–*Dlx6* positively regulate *Dlx3* expression. Therefore, one needs to examine further the expression of the other *Dlx* genes in order to interpret the mechanism(s) underlying mutant phenotypes. Herein, we do not evaluate *Dlx* gene expression under the various *Dlx* dosage conditions; this information, which we are in the process of obtaining, will be essential when giving fuller consideration to the mechanistic mode of the *Dlx* code operation.

Nonetheless, our dosage experiments do yield some mechanistic insights. Testing the combinatorial code with a subtractive strategy has demonstrated that the code is not strictly allelically additive, as evidenced, for example, by the transformation of *ala temporalis* morphology seen in the *Dlx1/2*^{+/-} heterozygote. In this compound heterozygote, the horizontal lamina is separated into diminished constituent parts to a greater degree than is seen in either the *Dlx1*^{+/-} or the *Dlx2*^{+/-} single heterozygotes, suggesting synergy between *Dlx1* and *Dlx2* in the development of this structure. Importantly, this disruption of morphology is not nearly as significant as that of either the *Dlx1*^{-/-} or the *Dlx2*^{-/-} homozygous mutants. The contribution of each individual allele is not therefore strictly additive nor proportional to the total number of expressed *Dlx* alleles: one *Dlx1* plus one *Dlx2* (i.e. two in total) are not functionally equivalent to two *Dlx1* or two *Dlx2* alleles.

This principle can further be seen with a comparison, among many others, of the phenotypes of the [*Dlx2*^{+/-}; *Dlx5*^{+/-}], [*Dlx2*^{-/-}; *Dlx5*^{+/-}], [*Dlx2*^{+/-}; *Dlx5*^{-/-}] and [*Dlx2*^{-/-}; *Dlx5*^{-/-}] mutants. Notwithstanding the alteration of *ala temporalis* development already seen in the *Dlx2*^{+/-} mice, the *Dlx2*^{+/-}; *Dlx5*^{+/-} mice are essentially phenotypically normal. Relative to the genotype–phenotype relationship of the *Dlx2*^{+/-}; *Dlx5*^{+/-} mice, one can com-

pare the additional loss of a single *Dlx2* allele with that of the loss of a single *Dlx5* allele (Fig. 20D). This comparison demonstrates that these mutants are distinct morphologically, and that the loss of a single allele of *Dlx5* is not equivalent to the loss of a single allele of *Dlx2*. (It might be suggested, however simplistically, that the similarity in mdBA1 derivative phenotype of the *Dlx2*^{+/-}; *Dlx5*^{-/-} and *Dlx2*^{-/-}; *Dlx5*^{+/-} mice indicates that a single copy of *Dlx5* was roughly equivalent to two copies of *Dlx2* in mdBA1 development.) It can be argued that while each gene compensates for the other to some degree, each gene contributes uniquely to the code; it may also be argued that *Dlx5* and *Dlx2* do not equally compensate/contribute. Indeed, *Dlx5* appears to be a more potent player in distal development.

The relative potency of *Dlx5*, compared with *Dlx2*, in controlling morphogenesis of the mandibular arch could be analogous to the mechanism underlying the posterior prevalence principle operating in the *Hox* gene system (see Duboule, 1994). *Hox* genes have a nested expression pattern along the anteroposterior axis of an embryo. As a rule, mutation of a *Hox* gene leads to alterations only at the anterior end of its expression domain. Likewise, over-expression of a particular *Hox* gene only leads to changes in anterior regions where more posterior *Hox* genes are not expressed. Hence, the posterior-most *Hox*-expressed gene appears to dominate, or prevail, in the development of a region. The jaw region disrupted in *Dlx5* null mice corresponds to the proximal part of the mandibular arch, where analogously *Dlx5* and *Dlx6* expression have their most 'proximal' expression (Fig. 3B). One might be tempted to consider *Dlx5* in this 'proximal prevalence' light; however, this idea falters with respect to *Dlx3*, which shows little prevalence over *Dlx1* and *Dlx2* and appears to be downstream of *Dlx5* and/or *Dlx6*.

It is also important to point out that the *Dlx* genes are expressed in regionally restricted patterns in both the mesenchyme and the ectoderm of the branchial arches and frontonasal prominences. For instance, *Dlx2* and *Dlx3* expression in the ectoderm is largely in regions overlying largely *Dlx*⁻; *Msx*⁺ mesenchyme in distal parts of the jaw primordia (Qiu et al. 1997; Thomas et al. 2000; Depew et al. 2002a). Although at this point we consider that most of the skeletal defects that are observed in the *Dlx* single and compound mutants result from defects in the *Dlx*⁺ ectomesenchyme, we do not exclude the possibility that aspects of the phenotypes,

particularly in compound mutants, might result from loss of *Dlx* expression in the ectoderm. This level of analysis will probably require the use of conditional mutants.

***Dlx* dosage in the BA1 development: regional specification and regional growth**

While testing the combinatorial code with a subtractive strategy may not definitively reveal the mode of operation of the code, it has revealed a number of substantive themes that provide insights into the molecular mechanisms that regulate branchial arch development. For instance, the effects of mutating, individually or in combination, *Dlx* genes centre on discrete regions along the proximo-distal axis of the arches, and supports the notion, based on comparative anatomy and evolutionary considerations, that the developing arches are constituted by discrete segment-like units that generate specific skeletal elements. Moreover, the BA are metameric within and are thus capable of homeotic transformation (i.e. they are homeomeric). Indeed, the homeotic transformation in the jaws seen in the *Dlx5/6*^{-/-} mutants is as great in scope as any transformation observed from the mutation of any other homeobox gene family.

Furthermore, although each genotype–phenotype relationship is unique, there are four general grades of transformations of mandibular (nested) structures observed with the loss-of-function of multiple *Dlx* alleles (Table 1). We categorize as Grade 1 those phenotypes where structures that we interpret to be primarily derived from the proximal half of the mandibular arch are mainly affected. With this grade, the proximal end of the body of Meckel's cartilage is bent or split, an ectopic os paradoxicum forms, and the proximal dentary is represented by juxtaposed condylar and angular processes, such as is seen with the *Dlx5*^{-/-} and *Dlx2*^{-/-}; *Dlx5*^{+/-} mutants.

Grade 2 phenotypes are those in which the mandibular contributions to both the 'primary' (i.e. malleal–incudal) and the 'secondary' (i.e. dentary–squamosal) jaw articulations are highly affected, and in which the maxillary contributions to the same are also slightly affected. With Grade 2 phenotypes, as exemplified by the *Dlx2*^{+/-}; *Dlx5*^{+/-} mutants, the proximal dentary is greatly reduced, lacks angular and coronoid processes and possesses just a rudimentary condylar process generally having a free floating osseous tip. An ectopic

os paradoxicum (much more extensive and elaborated than that of Grade 1) also develops, and the body of Meckel's cartilage is reminiscent of an ala temporalis (i.e. it is similar to, but not as overt as, that of the *Dlx5/6*^{-/-} mutants; discussed below). Moreover, the incus and malleus are fused, and the jaw-associated regions of the squamosal, such as the retrotympanic process and the glenoid cavity, are dysmorphic.

Grade 3 phenotypes exhibit a catastrophic loss of the primary and secondary jaws such as is evinced in the *Dlx2*^{-/-}; *Dlx5*^{-/-} mutants. Little remains of the body of Meckel's cartilage, the proximal dentary or the associated ectotympanic and gonial bones. What does remain consists largely of distal mandibular structures such as the rostral process of Meckel's cartilage, the incisors and associated alveolar bone – structures that are apparently under the control of the distally expressed *Msx* and *Bmp* genes. Neither a malleus nor an incus are seen, although a cartilaginous rudiment occupying their usual topography can be found. Moreover, the maxillary jaw-associated derivatives are affected in a manner similar to, but more severe than, the single *Dlx2*^{-/-} mutant. Scattered ectopic vibrissae are also found in association with the lower jaw.

Lastly, the Grade 4 phenotype, found with the *Dlx5/6*^{-/-} mutants, consists of a comprehensive homeotic transformation of the elements associated with the lower jaw into elements associated with the upper jaw. Concurrently, upper jaw soft tissue structures such as vibrissae and rugae develop within the lower jaw. It is noteworthy that while the *Dlx2*^{-/-}; *Dlx5*^{-/-} mutants essentially have a deletion of the proximal and middle parts of the mandibular arch, *Dlx5/6*^{-/-} mutants have a homeotic transformation of this region. Although the operational mode is unclear, that there are grades of alterations of structure might also argue for a developmental system of buffered thresholds.

The transformation of the body of Meckel's cartilage (a mandibular structure) toward a morphology similar to that of an ala temporalis (a maxillary structure) that is evinced in many of the *Dlx* mutants should not be overlooked. *Dlx2* is essential for making an ala temporalis, a structure that uniquely normally attaches to the neurocranial base; *Dlx2* is not, however, essential for making Meckel's cartilage. Loss of *Dlx5* results in the degradation of normal MC architecture, though not in the loss *per se* of MC itself; instead, in the *Dlx5*^{-/-} mutant the cells contributing to the MC, which splits and bends toward the neurocranial base, are influenced

by a patterning system that usually acts on the mxBA1, palatoquadrate cells alone. Hence, *Dlx5* – and ultimately *Dlx6* as well – is essential at some level to buffer mandibular cells from this system.

In the *Dlx2*^{-/-}; *Dlx5*^{+/-} mutants, the proximal mandibular structures are affected in a manner similar to the *Dlx5*^{-/-} single mutant. For instance, in both cases the dentary is truncated, has no coronoid, and the angular and condylar processes are juxtaposed. However, although MC is altered in both mutants, in the *Dlx2*^{-/-}; *Dlx5*^{+/-} mutants MC is split but does not bend to the same degree toward the neurocranial base as does MC of the *Dlx5*^{-/-} mutants. One interpretation of this difference is that the bend is an attempt to make an ala temporalis – a structure that requires a full complement of *Dlx2* to make – and so the lack of *Dlx2* in the *Dlx2*^{-/-}; *Dlx5*^{+/-} mutants translates into less of a bend. With the *Dlx2*^{+/-}; *Dlx5*^{-/-} mutants, then, MC is greatly reminiscent of an ala temporalis because there is no buffer from the neurocranial base system usually provided by *Dlx5* but there is still *Dlx2* present to translate signal into alar morphology. That the endogenous ala temporalis in the *Dlx2*^{+/-}; *Dlx5*^{-/-} mutants has been more affected than is seen with the loss of a single *Dlx2* allele in an otherwise *Dlx5* wild-type background might indicate, once compromised, some regional interdependence within the system.

Although the primary and secondary jaw articulations are essentially both lost in the *Dlx2*^{-/-}; *Dlx5*^{-/-} mutants, the presence of a single copy of *Dlx5* (i.e. in the *Dlx2*^{-/-}; *Dlx5*^{+/-}) greatly rescues the entire region; *Dlx5* is thus acting in a capacity greater than just as a buffer against a neurocranial base integration. This leads to the question: What is the significance in the substantive differences between the loss of *Dlx6* and that of *Dlx2* in a *Dlx5* null background? Is it because regulated BA growth and survival goes hand in hand with control of identity – and both are regulated by *Dlx*?

The similarities and differences in the phenotypes of the *Dlx2*^{-/-}; *Dlx5*^{-/-} mutants and the *Dlx5/6*^{-/-} mutants are worth further consideration. In the *Dlx5/6*^{-/-} mutants, mdBA1 skeletal elements are present but undergo a dramatic mirror-image homeotic transformation into maxillary-like structures. Importantly, this transformation is accompanied either by the loss of integration of the distal-most midline mdBA1 structures, including incisors, associated alveolar bone and the rostral process, or by the complete absence of midline mdBA1 structures. For example, just as with a normal maxilla, which

normally does not possess an incisor, the transformed dentary (now maxilla) does not possess an incisor; and when incisors do form, they are dissociated from this altered element. These skeletal changes are accompanied by acquisition in the lower jaw of ectopic soft tissue structures, such as vibrissae and rugae, usually associated with the mxBA1 and to some extent the frontonasal prominences (FNPs). Additionally, the olfactory placodes (a source of *Dlx5* and *Dlx6* expression) and associated frontonasal prominences fail to develop normally; subsequently, nasal capsular and premaxillary structures are affected. Notably, the maxillae of the *Dlx5/6*^{-/-} mutants also undergo a slight alteration, and indeed in some respects more resemble the ectopic maxillae that form in the lower jaws than they do wild-type maxillae.

Although there are a number of mechanistic explanations for how the anatomical mirror-image of the upper and lower jaws of the *Dlx5/6*^{-/-} mutants may have been generated, perhaps the most parsimonious is that a point source of positional information exists at the 'hinge' region that is the junction of the mxBA1 and mdBA1 primordia. The mirror-image duplication of the jaw apparatus in the *Dlx5/6*^{-/-} mutants would then result from the read-out of this source because mdBA1 and mxBA1 would be sharing the same *Dlx* code identities.

With the *Dlx2*^{-/-}; *Dlx5*^{-/-} mutants, by contrast, those structures usually associated with the hinge region between mdBA1 and mxBA1 are lost while the distal midline structures are present. Thus, rather than being transformed, the proximal dentary, gonial, ectotympanic, malleus and body of Meckel's cartilage are absent while incisors, rostral processes and alveolar bone are present. Losses in the lower jaw hinge region of mdBA1 derivatives are accompanied by alterations of the upper jaw hinge region of mxBA1 structures such as the squamosal. What remains of the dentary, moreover, is heterotopically associated with the maxilla. Indeed, the mirror image development of the jaws centred between the maxillary and mandibular arches in the *Dlx5/6*^{-/-} mutants is clearly not seen in the *Dlx2*^{-/-}; *Dlx5*^{-/-} mutants. Moreover, one further difference in hard tissue development from the *Dlx5/6*^{-/-} mutants is in the frequent presence of duplicated incisors in the *Dlx2*^{-/-}; *Dlx5*^{-/-} mutants. *Dlx2* and *Dlx5* are clearly essential, then, for both the realization of structure due to any hinge region signal and the pattern within the midline mandibular ectoderm. This leads to the speculation that perhaps, together, *Dlx5* and *Dlx2* (second-order

paralogues) regulate growth/survival of this region whereas, together, *Dlx5* and *Dlx6* (first-order paralogues) control its identity.

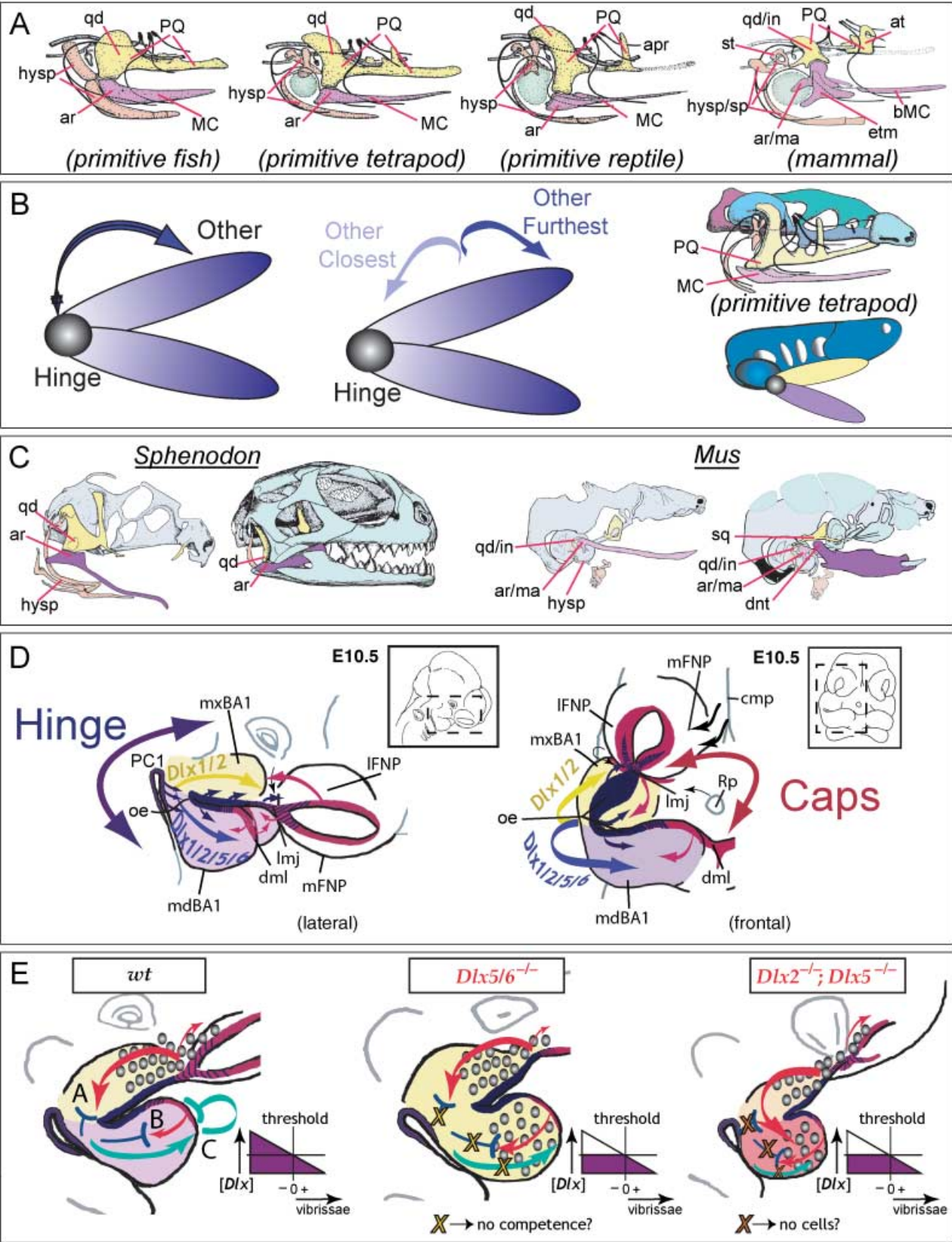
***Dlx* in the development and evolution of the jaw**

The phenotypes generated by the loss-of-function allelic series presented here demonstrate that an appropriate complement of *Dlx* gene expression is particularly important for the development of structures associated with both the 'primary' (i.e. malleal-incudal) and the functional 'secondary' (i.e. dentary-squamosal) jaw articulations. Although variously modified, expanded or reduced, by definition all gnathostomes (or jawed vertebrates, which comprise the vast majority of all vertebrates) possess hinged jaws (Fig. 21). Jaws are fundamental, functional cranial units that develop within the general context of the gnathostome bauplan as articulated, prehensile oral apparatuses, and are principally derived from the splanchnocranial, dermatocranial and associated dental elements of *mxBA1* and *mdBA1*, with a small yet significant contribution from the olfactory placode-associated FNPs. [Secondary, pharyngeal jaws utilizing skeletodontal structures derived from more caudal BAs in apposition to elements underlying the neurocranial base and palate have sporadically evolved (e.g. see Gregory, 1933), but they always form in addition to primary, or 'true', jaws.]

With respect to the functional architecture of jaws, a number of universal traits are apparent (see Reichert, 1837; Parker, 1866, 1869, 1871, 1873, 1876, 1877, 1878, 1879, 1881, 1882, 1883, 1885a,b; Huxley, 1869; Gegenbaur, 1888; Wiedersheim & Parker, 1897; Gaupp, 1898, 1899; Howes & Swinnerton, 1901; Gregory, 1904, 1913, 1933; Gaupp, 1905; Reynolds, 1913; Kindred, 1921; Wilder, 1923; Kingsley, 1925; Kingsbury, 1926; de Beer, 1937; Paterson, 1939; Nelsen, 1953; Romer, 1956, 1966; Jollie, 1957, 1962, 1977; Goodrich, 1958; Romanoff, 1960; Young, 1962; Schmalhausen, 1968; Allin, 1975; Presley & Steel, 1976; Crompton & Parker, 1978; Barghusen & Hopson, 1979; Bellairs & Kamal, 1981; Moore, 1981; Kuhn & Zeller, 1987; Radinsky, 1987; Carroll, 1988; Langille & Hall, 1989; Vorster, 1989; Allin & Hopson, 1992; Trueb & Hanken, 1992; Couly et al. 1993; Novacek, 1993; Schultze, 1993; Trueb, 1993; Zusi, 1993; Kimmel et al. 1995; Cubbage & Mabee, 1996; Kuratani et al. 1997; Depew et al. 2002a,b; Shigetani et al. 2005). Firstly, jaws contain a point of articulation (a joint or hinge) between the two appositional units that is

placed such that it allows relative motion of the two jaw units (Fig. 21A,B). As a consequence of this trait, polarity is an inherent character of jaws: there is 'hinge' and there is 'other'. Polarity must therefore also exist within each 'other' as minimally there is 'other closest-to-hinge' and 'other furthest-from-hinge'. Clearly, elements along the 'hinge to other furthest-from-hinge' axis of polarity must be kept in functional registration both within a jaw unit and between the apposed jaw unit. Secondly, relative to the rest of the organism, the two jaws are distinct as the upper jaw is placed in more intimate association with the neurocranium than the lower (Fig. 21B). Lastly, the articulations of all jaws appear to form in the same relative developmental position (Fig. 21C).

Elaborating the correct developmental patterning system is critical to the placement and function of the joint between the upper and lower jaws and hence to the manifestation of the above gnathostome traits. Because the jaw joint develops from structures that derive from within the primordia of BA1, the regulated development of BA1 into jaws is key to understanding this patterning event. According to a 'hinge and caps' model (Depew et al. 2002a,b; Depew and Simpson, under review; see also Shigetani et al. 2000, 2005; Kuratani, 2004, 2005), the developmental patterning system that keeps gnathostome jaws in functional registration, yet evolutionarily tractable to potential changes in functional demands, relies upon a system for the establishment of positional information where pattern and placement of the 'hinge' is driven by factors common to the junction of *mxBA1* and *mdBA1* and of the 'caps' (i.e. signals from the primordia associated with the 'other furthest-from-hinge' of above) by the signals emanating from the distal-most part of BA1 (i.e. the midline, *dml*) and the lambdoidal junction (*lmj*, where the maxillary BA1 meets the olfactory placode-associated FNPs) (Fig. 21D). In this particular model, then, the functional registration of jaws is achieved by the integration of 'hinge' and 'caps' signalling, with the 'caps' sharing at some critical level a developmental history that potentiates their own co-ordination. Moreover, in line with classical interpretations of what consists of 'maxillary' and 'mandibular', in this model maxillary and mandibular are placed in the context of where the hinge is placed and where the caps are placed; thus, 'maxillary' is understood to be that which connects the lower jaw articulations, and the signalling system engendering them, with the frontonasal



prominences and the signaling system at the lambdoidal junction. Although the relative importance and contributions toward the manifestation of specific structures of these two centres of patterning information is therefore idiosyncratic to a species and its ontogenetic functional demands, that they are integrated is patent.

Experimental evidence has implicated peri-oral and first pharyngeal cleftal tissues, such as those expressing *Fgf8*, as potential sources of hinge developmental information (e.g. Barlow & Francis-West, 1997; Neubüser et al. 1997; Bei & Maas, 1998; Tucker et al. 1998a,b, 1999a,b; Barlow et al. 1999; Trumpp et al.

Fig. 21 Model of jaw development and various factors integral to the development of the gnathostome jaw apparatus. (A) Comparisons of the constituent elements of the primary jaw articulations of a primitive fish, a primitive tetrapod, a primitive reptile and a mammal. The BA1-derived palatoquadrate (PQ), upper jaw components (including the quadrate, qd) are in yellow, while the Meckel's cartilage (MC) lower jaw components (including the articular, ar) are in lavender. The BA2 elements (hyps), which are developmentally and functionally integrated with those of BA1, are in salmon. The relative position of the tympanic membrane is coloured in green. Modified from Goodrich (1958). (B) Schemae demonstrating that polarity is an inherent character state of jaws. Jaws contain a point of articulation, or a 'hinge', between the two appositional units that is placed such that it allows the relative motion of the two jaw units. Thus, jaw polarity is inherent as there is 'hinge' and there is 'other' (left). Moreover, polarity is potentially differentially elaborated along the axis of a jaw as there is 'other closest-to-hinge' and 'other furthest-from-hinge' (centre). Moreover, relative to the rest of the organism, the two jaws are distinct (right-hand diagrams) as the upper jaw splanchnocranium (here in yellow) is placed in more intimate association with the neurocranium (green and blue) than the lower (depicted in lavender). (C) Neontological evidence to date indicates that the articulations of all jaws appear to form in the same relative developmental position, as exemplified here in a comparison of the jaw articulation of a representative reptile (*Sphenodon*, left) and a mammal (*Mus*, right). The functional jaw articulations are depicted in dark yellow (upper jaw) and dark lavender (lower jaw). With *Sphenodon* (modified from Bellairs & Kamal, 1981; Howes & Swinnerton, 1901), this means the quadrate (yellow) and articular (lavender); with *Mus*, this means the squamosal (yellow) and dentary (lavender). The 'primary' jaw articulation of the mammal, depicted here in light yellow (incus, quadrate homologue) and light lavender (malleus, articular homologue), has been modified for enhanced auditory functionality; nonetheless, the relative developmental position of the mammalian primary and secondary jaw apparatuses are as with all other gnathostomes. (D) Lateral and frontal views of an E10.5 mouse embryo schematizing a 'hinge and caps' model of pattern and polarity in the first branchial arch. The developmental patterning system that keeps gnathostome jaws in functional registration, yet evolutionarily tractable to changes in functional demands, is hypothesized to rely upon a 'hinge and caps' system of positional information. Pattern and placement of the 'hinge' is driven by the co-ordinated presence of factors, such as *Fgf8*, centred around the junction of mxBA1 and mdBA1 and the first pharyngeal plate (indicated in blue and purple). Non-hinge regional structures (the 'other' of above) are largely patterned by 'caps' signals (indicated in red) emanating from the distal-most part of BA1 (dml) and the lambdoidal junction (the junction where the maxillary BA1 meets the olfactory placode-associated FNP, or Imj). In this particular model, the functional registration of jaws is achieved by the integration of 'hinge' and 'caps' signalling, with the 'caps' importantly sharing at some critical level an earlier developmental history that informs their own co-ordination. This integrated system of signalling centres is subsequently regionally elaborated by the *Dlx*-positive ectomesenchyme, concentrated around the hinge region, and the interpretation and subsequent pattern and morphology depends on the combination of *Dlx* genes expressed. Other factors, such as *Msx*, *Alx* and *Prx*, are likewise centred at the caps. Modified from Depew et al. (2002a). (E) Schemae of BA development elaborating on the disconnection between skeletal and soft tissue patterning. In the wild-type, distinct complements of *Dlx* alleles distinguish between the maxillary (yellow) and mandibular (lavender) jaw systems. In the *Dlx5/6*^{-/-} mutant embryo (centre), a homeotic transformation has occurred and the maxillary complement of *Dlx* genes is replicated in the mandibular arch (thus both are depicted in yellow). This results in hinge region maxillary elements forming in place of mandibular, and is accompanied by ectopic vibrissae (indicated by the graded circles). Cap region integration with the hinge region, however, is compromised in these mutants. By contrast, with the *Dlx2*^{-/-}; *Dlx5*^{-/-} mutants the hinge region skeletal elements are essentially lost while those of the cap regions are maintained, albeit minus a large portion of their usual *Dlx* complement (reflected by orange and salmon BA1 primordia). Here, too, however, ectopic vibrissae develop. In the wild-type diagram, vibrissae follicles are restricted in their development to the maxillary and frontonasal primordial. 'A-C' in this diagram represent just three hypothetical systems for the restriction of vibrissae formation from the mandibular arch that are consistent with an underlying commonality between the 'caps' signals. In 'A', a competence signal (red arrows) emitted from the region of the lambdoidal junction is either imparted to the underlying mesenchyme (which subsequently acts to induce follicles) or through the ectoderm (creating competence to respond). Propagation of this signal is inhibited (blue 'T') by the mandibular complement of *Dlx* expression, and thus there are no mandibular vibrissae. In 'B', a similar signal (red arrow) is instead emitted from the distal midline mandibular ectoderm (that also happens to share a developmental history with the ectoderm of the lambdoidal junction as cephalic epiblast/ectoderm anterior to the developing neural plate), and inhibition (blue 'T') is generated by the appropriate complement of *Dlx* genes being expressed. In 'C', a signal emanates from the *Dlx*⁺ mesenchyme of the mandibular arch that subsequently informs the distal midline ectoderm to auto-inhibit (green bent 'T') a vibrissae signal such as indicated in B. All three models suggest the requirement for either an appropriate concentration (purple diagram) or complement of *Dlx* genes to be expressed. As depicted here, in both the *Dlx5/6*^{-/-} mutant and the *Dlx2*^{-/-}; *Dlx5*^{-/-} mutant this concentration has not been reached. It is further theorized that in the *Dlx5/6*^{-/-} mutant, the ability to inhibit has been lost while in the *Dlx2*^{-/-}; *Dlx5*^{-/-} mutant there are just not enough cells to propagate an inhibitory signal. See text for further discussion and list for abbreviations.

1999; Ferguson et al. 2000; Shigetani et al. 2000, 2005; Thomas et al. 2000; reviewed in Depew et al. 2002b; Francis-West et al. 2003). While integrated with, and balanced by, additional positional information coming from the 'caps' (which, for example, both express *Bmp*, *Msx*, *Alx*, *Prx*, etc.), this information is subsequently regionally elaborated by the *Dlx*-positive ectomesenchyme, and the interpretation and subsequent pattern and morphology depends on the combination of *Dlx* genes expressed (Depew et al. 2002a,b; Fig. 21D). We are currently addressing this integration of hinge and caps signalling at different levels, including, for instance, through an assessment of the genetic interactions of the *Dlx* and *Msx* genes in patterning the proximo-distal axes of the BA and FNP.

In this regard, our loss-of-function studies have demonstrated that the elaboration of the *Dlx* code is particularly integral to the development of structures in and around the hinge region. For instance, the loss of *Dlx1* and *Dlx2* transforms the upper jaw components of the primary and secondary jaw articulations leaving those of the lower jaw relatively spared. The variable loss of *Dlx* genes in the first nested region (where there is overlap of *Dlx1*, *Dlx2*, *Dlx5* and *Dlx6*), however, leads to an alteration of hinge region architecture, while the loss of both *Dlx2* and *Dlx5* essentially deletes the entire hinge region. Furthermore, the loss of *Dlx5* and *Dlx6* results in a homeotic transformation of the mandibular components at, and below, the hinge and results in a mirror-image structural development about the hinge. It is also notable that vertebrates without brachial arch hinge regions, namely lampreys, apparently possess multiple *Dlx* genes which are not, however, nested within their BA primordia (Neidert et al. 2001).

Soft tissue phenotypes in the jaws of *Dlx5/6*^{-/-} and *Dlx2*^{-/-}; *Dlx5*^{-/-} mutants

Although the skeletal phenotypes of the *Dlx5/6*^{-/-} and *Dlx2*^{-/-}; *Dlx5*^{-/-} mutants are divergent, they do share features of soft tissue transformations, in particular in their possession of ectopic vibrissae on their lower jaws. How is it possible that such disparate skeletal changes are accompanied by such apparently similar soft tissue changes? Perhaps the answer lies in the manner in which vibrissae are generated. It is unclear precisely how the restriction of murine vibrissae development to the mxBA1-FNP region takes place. The entire cephalic surface ectoderm (or perhaps just a

large subset of it, such as the midline) might be competent to respond and spatial restriction could then come from a specific subpopulation of mesenchyme that alone can induce the follicles. The issue would then become one of the specification of this mesenchymal subpopulation, which might come about either by an active conferral on this subpopulation of inductive capacity or by an active repression of inductive capacities in all but a subset of the mesenchyme. Otherwise, the mesenchyme might be universally capable of induction with restriction due either to focal activation or to near universal repression of competence within the ectoderm. Alternatively, vibrissae (and rugae) might result from multiple mechanisms, acting in various steps and sites, establishing mesenchymal and ectodermal competence. At this point, it is not entirely clear whether development of the vibrissae is encoded by region-specific factors that are expressed in the ectoderm, mesenchyme or both.

Whatever the mechanism, it must allow for two mesenchymal populations distinct in their complement of *Dlx* expression and skeletal patterning capacity to both generate vibrissae (Fig. 21E). The lack of frontonasal mesenchymal *Dlx* expression coupled with loss-of-function evidence suggests that *Dlx1*, *Dlx2*, *Dlx5* and *Dlx6* are not essential to the formation of vibrissae; and while the *Dlx5/6*^{-/-} mutants appear to have lost both molecular and structural mdBA1 identity and to have gained mxBA1 identity, the same cannot be said of the *Dlx2*^{-/-}; *Dlx5*^{-/-} mutants. Thus, if the presence of mandibular vibrissae were the result of a change of the inductive capacity of the mesenchyme in both the *Dlx5/6*^{-/-} and the *Dlx2*^{-/-}; *Dlx5*^{-/-} mutants, it seems most parsimonious to suggest that both mutants have lost the normal repression of inductive capacity rather than that each, actively and independently, have acquired inductive capacities (Fig. 21E). Thus, it is possible that a '*Dlx*' threshold is essential for the inhibition, or repression, of vibrissae in mdBA1. Such a threshold would, of course, be higher than what normally exists in the mxBA1 primordia and would not be reached in either the *Dlx2*^{-/-}; *Dlx5*^{-/-} or the *Dlx5/6*^{-/-} mutants (Fig. 21E).

This raises various questions; for example: What would the mechanics of such a theoretical repression be, and would they be the same for both mutants? In one scenario, a repressive signal from the hinge region, perhaps originating around the first pharyngeal plate (where the endoderm and ectoderm meet), would normally be propagated through the mdBA1 mesenchyme.

In turn, this mesenchyme would act in either an autocrine fashion within the mesenchymal population to inhibit induction of vibrissae or in a paracrine fashion to inhibit competence in the ectoderm (Fig. 21E). The loss of inhibition could arise from different circumstances, such as either a lack of competence in a population of mesenchyme to propagate the signal or a lack of an appropriate population of cells competent to propagate the signal; for instance, the *Dlx5/6*^{-/-} mutants might lack the competence to propagate the repressive signal while the *Dlx2*^{-/-}; *Dlx5*^{-/-} mutants might just lack the population of cells.

Whether the nature and identity of the vibrissae in the *Dlx5/6*^{-/-} and *Dlx2*^{-/-}; *Dlx5*^{-/-} mutants is the same is also unclear. As stated above, vibrissae usually form in the ectoderm of prominences associated with the lambdoidal junction where mxBA1 meets the fronto-nasal prominences. Although most vibrissae are maxillary in nature, some are premaxillary in origin; it is possible, however unlikely, that the generation of maxillary and premaxillary vibrissae occur through distinct mechanisms. Likewise, it is possible that the manifestation of ectopic vibrissae has been achieved by independent means in the *Dlx2*^{-/-}; *Dlx5*^{-/-} and *Dlx5/6*^{-/-} mutants, which might have taken place, for instance, if the mutants have differentially altered the fundamental relationships of the hinge and caps signalling centres with the associated mesenchyme. To address the above and other possible scenarios we are further characterizing and comparing the developmental and molecular characteristics of the compound *Dlx* mutants, including the *Dlx5/6*^{-/-} and *Dlx2*^{-/-}; *Dlx5*^{-/-} mutants.

Implications of the *Dlx* mutants for human developmental disorders

This is the first study demonstrating that mice lacking one allele of a *Dlx* gene are phenotypically abnormal. The *Dlx1*^{+/-} and *Dlx2*^{+/-} mutants each exhibit alterations of the ala temporalis, the physiological and functional ramifications of which are not known. *Dlx1*^{-/-} mutants are viable, and exhibit ala temporalis and middle bone defects; the latter could affect hearing. Furthermore, *Dlx* compound heterozygotes (e.g. [*Dlx2*^{+/-}; *Dlx5/6*^{+/-}], [*Dlx1/2*^{+/-}; *Dlx5/6*^{+/-}] and [*Dlx1*^{+/-}; *Dlx2*^{+/-}; *Dlx3*^{+/-}; *Dlx5*^{+/-}; *Dlx6*^{+/-}]) exhibit a range of significant craniofacial defects, including otosclerosis (and other malformations of the middle ear bones) and cleft palate. Therefore, in addition to the developmental and evolutionary considerations,

we believe that humans with altered *Dlx* dosage (alone or in combination with interacting genes) could be at risk for craniofacial and hearing defects. *Dlx* function is also required for limb development, as *Dlx5/6* and *Dlx2/5* mutants have distal limb malformations (Merlo et al. 2002; Robledo et al. 2002; Depew and Rubenstein, unpublished), and significantly one form of human ectrodactyly maps to the region of the *Dlx5/6* locus (Crackower et al. 1996). Additionally, *Dlx3* mutations are now implicated in dental and osseous defects in patients with autosomal dominant amelogenesis imperfecta with taurodontism (Dong et al. 2005) and tricho-dento-osseous syndrome (Haldeman et al. 2004).

We have recently demonstrated, moreover, that adult *Dlx1*^{-/-} mice have cortical interneuron deficiencies and epilepsy (Cobos et al. 2005). Thus, *Dlx* dosage is critical for the development and function of forebrain, craniofacial, auditory, olfactory and limb structures (among others). This is particularly important given recent evidence that the *Dlx5* locus is partially imprinted in humans, but apparently not in mice (Kimura et al. 2004), and that there are alterations in chromatin structure in this region caused by loss of *MECP2* expression which lead to over-expression of *Dlx5* (Horike et al. 2005). Loss of *MECP2* function causes Rett syndrome, which at early stages resembles autism (Zoghbi, 2003). Given all of this information, we are intrigued by the observation that several non-synonymous mutations are present in *Dlx2* and *Dlx5* in subsets of patients with autism (Hamilton, Woo, Carlson, Ghanem, Ekker, and Rubenstein, under review). Although it is unknown whether these heterozygous mutations contribute to causing autism, the fact that development in the mouse is sensitive to *Dlx* dosage increases the possibility that subtle alterations in *Dlx* dose and function can have important functional ramifications.

Summary

We conclude, then, that the *Dlx* gene family is essential for the development, pattern and morphogenesis of the branchial arches, and that the nested expression pattern of the *Dlx* genes within the murine branchial arches regulates intra-arch skeletal identity. We have found, contrary to initial reports, that *Dlx1*, *Dlx2* and *Dlx1/2* heterozygotes exhibit alterations of branchial arch structures and that *Dlx2*^{-/-} and *Dlx1/2*^{-/-} mutants have slight alterations of structures derived from the distal portions of the branchial arches. We have further

demonstrated that the BA of mice are sensitive to *Dlx* (including to *Dlx3*) dosage, that compound *Dlx* mutants reveal four grades of mandibular arch transformations, and that the genetic interactions of *cis* first-order, *trans* second-order and *trans* third-order paralogues result in significant and distinct morphological differences in BA development. Lastly, we show that the development of the BA soft tissues and skeletal tissues might be un-coupled, present a generalized model for gnathostome jaw development, and suggest that *Dlx* dosage may have functional and physiological ramifications for human development as they do in mice.

Acknowledgements

We would like to thank Fiona Wong, Nadia David and Anastasios Karydis for assistance with the project, and Kim Haworth, Isabelle Miletich and Paul Sharpe for discussion of various points. Our work described herein was aided by grants funding J.L.R.R. (Nina Ireland, NIH K05 MH065670, NIDCD R01 DC005667, the Hillblom Foundation and the March of Dimes) and M.J.D. (ARCS, T32DE07204 and the Royal Society, UK).

List of abbreviations

acc, aliochlear commissure; **agp**, angular process; **alat**, anterolateral process of ala temporalis; **alf**, alisphenoid foramen; **alf***, ectopic alisphenoid foramen; **alo**, ala orbitalis; **als**, alisphenoid; **amx**, alveolus of maxilla; **amx***, ectopic maxillary alveolus; **apet**, anterior process of ectotympanic; **apr**, ascending process; **ar**, articular; **at**, ala temporalis; **at***, ectopic ala temporalis cartilage; **BA1**, first branchial arch; **BA2**, second branchial arch; **BA3**, third branchial arch; **bh**, body of hyoid; **bMC**, body of Meckel's cartilage; **bMC1**, ectopic rostro-medial projection from the body of Meckel's cartilage; **bMC2**, ectopic rostro-lateral projection from the body of Meckel's cartilage; **bo**, basioccipital; **bs**, basisphenoid; **btp**, basitrabecular process; **cart**, articular cartilage; **cbi**, crus brevis of incus; **cbp**, cribiform plate; **ccri**, cricoid cartilage; **cdp**, condylar process; **cin**, corpus of the incus; **cli**, crus longus of incus; **cmp**, commissural plate; **cna**, cupola nasi anterior of nasal capsule; **cpr**, crista parotica; **cps**, caudal process of squamosal; **crp**, coronoid process; **cthy**, thyroid cartilage; **ctra**, tracheal cartilage; **dml**, distal midline of mandibular arch; **dnt**, dentary; **e-ch**, ectopic cartilage; **e-LI**, ectopic lower incisor; **eo**, exoccipital; **e-os**, ectopic ossification; **etm**,

ectotympanic process; **fmx**, frontal process of maxilla; **fmx***, ectopic frontal process of maxilla; **FNP**, frontonasal process; **fop**, orbitonasal fissure; **fr**, frontal; **ghh**, greater horn of the hyoid; **gn**, gonial; **hrt**, heart; **hzi**, horizontal lamina; **hysp**, hyoid arch splanchnocranium; **in**, incus; **in***, ectopic incus; **ina**, incisive alveolus of dentary; **iof**, infraorbital foramen of maxilla; **iof***, ectopic infraorbital foramen of maxilla; **iov**, incisura ovale; **ip**, interparietal; **jg**, jugal; **jg***, ectopic jugal; **la**, lacrimal; **laat**, lamina ascendens ala temporalis; **IFNP**, lateral frontonasal process; **lhh**, lesser horn of hyoid; **LI**, lower incisor; **LJ**, lower jaw; **lmj**, lambdoidal junction; **Lmo**, lower molar; **Lmo***, ectopic lower molar; **lo**, lamina obturans; **lo***, ectopic lamina obturans; **lsq**, squamosal lamina; **ma**, malleus; **MC**, Meckel's cartilage; **mdBA1**, mandibular first branchial arch (distal); **mFNP**, medial frontonasal process; **mm**, manubrium of the malleus; **mmx**, maxillary molar alveolus; **mmx***, ectopic maxillary molar alveolus; **moa**, molar alveolus of dentary; **mx**, maxilla; **mx***, ectopic maxilla; **mxBA1**, maxillary first branchial arch (proximal); **mxxp**, maxillary process; **mxxp***, ectopic maxillary process; **na**, nasal bone; **nc**, nasal capsule; **ncb**, neurocranial base; **oe**, oral ectoderm; **olf plc**, olfactory placode; **os 1**, sidewall ossification 1; **os 2**, sidewall ossification 2; **os 3**, sidewall ossification 3; **os 4**, sidewall ossification 4; **ospdx**, os paradoxicum; **pbvm**, processus brevis of the malleus; **pc**, paraseptal cartilage; **PC1**, first pharyngeal cleft; **pca**, pars canalicularis; **pco**, pars cochlearis; **pfi**, processus folii of the malleus; **pl**, palatine; **pl***, ectopic palatine; **pmp**, posterior maxillary process; **pmx**, premaxilla; **pn-nc**, paries nasi – nasal capsule; **pp**, parietal plate; **ppat**, pterygoid process of ala temporalis; **ppet**, posterior process of ectotympanic; **ppi (nc)**, prominentia pars intermedia (nasal capsule); **ppmx**, palatal process of maxilla; **ppmx***, ectopic maxillary palatal process; **pppl**, palatal process of palatine; **pppx**, palatal process of premaxilla; **PQ**, **pq**, palatoquadrate cartilage; **PQ***, **pq***, ectopic palatoquadrate cartilage; **pr**, parietal; **ps**, presphenoid; **ptg**, pterygoid; **ptg***, ectopic pterygoid; **qd**, quadrate; **Rp**, Rathke's pouch; **rpMC**, rostral process of Meckel's cartilage; **rtp**, retrotympanic process; **rug**, rugae; **rug***, ectopic rugae; **scth**, superior cornu of the thyroid; **slh**, stylohyal; **so**, supraoccipital; **sp**, styloid process; **sq**, squamosal; **sq***, ectopic squamosal; **sql**, squamosal lamina; **st**, stapes; **stm**, stomodeum; **strt***, ectopic basitrabecular strut; **tbp**, trabecular basal plate; **tgt**, tegman tympani; **thyc**, cartilago thyroidea; **tm**, taenia marginalis; **tmh**, tympanohyal; **tp-ns**, trabecular

basal plate – nasal septum; **tymb**, tympanic membrane; **UI**, upper incisor; **UJ**, upper jaw; **UJ***, ectopic upper jaw; **V2**, maxillary branch of trigeminal; **V2***, ectopic maxillary branch of trigeminal; **vbf**, vibrissae follicle; **vbf***, ectopic vibrissae follicle; **Vg**, trigeminal ganglia; **vm**, vomer; **zar**, zygomatic arch; **zmx**, zygomatic process of maxilla; **zps**, zygomatic process of squamosal; **2agp**, secondary cartilage of angular parocess; **2cdp**, secondary cartilage of condylar process.

References

- Acampora D, Merlo GR, Paleari L, et al.** (1999) Craniofacial, vestibular and bone defects in mice lacking the *Distal-less*-related gene *Dlx5*. *Development* **126**, 3795–3809.
- Adelmann HB** (1966) *Marcello Malpighi and the Evolution of Embryology*. Ithaca, NY: Cornell University Press.
- Allin EF** (1975) The evolution of the mammalian middle ear. *J Morph* **147**, 403–438.
- Allin EF, Hopson A** (1992) Evolution of the auditory system in Synapsida ('Mammal-like reptiles' and primitive mammals) as seen in the fossil record. In *The Evolutionary Biology of Hearing* (eds Webster DB, Fay RR, Popper AN), pp. 587–614. New York: Springer-Verlag.
- Anderson S, Qiu M, Bulfone A, et al.** (1997) Mutations of the homeobox genes *Dlx-1* and *Dlx-2* disrupt the striatal subventricular zone and differentiation of late-born striatal cells. *Neuron* **19**, 27–37.
- von Baer CE** (1827) Ueber die Kiemen und Kiemengefäße in den Embryonen der Wirbelthiere. *Archiv für Anatomie, Physiologie und wissenschaftl. Medizin* **556–568**.
- Barghusen HR, Hopson A** (1979) The endoskeleton: the comparative anatomy of the skull and visceral skeleton. In *Hyman's Comparative Anatomy* (ed. Wake M), pp. 265–326. Chicago: University of Chicago Press.
- Barlow AJ, Francis-West PH** (1997) Ectopic application of recombinant BMP-2 and BMP-4 can change patterning of developing chick facial primordia. *Development* **124**, 391–398.
- Barlow AJ, Bogardi JP, Ladher R, Francis-West P** (1999) Expression of chick *Barx-1* and its differential regulation by FGF-8 and BMP4 signaling in the maxillary primordia. *Dev Dyn* **214**, 291–302.
- de Beer GR, Barrington EJW** (1934) The segmentation and chondrification of the skull of the duck. *Phil Trans Royal Soc London* **223**, 411–467.
- de Beer GR, Moy-Thomas JA** (1935) On the skull of the Holocephali. *Phil Trans Royal Soc London* **224**, 287–312.
- de Beer GR** (1937) *The Development of the Vertebrate Skull*. Chicago: University of Chicago Press.
- Bei M, Maas R** (1998) FGFs and BMP4 induce both *Msx1*-independent and *Msx1*-dependent signaling pathways in early tooth development. *Development* **125**, 4325–4333.
- Bellairs A d'A, Kamal AM** (1981) The chondrocranium and the development of the skull in recent reptiles. In *Biology of the Reptilia*, Vol. 11 (eds Gans C, Parsons TS), pp. 1–263. London: Academic Press.
- Beverdam A, Merlo GR, Paleari L, et al.** (2002) Jaw transformation with gain of symmetry after *Dlx5/Dlx6* inactivation: mirror of the past? *Genesis* **34**, 221–227.
- Bulfone A, Kim HJ, Puelles L, Porteus MH, Grippo JF, Rubenstein JL** (1993) The mouse *Dlx-2* (*Tes-1*) gene is expressed in spatially restricted domains of the forebrain, face and limbs in midgestation mouse embryos. *Mech Dev* **40**, 129–140.
- Carroll RL** (1988) *Vertebrate Paleontology and Evolution*. New York: W.H. Freeman.
- Cobos I, Calcagnotto ME, Vilaythong AJ, Noebels J, Baraban SC, Rubenstein JLR** (2005) Mice lacking the *Dlx1* transcription factor exhibit subtype-specific loss of interneurons, reduced synaptic inhibition and epilepsy. *Nat Neurosci* **8**, 1059–1068.
- Cohen SM, Jurgens G** (1989) Proximal–distal pattern formation in *Drosophila* – Graded requirement for *Distal-Less* gene activity during limb development. *Roux Arch Dev Biol* **198**, 157–169.
- Couly GF, Coltey PM, Le Douarin NM** (1993) The triple origin of skull in higher vertebrates: a study in quail–chick chimeras. *Development* **117**, 409–429.
- Crackower MA, Scherer SW, Rommens JM, et al.** (1996) Characterization of the split hand/split foot malformation locus SHFM1 at 7q213–q221 and analysis of a candidate gene for its expression during limb development. *Hum Mol Genet* **5**, 571–579.
- Crompton AW, Parker P** (1978) Evolution of the mammalian masticatory apparatus. *Am Sci* **66**, 192–201.
- Cubbage CC, Mabey PM** (1996) Development of the cranium and paired fins in the zebrafish *Danio rerio* (Ostariophysi, Cyprinidae). *J Morph* **229**, 121–160.
- Depew MJ, Liu JK, Long JE, et al.** (1999) *Dlx5* regulates regional development of the branchial arches and sensory capsules. *Development* **126**, 3831–3846.
- Depew MJ, Lufkin T, Rubenstein JL** (2002a) Specification of jaw subdivisions by *Dlx* genes. *Science* **298**, 381–385.
- Depew MJ, Tucker A, Sharpe A** (2002b) Craniofacial development. In *Mouse Development: Patterning, Morphogenesis, and Organogenesis* (eds Rossant J, Tam PPL), pp. 421–498. London: Academic Press.
- Dolle P, Price M, Duboule D** (1992) Expression of the murine *Dlx-1* homeobox gene during facial, ocular and limb development. *Differentiation* **49**, 93–99.
- Dong J, Amor D, Aldred MJ, Gu T, Escamilla M, MacDougall M** (2005) *DLX3* mutation associated with autosomal dominant amelogenesis imperfecta with taurodontism. *Am J Med Genet* **133**, 138–141.
- Duboule D** (1994) Temporal colinearity and the phylotypic progression: a basis for the stability of a vertebrate Bauplan and the evolution of morphologies through heterochrony. *Development* **103** (Suppl.), 135–142.
- Ellies DL, Stock DW, Hatch G, Giroux G, Weiss KM, Ekker M** (1997) Relationship between the genomic organization and the overlapping embryonic expression patterns of the zebrafish *dlx* genes. *Genomics* **45**, 580–590.
- Fawcett E** (1922) The primordial cranium of *Xerus* (spiny squirrel) at the 17 and 19 millimeters stages. *J Anat* **57**, 221–237.
- Ferguson CA, Tucker AS, Sharpe PT** (2000) Temporospatial cell interactions regulating mandibular and maxillary arch patterning. *Development* **127**, 403–412.

- Francis-West PH, Robson L, Evans DJ (2003) Craniofacial development: the tissue and molecular interactions that control the development of the head. *Adv Anat Embryol Cell Biol* **169**, 1–138.
- Gaupp EWT (1898) Die Metamerie des Schädels. *Erg Anat Ent -Ges* **7**, 793–885.
- Gaupp EWT (1899) Ontogenese und Phylogenese des Schallleitenden Apparates bei den Wirbeltieren. *Ergebn D Anat U Entw* **VIII**, 990–1149.
- Gaupp EWT (1905) Das Hyobranchialskelet der Wirbeltiere. *Ergebn D Anat U Entw* **XIV**, 807–1048.
- Gegenbaur C (1888) Die Metamerie des Kopfes. *Morph Jahrb* **13**, 1–114.
- Gendron-Maguire M, Mallo M, Zhang M, Gridley T (1993) *Hoxa-2* mutant mice exhibit homeotic transformation of skeletal elements derived from cranial neural crest. *Cell* **75**, 1317–1331.
- Ghanem N, Jarinova O, Amores A, et al. (2003) Regulatory roles of conserved intergenic domains in vertebrate *Dlx* bigene clusters. *Genome Res* **13**, 533–543.
- Goodrich ES (1958) *Studies on the Structure and Development of Vertebrates*. New York: Dover Publications.
- Graham A (2001) The development and evolution of the pharyngeal arches. *J Anat* **199**, 133–141.
- Gregory WK (1904) The relations of the anterior visceral arches to the chondrocranium. *Biol Bul (Woods Hole, Mass)* **7**, 55–69.
- Gregory WK (1913) Critique of recent work on the morphology of the vertebrate skull, especially in relation to the origin of mammals. *J Morph* **24**, 1–42.
- Gregory WK (1933) Fish skulls: a study of the evolution of natural mechanisms. *Am Philosoph Soc* **23**, 412–449.
- Haldeman RJ, Cooper LF, Hart TC, et al. (2004) Increased bone density associated with *DLX3* mutation in the tricho-dentosseous syndrome. *Bone* **35**, 988–997.
- Hall BK (1999) *Evolutionary Developmental Biology*. London: Kluwer.
- Hanken J, Klymkowsky MW, Summers CH, Seufert DW, Ingebrigtsen N (1992) Cranial ontogeny in the direct-developing frog, *Eleutherodactylus coqui* (Anura: Leptodactylidae), analyzed using whole-mount immunohistochemistry. *J Morph* **211**, 95–118.
- His W (1881) Mittheilungen zur Embryologie der Säugethiere und des Menschen. *Archiv für Anatomie, Physiologie Anat. Abth Jhrg* **303–329**.
- Horike S, Cai S, Miyano M, Cheng JF, Kohwi-Shigematsu T (2005) Loss of silent-chromatin looping and impaired imprinting of *DLX5* in Rett syndrome. *Nat Genet* **37**, 31–40.
- Howes GB, Swinnerton HH (1901) On the development of the skeleton of the tuatara, *Sphenodon punctatus*. *Trans Zool Soc Lond* **16**, 1–86.
- Hunt P, Whiting J, Muchamore I, Marshall H, Krumlauf R (1991a) Homeobox genes and models for patterning the hindbrain and branchial arches. *Development Suppl.*, 187–196.
- Hunt P, Wilkinson D, Krumlauf R (1991b) Patterning the vertebrate head: murine *Hox 2* genes mark distinct subpopulations of premigratory and migrating cranial neural crest. *Development* **112**, 43–50.
- Huschke E (1827) Über die Kiemenbogen und Kiemengefäße bey m bebrüteten Hühnchen. *Isis Von Oken, Jhrg* **1827**, 401–403.
- Huxley TH (1869) On the representatives of the malleus and the incus of the Mammalia in the other Vertebrata. *Proc Zool. Soc Lond* **391–407**.
- Huxley TH (1876) On the nature of the craniofacial apparatus of *Petromyzon*. *J Anat Physiol* **10**, 412–429.
- Janvier P (1996) *Early Vertebrates*. Oxford Monographs in Geology and Geophysics, 33. Oxford: Oxford University Press.
- Jarvik E (1980) *Basic Structure and Evolution of Vertebrates*. New York: Academic Press.
- Jollie M (1957) The head skeleton of the chicken and remarks on the anatomy of this region in other birds. *J Morph* **100**, 389–436.
- Jollie M (1962) *Chordate Morphology*. New York: Reinhold.
- Jollie M (1977) Segmentation of the vertebrate head. *Am Zool* **17**, 323–333.
- Kimmel CB, Ballard WW, Kimmel SR, Ullmann B, Schilling TF (1995) Stages of embryonic development of the zebrafish. *Dev Dynamics* **203**, 253–310.
- Kimmel CB, Miller CT, Keynes RJ (2001) Neural crest patterning and the evolution of the jaw. *J Anat* **199**, 105–120.
- Kimura MI, Kazuki Y, Kashiwagi A, et al. (2004) *Dlx5*, the mouse homologue of the human-imprinted *DLX5* gene, is biallelically expressed in the mouse brain. *J Hum Genet* **49**, 273–277.
- Kindred JE (1921) The chondrocranium of *Syngnathus fuscus*. *J Morph* **35**, 425–456.
- Kingsbury BF (1926) Branchiomerism and the theory of head segmentation. *J Morph* **42**, 83–109.
- Kingsley JS (1925) *The Vertebrate Skeleton from the Developmental Standpoint*. Philadelphia: P. Blakiston.
- Krumlauf R (1993) Hox genes and pattern formation in the branchial region of the vertebrate head. *Trends Genet* **9**, 106–112.
- Kuhn H, Zeller U (1987) The cavum epiptericum in monotremes and therian mammals. In *Morphogenesis of the Mammalian Skull* (eds Zeller U, Kuhn H), pp. 51–70. Hamburg: Parey.
- Kuratani S, Matsuo I, Aizawa S (1997) Developmental patterning and evolution of the mammalian viscerocranium: genetic insights into comparative morphology. *Dev Dynamics* **209**, 139–155.
- Kuratani S (2003a) Evolutionary developmental biology and vertebrate head segmentation: a perspective from developmental constraint. *Theory Biosci* **122**, 230–251.
- Kuratani S (2003b) Evolution of the vertebrate jaw: homology and developmental constraints. *Palaeontol Res* **7**, 89–102.
- Kuratani S (2004) Evolution of the vertebrate jaw: comparative embryology and molecular developmental biology reveal the factors behind evolutionary novelty. *J Anat* **205**, 335–347.
- Kuratani S, Murakami Y, Nobusada Y, Kusakabe R, Hirano S (2004) Developmental fate of the mandibular mesoderm in the lamprey, *Lethenteron japonicum*: comparative morphology and development of the gnathostome jaw with special reference to the nature of the trabecula cranii. *J Exp Zool (Mol Dev Evol)* in press.
- Kuratani S (2005) Craniofacial development and the evolution of the vertebrates: the old problems on a new background. *Zool Sci* **22**, 1–19.

- Langille RM, Hall BK** (1989) Developmental processes, developmental sequences and early vertebrate phylogeny. *Biol Rev Cambridge Philosoph Soc* **64**, 73–91.
- Lawrence PA** (1992) *The Making of a Fly: the Genetics of Animal Design*. Oxford: Blackwell Scientific.
- Lewis EB** (1978) A gene complex controlling segmentation in *Drosophila*. *Nature* **276**, 565–570.
- Liessner E** (1888) Ein Beitrag zur Kenntnis der Kiemerspalten und ihrer Anlagen bei amnioten Wirbeltieren. *Morph Jahrb* **XIII**, 402–425.
- Lumsden AG** (1988) Spatial organization of the epithelium and the role of neural crest cells in the initiation of the mammalian tooth germ. *Development* **103** (Suppl.), 155–169.
- Matsuo I, Kuratani S, Kimura C, Takeda N, Aizawa S** (1995) Mouse *Otx2* functions in the formation and patterning of rostral head. *Genes Dev* **9**, 2646–2658.
- McGinnis W, Krumlauf R** (1992) Homeobox genes and axial patterning. *Cell* **68**, 283–302.
- McLeod MJ** (1980) Differential staining of cartilage and bone in whole mouse fetuses by alcian blue and alizarin red S. *Teratology* **22**, 299–301.
- Meckel JH** (1809–1811) *Beyträge zur vergleichenden Anatomie*. 2 volumes. Leipzig.
- Merlo GR, Paleari L, Mantero S, et al.** (2002) Mouse model of split hand/foot malformation type I. *Genesis* **33**, 97–101.
- Moore WJ** (1981) *The Mammalian Skull*. Cambridge: Cambridge University Press.
- Morasso MI, Grinberg A, Robinson G, Sargent TD, Mahon KA** (1999) Placental failure in mice lacking the homeobox gene *Dlx3*. *Proc Natl Acad Sci USA* **96**, 162–167.
- Neider AH, Virupannavar V, Hooker GW, Langeland JA** (2001) Lamprey *Dlx* genes and early vertebrate evolution. *Proc Natl Acad Sci USA* **98**, 1665–1670.
- Nelsen OE** (1953) *Comparative Embryology of the Vertebrates*. New York: Blakiston Co.
- Neubüser A, Peters H, Balling R, Martin GR** (1997) Antagonistic interactions between FGF and BMP signaling pathways: a mechanism for positioning the site of tooth formation. *Cell* **90**, 247–255.
- Noden DM** (1991) Vertebrate craniofacial development: the relation between ontogenetic process and morphological outcome. *Brain, Behavior and Evolution* **38**, 190–225.
- Norman JR** (1926) The development of the chondrocranium of the Eel (*Anguilla vulgaris*), with observations on the comparative morphology and development of the chondrocranium in bony fishes. *Phil Trans Royal Soc Lond* **214**, 369–464.
- Northcutt RG** (1990) Ontogeny and phylogeny: a re-evaluation of conceptual relationships and some applications. *Brain, Behavior and Evolution* **36**, 116–140.
- Novacek MJ** (1993) Patterns of diversity in the mammalian skull. In *The Skull, Vol. 2: Patterns of Structural and Systematic Diversity* (eds Hanken J, Hall BK), pp. 438–545. Chicago: University of Chicago Press.
- Nüsslein-Volhard C, Wieschaus E** (1980) Mutations affecting segment number and polarity in *Drosophila*. *Nature* **287**, 795–801.
- Panganiban G, Irvine SM, Lowe C, et al.** (1997) The origin and evolution of animal appendages. *Proc Natl Acad Sci USA* **94**, 5162–5166.
- Panganiban G, Rubenstein JL** (2002) Developmental functions of the *Distal-less/Dlx* homeobox genes. *Development* **129**, 4371–4386.
- Parker WK** (1866) On the structure and development of the skull in the ostrich tribe. *Phil Trans Royal Soc Lond* **156**, 113–183.
- Parker WK** (1869) On the structure and development of the skull of the common fowl (*Gallus domesticus*). *Phil Trans Royal Soc London* **159**, 755–807.
- Parker WK** (1871) On the structure and development of the skull of the common frog (*Rana temporaria*, L.). *Phil Trans Royal Soc London* **161**, 137–211.
- Parker WK** (1873) The Bakerian lecture: on the structure and development of the skull in the salmon (*Salmo salar*, L.). *Phil Trans Royal Soc London* **163**, 95–114.
- Parker WK** (1876) On the structure and development of the skull in the Batrachia. Part II, I. *Phil Trans Royal Soc London* **166**, 601–669.
- Parker WK** (1877) On the structure and development of the skull in the urodelous Amphibia. Part I. *Phil Trans Royal Soc London* **167**, 529–597.
- Parker WK** (1878) On the Structure and Development of the Skull in the Common Snake (*Tropidonotus natrix*). *Phil Trans Royal Soc London* **169**, 385–417.
- Parker WK** (1879) The Croonian Lecture: On the Structure and Development of the Skull in the Lacertilia. Part I. On the Skull of the Common Lizards (*Lacerta agilis*, L. *viridis*, and *Zootoca vivipara*). *Phil Trans Royal Soc London* **170**, 595–640.
- Parker WK** (1881) On the structure and development of the skull in the Batrachia. Part III. *Phil Trans Royal Soc London* **172**, 1–266.
- Parker WK** (1882) On the structure and development of the skull in sturgeons (*Acipenser ruthenus* and *A. sturio*). *Phil Trans Royal Soc London* **173**, 139–185.
- Parker WK** (1883) On the skeleton of the marsipobranch fishes. Part II. Petromyzon. *Phil Trans Royal Soc London* **174**, 373–409.
- Parker WK** (1885a) On the structure and development of the skull in the Mammalia. Part II. Edentata. *Phil Trans Royal Soc London* **176**, 1–119.
- Parker WK** (1885b) On the structure and development of the skull in the Mammalia. Part III. Insectivora. *Phil Trans Royal Soc London* **176**, 121–275.
- Paterson N** (1939) The head of *Xenopus laevis*. *Q J Microsc Sci* **81**, 161–234.
- Presley R, Steel FLD** (1976) On the homology of the alisphenoid. *J Anat* **121**, 441–459.
- Qiu M, Bulfone A, Martinez S, et al.** (1995) Null mutation of *Dlx-2* results in abnormal morphogenesis of proximal first and second branchial arch derivatives and abnormal differentiation in the forebrain. *Genes Dev* **9**, 2523–2538.
- Qiu M, Bulfone A, Ghattas I, et al.** (1997) Role of the *Dlx* homeobox genes in proximodistal patterning of the branchial arches: mutations of *Dlx-1*, *Dlx-2*, and *Dlx-1* and *-2* alter morphogenesis of proximal skeletal and soft tissue structures derived from the first and second arches. *Dev Biol* **185**, 165–184.
- Radinsky LB** (1987) *The Evolution of Vertebrate Design*. Chicago: University of Chicago Press.

- Rathke MH (1825a) Kiemen bey Säugethieren. *Isis Von Oken, Jhrg I*, 747–749.
- Rathke MH (1825b) Kiemen bey Vögeln. *Isis Von Oken, Jhrg II*, 1100–1101.
- Rathke MH (1828) Ueber das Daseyn von Kiemenandeutungen bey menschlichen Embryonen. *Isis Von Oken, Jhrg* 80–85.
- Rathke MH (1839) *Entwicklungsgeschichte der Natter*. Koenigsberg.
- Rathke MH (1843) Ueber die Entwicklung der Arterien, welche bei den Säugethieren von dem Bogen der Aorta ausgehen. *Archiv für Anatomie, Physiologie und wissenschaftl. Medicin Jhrg* 276–313.
- Rathke MH (1857) Untersuchungen über die Aortenwurzeln und die von ihnen ausgehenden Arterien der Surier. *Denkschr Kaiserl Akad D Wiss Wien, Math-Naturwiss Kl XIII*, 51–142.
- Reichert C (1837) Über die Visceralbogen der Wirbeltiere im Allgemeinen und deren Metamorphosen bei den Vögeln und Säugethieren. *Archiv für Anatomie, Physiologie und wissenschaftl. Medicin Jhrg* 120–222.
- Reynolds SH (1913) *The Vertebrate Skeleton*. Cambridge: Cambridge University Press.
- Rijli FM, Mark M, Lakkaraju S, Dierich A, Dollé P, Chambon P (1993) A homeotic transformation is generated in the rostral branchial region of the head by disruption of *Hoxa-2*, which acts as a selector gene. *Cell* 75, 1333–1349.
- Robinson GW, Mahon KA (1994) Differential and overlapping expression domains of *Dlx-2* and *Dlx-3* suggest distinct roles for *Distal-less* homeobox genes in craniofacial development. *Mech Dev* 48, 199–215.
- Robledo RF, Rajan L, Li X, Lufkin T (2002) The *Dlx5* and *Dlx6* homeobox genes are essential for craniofacial, axial, and appendicular skeletal development. *Genes Dev* 16, 1089–1101.
- Romanoff AL (1960) *The Avian Embryo: Structural and Functional Development*. New York: Macmillan.
- Romer AS (1956) *The Osteology of the Reptilia*. Chicago: University of Chicago Press.
- Romer AS (1966) *The Vertebrate Body*. Chicago: University of Chicago Press.
- Romer AS (1972) The vertebrate as a dual animal – somatic and visceral. *Evol Biol* 6, 121–156.
- Santagati F, Rijli FM (2003) Cranial neural crest and the building of the vertebrate head. *Nat Rev Neurosci* 4, 806–818.
- Schmalhausen II (1968) *The Origin of Terrestrial Vertebrates*. New York: Academic Press.
- Schultze HP (1993) Patterns of diversity in the skulls of jawed fishes. In *The Skull, Vol. 2: Patterns of Structural and Systematic Diversity* (eds Hanken J, Hall BK), pp. 189–254. Chicago: University of Chicago Press.
- Selleri L, Depew MJ, Jacobs Y, et al. (2001) Requirement for Pbx1 in skeletal patterning and programming chondrocyte proliferation and differentiation. *Development* 128, 3543–3557.
- Sewertzoff AN (1911) Die Kiemenbogennerven der Fische. *Anat Anz* 38, 487–495.
- Sewertzoff AN (1928) The head skeleton and muscles of *Acipenser ruthenus*. *Acta Zool* 9, 1–127.
- Shigetani Y, Nobusada Y, Kuratani S (2000) Ectodermally derived FGF8 defines the maxillomandibular region in the early chick embryo: epithelial–mesenchymal interactions in the specification of the craniofacial ectomesenchyme. *Dev Biol* 228, 73–85.
- Shigetani Y, Sugahara F, Kawakami Y, Murakami Y, Hirano S, Kuratani S (2002) Heterotopic shift of epithelial–mesenchymal interactions for vertebrate jaw evolution. *Science* 296, 1316–1319.
- Shigetani Y, Sugahara F, Kuratani S (2005) A new evolutionary scenario for the vertebrate jaw. *Bioessays* 27, 331–338.
- Simeone A, Acampora D, Pannese M, et al. (1994) Cloning and characterization of two members of the vertebrate *Dlx* gene family. *Proc Natl Acad Sci USA* 91, 2250–2254.
- Slack JMW, Holland PWH, Graham CF (1993) The zootype and the phylotypic stage. *Nature* 361, 490–492.
- von Sömmerring ST (1799) *Icones embryonum humanorum*. Francofurti ad Moenum.
- Stock DW, Ellices DL, Zhao Z, Ekker M, Ruddle FH, Weiss KM (1996) The evolution of the vertebrate *Dlx* gene family. *Proc Natl Acad Sci USA* 93, 10858–10863.
- Stock DW (2005) The *Dlx* gene complement of the Leopard Shark, *Triakis semifasciata*, resembles that of mammals: implications for genomic and morphological evolution of jawed vertebrates. *Genetics* 169, 807–817.
- Sumiyama K, Ruddle FH (2003) Regulation of *Dlx3* gene expression in visceral arches by evolutionarily conserved enhancer elements. *Proc Natl Acad Sci USA* 100, 4030–4034.
- Takio Y, Pasqualetti M, Kuraku S, Hirano S, Rijli FM, Kuratani S (2004) Lamprey *Hox* genes and the evolution of jaws. *Nature* 429 (6989), 262.
- Thomas BL, Liu JK, Rubenstein JL, Sharpe PT (2000) Independent regulation of *Dlx2* expression in the epithelium and mesenchyme of the first branchial arch. *Development* 127, 217–224.
- Trainor PA, Melton KR, Manzanares M (2003) Origins and plasticity of neural crest cells and their roles in jaw and craniofacial evolution. *Int J Dev Biol* 47, 541–553.
- Trueb L, Hanken J (1992) Skeletal development in *Xenopus laevis* (Anura: Pipidae). *J Morph* 214, 1–41.
- Trueb L (1993) Patterns of cranial diversity among the Lissamphibia. In *The Skull, Vol. 2: Patterns of Structural and Systematic Diversity* (eds Hanken J, Hall BK), pp. 255–343. Chicago: University of Chicago Press.
- Trumpp A, Depew MJ, Rubenstein JLR, Bishop JM, Martin GR (1999) Cre-mediated gene inactivation demonstrates that FGF8 is required for cell survival and patterning of the first branchial arch. *Genes Dev* 13, 3136–3148.
- Tucker AS, Al Khaimis A, Sharpe PT (1998a) Interactions between *Bmp-4* and *Msx-1* act to restrict gene expression to odontogenic mesenchyme. *Dev Dynamics* 212, 533–539.
- Tucker AS, Matthews KL, Sharpe PT (1998b) Transformation of tooth type induced by inhibition of Bmp signaling. *Science* 282, 1136–1138.
- Tucker AS, Khamis AA, Ferguson CA, Bach I, Rosenfeld MG, Sharpe PT (1999a) Conserved regulation of mesenchymal gene expression by *Fgf-8* in face and limb development. *Development* 126, 221–228.
- Tucker AS, Yamada G, Grigoriou M, Pachnis V, Sharpe PT (1999b) Fgf-8 determines rostral–caudal polarity in the first branchial arch. *Development* 126, 51–61.
- Tucker A, Sharpe P (2004) The cutting-edge of mammalian

- development; how embryos make teeth. *Nature Rev Genet* **5**, 499–508.
- Vorster W** (1989) The development of the chondrocranium of *Gallus gallus*. *Adv Anat Embryol Cell Biol* **113**, 1–75.
- Wiedersheim R, Parker WN** (1897) *Elements of the Comparative Anatomy of Vertebrates*. London: Macmillan.
- Wilder HH** (1923) *The History of the Human Body*. New York: H. Holt.
- Wolff CF** (1769) De formatione intestinorum praecipue, tum et de amnio spurio, aliisque partibus embryonic gallinacei, nondum visis. *Novi Commentarii Acad Sci Imp Petropolitanae* **XII**, 403–507; **XIII**, 478–530.
- Yang L, Zhang H, Hu G, Wang H, Abate-Shen C, Shen MM** (1998) An early phase of embryonic *Dlx5* expression defines the rostral boundary of the neural plate. *J Neurosci* **18**, 8322–8230.
- Young JZ** (1962) *The Life of Vertebrates*. New York: Oxford University Press.
- Zoghbi HY** (2003) Postnatal neurodevelopmental disorders: meeting at the synapse? *Science* **302**, 826–830.
- Zusi RL** (1993) Patterns of Diversity in the Avian Skull. In *The Skull, Vol. 2: Patterns of Structural and Systematic Diversity* (eds Hanken J, Hall BK), pp. 391–437. Chicago: University of Chicago Press.